COMPARISON OF THE PERSISTING EFFECTS OF BISPHOSPHONATE TREATMENTS PRIOR TO HINDLIMB UNLOADING ON MECHANICAL AND DENSITOMETRIC PROPERTIES IN THE TIBIA OF ADULT MALE RATS

A Thesis

by

JEREMY MICHAEL BLACK

Submitted to the Office of Graduate and Professional Studies of
Texas A&M University
in partial fulfillment of the requirements for the degree of

MASTER OF SCIENCE

Chair of Committee,	Harry A. Hogan
Committee Members,	Susan A. Bloomfield
	Bruce Tai
Head of Department,	Andreas Polycarpou

December 2016

Major Subject: Mechanical Engineering

Copyright 2016. Jeremy Michael Black

ABSTRACT

Bisphosphonates have been shown to be an effective method to treat detrimental bone loss that is associated with osteoporosis. In microgravity, astronauts experience mechanical unloading of the skeleton. This can cause detrimental bone loss. Bisphosphonates offer astronauts a pharmacological method to combat the negative effect of space flight. This study looked at the effectiveness of two bisphosphonate drug treatments administered prior to hindlimb unloading (HU) and their effect as a countermeasure to disuse induced bone loss and recovery following reambulation.

The model used to mimic space flight was the adult HU rat model, specifically 6-month old, male, Sprague-Dawley rats. The rats underwent 28 days of pre-treatment, 28 days of HU and 56 days of recovery. The rats were divided into four treatment groups. The groups included an age-matched control group (AC) that did not undergo HU. The other groups that underwent HU were hindlimb unloaded control (HUC), alendronate pre-treated (ALN), and risedronate pre-treated (RIS). The effects of pre-treatment and the differences between the two drugs were explored. Data were collected ex vivo from left tibia using peripheral Quantitative Computed Tomography (pQCT) and mechanical testing at both the proximal metaphysis and the mid-diaphysis.

The results of this study showed that bisphosphonates were able to prevent the bone loss that was seen in the HUC animals, and maintain bone at levels that were not statistically different from AC. Metaphysis pQCT scans showed that the drugs were able to significantly combat losses due to HU and were specifically effective in the

cancellous bone. Reduced platen compression tests showed that ALN and RIS were able to maintain cancellous strength in the metaphysis. Mid-diaphysis pQCT scans and 3-point bend tests showed no significant changes in cortical bone due to the drug treatments or HU. Over recovery there were no indications that bisphosphonate pre-treated animals fared worse than AC, despite the fact that they did not completely recover all lost bone. They also did not exhibit age related decline in cancellous bone. The drug pre-treatments did not show any significant differences when compared to each other.

ACKNOWLEDGEMENTS

As with any project as large as this there are plenty of people to thank for their contributions to this work. First, I would like to thank Dr. Tai for taking the time to serve on my thesis committee. I would like to thank Dr. Hogan, my committee chair, for his support of my work in this project, both in providing my funding and his intellectual contributions to the study. He has helped me to grow as both a person and a student and I thank him for that. I would additionally like to thank Dr. Bloomfield for both her participation as a member of my thesis committee and as a collaborator on this research project. The funding for this study was through NASA grant #NNX13AM43G.

I would personally like to thank each and every member of the Bone Biomechanics Lab and the Bone Biology Lab. Countless hours of work have been put in by both graduate and undergraduate students in animal care, data collection, and data analysis. This thesis project could not be completed without this help.

TABLE OF CONTENTS

Page

Page

LIST OF FIGURES

Page

Page

LIST OF TABLES

Page

1. INTRODUCTION

With the advent of spaceflight, humanity has used the power of scientific understanding to overcome a host of difficulties. From rocket propulsion to growing food in space, an increased understanding of space has improved humanity's understanding of how to do things on Earth. One such challenge that has a profound impact outside of space travel is the performance of bone in space. Due to the mechanical unloading that accompanies microgravity in space, the musculoskeletal system undergoes significant changes [1] that can lead to bone mass losses on the order of 1-1.5% per month [1] - [6].

There are a variety of ways to combat bone loss that occurs in space. This includes exercise [7] - [9], drug interventions [7], [8], [10], and even dietary measures [6], [11]. Specifically, when it comes to drug interventions, LeBlanc et al. investigated using a bisphosphonate treatment of alendronate in conjunction with aerobic exercise on astronauts aboard the International Space Station [8]. Alendronate is a common treatment for osteoporosis and has been shown to be effective in reducing fracture risk in postmenopausal women. It has also been shown in human bed rest [12], rat hindlimb unloading (HU) [13], [14], and human spaceflight [8] to be an effective bone loss intervention when administered concurrently with disuse. The current study was designed to analyze the effect of bisphosphonate pre-treatments on rats prior to a period of HU and, following unloading, a return to normal ambulation.

Bone is a complicated biological structure that is constantly changing to adapt to its environment. Exposure to microgravity causes an overall reduction in skeletal loading,

and bone responds by reducing bone mass to meet the new loading requirements. Bone is primarily able to adapt through a process known as remodeling. Bone remodeling is split into two mechanisms, resorption and formation. During resorption, old bone tissue is removed from the matrix. Formation follows resorption and is the process by which new bone tissue is added. Under ordinary circumstances, the processes of formation and resorption are coupled together in such a way that there is not a net change in bone mass. For this reason, remodeling is also referred to as bone homeostasis. This is an important aspect of bone's response to environmental stimuli and it results in changes to bone structure and architecture. One method to reduce spaceflight induced bone loss is to modify remodeling with drug interventions such as bisphosphonate treatments.

Bisphosphonates are used to combat the effects of age-related bone loss that occurs due to osteoporosis [15]. These drugs work by slowing and even stopping bone resorption [16]. This means that, in addition to halting resorption, the formation that occurs to complete the cycle of remodeling does not occur. The only growth that continues to occur is due to modeling, formation that occurs independent of resorption, and not from remodeling. Blocking resorption is an effective countermeasure against age related decline [15], but is not without its drawbacks. As the average life span increases and the age at onset of osteoporosis is similar, the duration of drug treatment to prevent fracture continues to increase. There is an increasing amount of concern that extended use of these drugs over long periods of time can actually reverse improvements in fracture risk reduction [17], [18]. Clinically, it is now being recommended to for some patients to take a hiatus from drug treatment so that the bisphosphonate stored in bone

gets depleted allowing bone remodeling to begin again. This can mitigate an excessive buildup of old bone tissue which has been linked to rises in fracture risk during bisphosphonate treatment [17], [18]. This drug holiday is merely a means to reduce potential negative side effects of long term bisphosphonate use. Bisphosphonates are still a viable, effective means to reduce fracture risk in patients with a variety of conditions.

The current investigation was designed to examine at the effects of two bisphosphonates and their persisting effects on spaceflight induced bone loss. This was studied by using a bisphosphonate drug pre-treatment before a period of HU. While a drug pre-treatment does not exactly emulate the current countermeasures that are used to combat mechanical unloading, it is still completely relevant and has a few advantages. By using a pre-treatment, it is possible to understand how the persisting effect of bisphosphonates will impact bone during HU. The effects will persist through the return to weight bearing post-HU and will shed light on how bisphosphonates effect the recovery of bone. A pre-treatment protocol is also optimal for possible animal spaceflight experiments, by limiting astronaut crew time involved with the experiment inflight to a minimum. Although not explored in this study, there are also a variety of negative side effects from bisphosphonate treatment. A pre-treatment could possibly be used to prevent some of these side effects from occurring while in space, where some side effects could prove to be much more problematic than on earth.

This study also sought to examine the effectiveness of bisphosphonate drug pre-treatments by comparing two bisphosphonates with different binding affinities, alendronate and risedronate. The hypothesis was centered on the idea that the long

retention times of bisphosphonates would allow the drugs to continue to be effective after treatment through a period of HU. After a 28-day pre-treatment, 6 month-old, Sprague-Dawley, male rats were exposed to a 28-day period of HU. HU is used to study bone loss in a variety of animals. A rat model was chosen, not only for its feasibility, but because the bone loss observed in the rat model matches the magnitude of the bone loss in human spaceflight when minimal countermeasures are taken to combat spaceflight induced bone loss [19], [20]. After HU, the rats were allowed to reambulate and recover for 56 days. It was additionally hypothesized that risedronate would show a decline quicker than alendronate, which would give it an advantage over alendronate during the recovery period. These time periods corresponded with the four termination time points: baseline, end of pre-treatment (day 28), end of HU (day 56) and end of recovery (day 112). The study utilized an unbalanced design, with an age matched control that had no treatment, and an HU control group that was unloaded but had no pre-treatment. All of the animals given alendronate and risedronate underwent HU.

The area of interest when studying human bone is typically the femoral neck or the lumbar spine. The femoral neck has been shown to be an incredibly dangerous area of fracture in postmenopausal osteoporosis [21] and has been an area of focus for spaceflight induced bone loss [3]. For rats, the sites that best replicate the bone composition as seen in the human femoral neck are the proximal tibia metaphysis [22] and the distal femur metaphysis. The site of primary interest in this study is the proximal tibia metaphysis, but the tibia mid-diaphysis will also be examined.

The left tibia of all of the rats was analyzed post mortem with three different techniques. These techniques included peripheral Quantitative Computed Tomography, 3-point bend mechanical testing, and reduced platen compression mechanical testing. Each of these techniques offer a unique look at how differences in mineralization, geometry and mechanical strength were caused by changes in treatment. The differences between these methods of analysis will offer insight into how the rat bone changes based on treatment and time. With the analysis of the data from this rodent model, it could be possible to better understand methods to prevent spaceflight induced bone loss and understand how two different bisphosphonates affect bone strength.

2. OBJECTIVES

This investigation has two major areas of interest. The first is to understand how the two drug pre-treatments alter bone during hindlimb unloading (HU) and recovery. The second focus is to see what differences, if any, arise between the use of alendronate and risedronate. The objectives of this investigation were as follows:

1. To characterize the effects of two different bisphosphonate treatments administered prior to a bout of HU on both a period of HU and a period of recovery using densitometric and geometric properties of the rat left tibia.
2. To characterize the effects of two different bisphosphonate treatments administered prior to a bout of HU on both a period of HU and a period of recovery using mechanical properties of the rat left tibia.
3. To further understand how changes in densitometric properties compare to changes in intrinsic and extrinsic mechanical properties.

Based on these objectives, I hypothesize that both bisphosphonate pre-treatments before unloading will protect against bone loss, particularly in the cancellous region, during the subsequent unloading period. The use of a bisphosphonate pre-treatment will not hinder the recovery of bone upon return to weight bearing following unloading.

Additionally, I also hypothesize that if differences arise between the drug pre-treatments, risedronate will show a more positive affect over recovery compared to alendronate upon return to weight bearing. ALN will be more likely to negatively impact the recovery process because its higher binding affinity will introduce stronger and more persistent suppression of remodeling.

3. BACKGROUND

This experiment was conducted as part of a larger study funded by the National Aeronautics and Space Administration (NASA) as a part of NASA Space Biology grant number #NNX13AM43G. The aim of the study was to assess the efficacy of two different drug pre-treatments to combat space flight induced bone loss and recovery from space flight. This was done using a rat hindlimb unloading (HU) model. The model utilized a 28-day period of unloading followed by 56 days of return to normal ambulation (recovery). The treatments used in the study were two anti-catabolic drug treatments, both bisphosphonates, alendronate (ALN) and risedronate (RIS). This experiment was focused on understanding changes in the tibia by using two different methods of measuring mechanical and densitometric properties. The data collected will offer insight into how the two bisphosphonate drugs affect skeletal integrity in the long term, and, especially, for astronauts. These results will offer new and insightful results that can be used to better inform decisions about how to treat astronauts in space, and how to treat other users of bisphosphonates on earth.

3.1. The Basics of Bone Biology

Bone is the part of the body that gives it shape and structure. Like every other part of the body, it has the ability to adapt to the environment around it, which makes it truly impressive. Bone is composed of two different types of bone, cortical and cancellous bone.

Cortical bone is largely composed of a mineralized collagen framework made up of an interior of calcium phosphate and water. This structure is organized in a lamellar

fashion that is initially determined by a genetic model [23]. These layers form cylindrical structures known as osteons (Figure 1). Osteons are concentric layers of cortical bone that surround what is known as the Haversian canal. This canal houses vessels and nerves and is used to deliver nutrients to the interior of the bone.

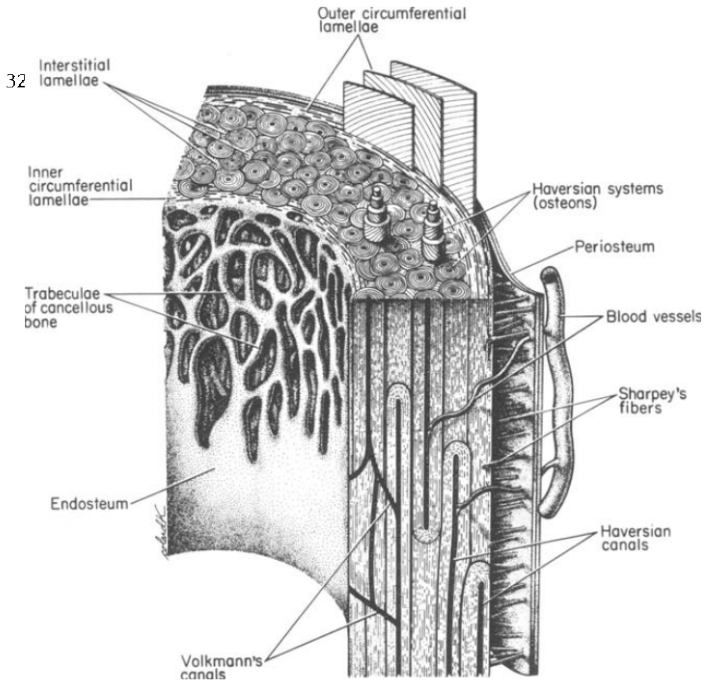

Figure 1. Sketch of Important Features of Long Bone. [23]

An important thing to consider for this experiment is that Haversian canals and osteons are not present in rat cortical bone [23]. This is an important difference between the actual structure and behavior of rat bone compared to human bone. This limits the scope of comparison between humans and rats for the study of intracortical bone

remodeling, but rat models are very effective in predicting the outcomes of similar treatments to human cancellous bone.

The other type of bone is cancellous bone as shown in Figure 2. This bone is unique in that it is made of individual trabeculae which form a porous network [23]. It can be found in vertebrae, flat bones, and the ends of long bones. This bone is 75-95% porous with marrow cells filling the interconnected pores. These pores are formed by individual trabeculae that are around 200 μm thick [24]. The structure of the trabeculae is unique in a few ways. The first is that all animals show the exact same size of trabeculae [24]. This means that the only difference between humans and rats is the volume of cancellous bone, not the actual size of the trabeculae that make up the bone.

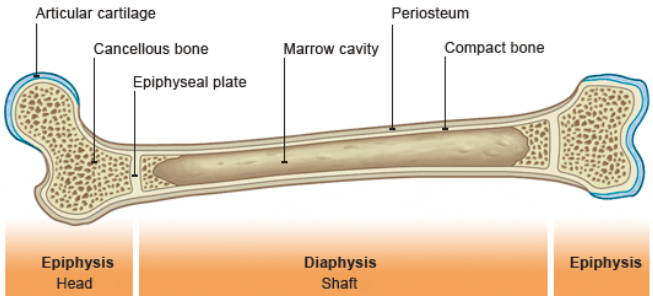

Figure 2. Diagram of Cortical and Cancellous Regions of Bone. [25]

Cancellous bone is a region of bone that also shows the most rapidly, depending on the local environmental conditions. It is widely believed that the trabeculae in these compartments are able to align themselves so that they are in the direction of maximum

loading [26], [27]. Cancellous bone is useful because individual trabeculae are smaller than the layers that make up cortical bone, meaning that it can be modified quickly, through bone resorption or formation, to adapt to the environment. The porous structure of the bone allows it to absorb more impact than cortical bone and that is why it can be found in the locations it is throughout the body; these are locations of high impact such as the long bones and spine.

These descriptions of cortical and cancellous bone are missing a very important part, the biology behind how they work. Bone is more than just a structural support. It is a living part of the body that is constantly changing. Bone undergoes two processes that make up this cycle of change: formation and remodeling.

Bone formation is basic growth of bone. Bone is added layer by layer in a lamellar structure. This process occurs at a high rate during early development and once skeletal maturity is reached, the rate of formation slows [23]. The occurrence of bone formation remains relatively constant after skeletal maturity, except during cases of fracture healing or other severe damage to the bone.

Remodeling is the process by which bone adapts to environmental conditions. This process involves a three step cycle: activation, resorption and formation [23]. In activation, osteoclasts, a specialized bone cell, begin to move to sites in the bone where tissue is to be removed. In resorption, the osteoclasts work to remove the old tissue. In formation, another bone cell, known as an osteoblast, replaces the removed tissue with new bone. This process is shown in Figure 3. This process seems simple in concept, but understanding this process and how it affects bone is a large area of research in bone

biology. Small changes in hormones and other regulatory functions in the body can drastically effect the way that osteoclasts and osteoblasts behave. This experiment, which uses hindlimb unloading, is also looking at how changes in remodeling or after a period of disuse affect the resulting bone structure.

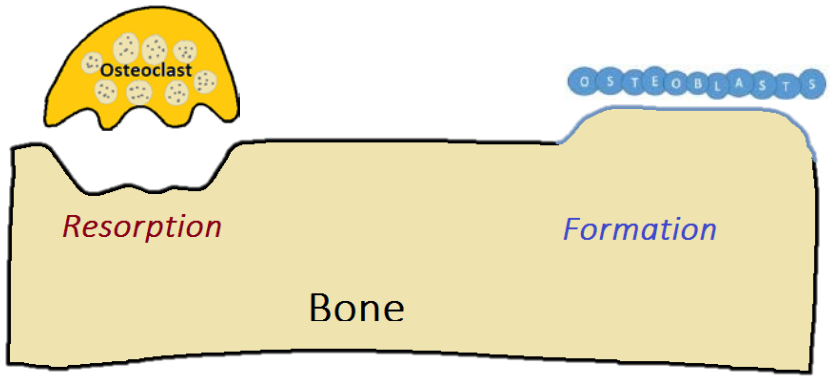

Figure 3. Osteoclasts and Osteoblasts in the Bone Remodeling Cycle.

When experiencing spaceflight or hindlimb unloading, bone adapts to the lack of mechanical loading on the skeleton by removing bone. This would not be a major problem if astronauts were to stay in space; however, if the skeleton is completely adapted to space, it will not be able to handle the much higher mechanical load on the skeleton due to earth's gravity at the end of a mission.

3.1.1. Mechanical Adaptation of Bone

Changes in the loading of bone can drastically alter how bone is structured. Bone can undergo a wide variety of adaptations and depart greatly from what could be called "normal" structure. These changes are described by what is known as Wolff's law. This

law states that bone in all vertebrates will adapt to the current mechanical loading conditions to which it is subjected [28]. This means that as loading changes, formation and remodeling are used to modify both the cortical and cancellous bone. This ability to alter bone is based on what is known as mechanotransduction. There are special cells in the bone matrix that are able to detect changes in loading and these then instruct the osteoclasts and osteoblasts to begin their work in new formation and remodeling. In unique cases, these changes can cause bone to change so rapidly that it does not structure itself in a lamellar fashion.

The process of HU triggers a response in the mechanotransduction cells that causes a drastic increase in resorption, resulting in rapid bone loss. This is a risk because, upon returning to earth, astronauts no longer have the bones with the same strength as when they departed to space.

3.2. Understanding Mechanical Testing Data

Destructive testing of materials can be useful in understanding how and why they fail. This is especially useful in understanding the mechanical strength of bone. Mechanical testing allows bone fracture risk to be explored in much more depth. This not only includes the maximum stresses that a material can withstand, but how much deformation the material can undergo and how the progression of deformation reflects other properties of the material. Figure 4 shows a typical mechanical testing output that is used to measure mechanical properties.

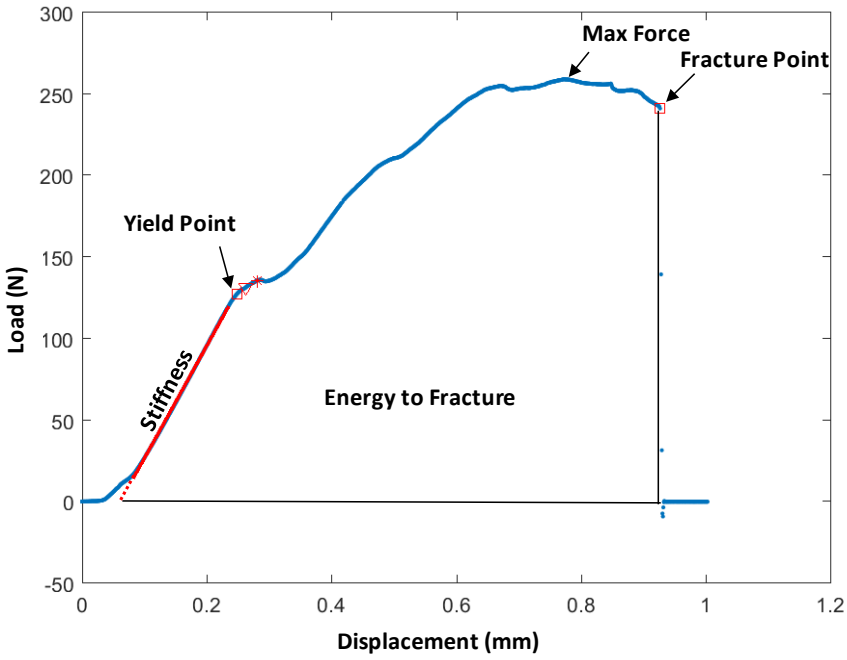

Figure 4. Graphical Representation of Extrinsic Force-Displacement Data with Important Data Markers.

There are three important points in Figure 4. The most basic two points are the point of maximum force and the point of fracture force. The other point is the yield point. This point is where the material begins to undergo irreversible changes. This point marks the point of plastic deformation. The linear region to the left of this point is where elastic deformation occurs. The yield point is defined by the end of this linear region of deformation.

The area under this curve is used to calculate energy, sometimes referred to as work. This is the amount of energy that the material is able to absorb. For instance, if the area was calculated from the yield point to the fracture point this would be the energy from

yield to fracture. Energy can be used to compare how the material undergoes deformation and can be used to determine if the material is ductile or brittle.

These material properties are only extrinsic properties. This means that these are measured values that are independent of any contributing factors that could vary between specimens. For example, these properties do not take into account any aspect of the geometry of the specimen tested. For this experiment, the intrinsic properties are directly related to the varying cross-sections of the specimens tested. The 3-point bend test uses cross-sectional moment of inertia and the reduced platen compression test uses area to calculate intrinsic properties from the directly measured extrinsic properties.

Since these intrinsic measurements depend on the cross-section, that means that there can be differences seen in these properties even if the extrinsic properties show no difference. Due to the fact that the drugs used in this study are both bisphosphonates, their method of intervention is incredibly similar. When it comes to finding differences between the drugs, the comparison of extrinsic and intrinsic properties will offer an interesting perspective on how the drugs may be affecting the bone in different ways.

3.3. The Effect of Bisphosphonates on Bone Biology

This experiment used two different bisphosphonate drug treatments to combat the induced bone loss of hindlimb unloading. Bisphosphonates are a catabolic treatment used to combat osteoporosis [15]. These drugs work by slowing and even stopping bone resorption and only allowing new bone formation [16]. In other words, bone is allowed to grow, but not allowed to resorb old bone tissue. There is not a complete consensus on whether the bisphosphonates act directly on the osteoclasts or the osteoblasts [16], but it

is generally considered to affect the osteoclast. The drug works by binding to hydroxyapatite in the matrix of the bone. During resorption, old crystals are dissolved and this releases the bisphosphonate. This is the point where the drug begins to take effect. Since these drugs take effect after osteoclasts begin the resorption process, they do not limit primary formation of bone; however, they do suppress overall formation because formation due to remodeling is essentially halted. Remodeling is the main source of formation after skeletal maturity is reached. This process is shown in Figure 5. In the context of this study, this means that the effect of the drugs will not be pronounced until massive resorption begins, during HU.

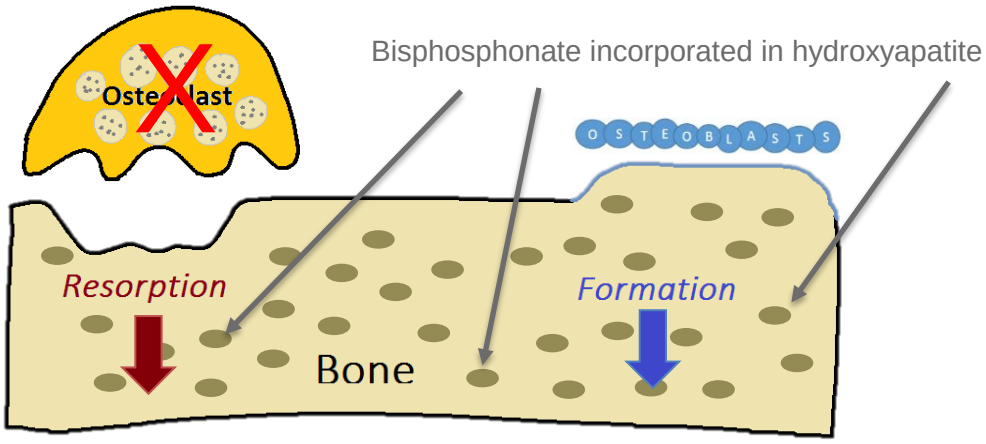

Figure 5. Bisphosphonates and the Remodeling Cycle.

There are a few other important things to note about bisphosphonates. First, is that because the drugs need a surface to bind to, the high surface area of the cancellous region is an optimal site for the drugs to bind. Another important bisphosphonate

specific effect is binding affinity. This is simply how well the drug can bind to the hydroxyapatite. High binding affinity drugs are unable to penetrate as deep into the bone matrix because they bind very rapidly. Low binding affinity drugs are able to penetrate deeper into the matrix because they do not bind as readily to hydroxyapatite [29].

The drugs also have another interesting effect. Since they have to be dissolved out of the matrix to be released, they remain in the mineralized for quite some time. Some of the drugs have been shown to remain in the skeleton for an incredibly long time [30], [31], depending on the treatment procedure. The clinical effectiveness of these drugs is based on their binding affinity [30]. The binding affinity and the retention time in the skeleton are directly related and the higher the binding affinity [31], the more clinically effective the drug is considered to be [32].

The only remaining thing to consider in regards to binding affinity is how it affects the initial time of the treatment. There are differences in the effect of some of the drugs depending on the method of administration. Injections have shown to be the best method for treatment as they limit secondary complications and do no inhibit the effectiveness of the drug [16]. Bisphosphonates have poor absorption through oral administration, and this limitation does not seem to vary between drug binding affinities [16]. There also does not seem to be a relationship between initiation of the effects of bisphosphonates and binding affinity.

An interesting aspect of a bisphosphonate treatment is how exercise can modify the effects of the treatment. Studies have shown that resistance exercise [33] and regular exercise [34] did not alter the results of the drug treatments. The combination of

alendronate and resistance exercise have been tested in space and the results indicated that this can greatly reduce bone loss [8]. Unfortunately, there is no data to compare this to a group treated with only bisphosphonates during spaceflight.

These drugs are an effective countermeasure against age-related decline [16] in bone mass, but not without any drawbacks. As the average life span increases, the duration of drug treatment to prevent fracture continues to increase. A concern arises from the fact that bisphosphonates eventually begin to limit new formation and can cause an increase in bone brittleness. This change in bone is due to the overall lack of formation. Since new bone formation slows after skeletal maturity, this becomes the only method of bone formation once remodeling, which has a secondary method of bone formation, is halted by bisphosphonate treatment. Clinicians have become increasingly concerned about how these changes could affect bone over a long period of time. The concern is that the extended use of bisphosphonates over long periods of time could actually reverse improvements in fracture risk reduction [17].

These drugs can be used for a variety of situations involving bone loss and have previously been used on NASA missions aboard the International Space Station. They have been shown to work to combat bone loss effectively in both astronauts and comparable rat hindlimb unloading models. Therefore, this study seeks to build upon this body of research to discover how the lingering effect of two different bisphosphonate pre-treatments will affect bone during a subsequent period of hindlimb unloading and recovery.

4. EXPERIMENTAL METHODS

This experiment examined the ability of pre-treatments to improve the performance of bone in space. The study used two bisphosphonate drug treatments as interventions against bone loss, alendronate and risedronate. Effects of the treatments on the left tibia were evaluated using peripheral Quantitative Computed Tomography (pQCT), and two tests to measure bone mechanical properties: 3-point bending, and reduced platen compression (RPC) testing.

4.1. Animal Study Background

This experiment used 140 Sprague-Dawley rats acquired from Harlan Sprague Dawley Inc. (Houston, TX) as a part of a protocol approved by the Institutional Animal Care and Use Committee (IACUC). The rats were purchased at approximately 5.5 months old where they have reached skeletal maturity. They were allowed to acclimate for two weeks before beginning the study. After acclimation, the animals were divided into different treatment groups based on body weight and total volumetric bone mineral density (vBMD) from in vivo pQCT at the proximal tibia.

The use of a pre-treatment does not actually emulate the typical countermeasures that are used to combat the unloading effects of microgravity, which are implemented concurrently with spaceflight. Instead, it was used to characterize the time course of effects through a period of HU and recovery following HU. This recovery period is a full return to complete normal weight bearing and ambulatory activity. The protocol was optimized for potential animal spaceflight experiments, by eliminating astronaut crew time required for the experiment as would be the case with a concurrent treatment. This

experiment was additionally aimed at comparing the efficacy of two bisphosphonates with different binding affinities. This investigation has broader implications outside of space flight because of the use of these two drugs. These drugs are widely used to treat osteoporosis but also periods of prolonged disuse, such as bed rest, show comparable effects of bone loss that could possibly be treated with the use of these treatments.

4.1.1. Choice of Bisphosphonates

The major point of treatment comparison centered around two different bisphosphonate drugs. One of the drugs, alendronate, was chosen based on past usage in spaceflight [8]. It is also a common method for treating postmenopausal osteoporosis and is one of the most widely used bisphosphonates. The only issue with the past usage in space is that it was tested in conjunction with exercise and it was not ever used as a singular intervention in space. For this reason, it is not clear what the extent of the effects of the drug are in space. This study sought to use this drug to better understand its effect on microgravity bone loss with a rat hindlimb unloading study.

The other drug, risedronate was selected based on its binding affinity. Binding affinity simply refers to how tightly the bisphosphonate binds to the ligand which is solely a characterization of intermolecular forces between the bisphosphonate and the hydroxyapatite. It is important to note that binding affinity is a determinant of the duration of bisphosphonate effectiveness and does not necessary offer any indication of potency. Risedronate has a lower binding affinity than alendronate, which allows this study to investigate how differences in binding affinity will affect the observed changes in bone over HU and recovery. The expectation is that the differences in binding affinity

may cause a difference between risedronate and alendronate to become apparent over the course of the study. Due to differences in the lingering effects of the two pre-treatments, it is possible that risedronate could provide a better overall response. The lower binding affinity could reduce the chances of inhibiting the recovery that needs to occur in bone upon return to weight bearing.

4.1.2. Comparing Rat and Human Bone

There are several important things to consider when trying to interpret these results and put them in the context of the implications of these results in terms of human spaceflight. The first of these is comparisons between rat and human aging. Correlating rat to human ages can be difficult because rat development varies widely during their lifespan; but, during the period of HU, 10-15 rat days roughly correspond to 1 human year [35]. This means that the 28 day HU is roughly equivalent to 2 years in terms of humans.

Typically, over this 28 day HU period, bone responses similarly to astronauts taking minimal countermeasures to combat bone loss. The HU model in 6-month old rats shows bone loss during 28-days in accordance with 4-6 months of astronaut spaceflight. Previous work by Shirazi et al. demonstrated these results [8], [22].

One of the major sites of concern for fracture risk in humans is the femoral neck. This location has a thin cortical shell that surrounds a central region made up of cancellous bone. In the rat, the femoral neck is mainly cortical bone. This can be seen in Figure 6.

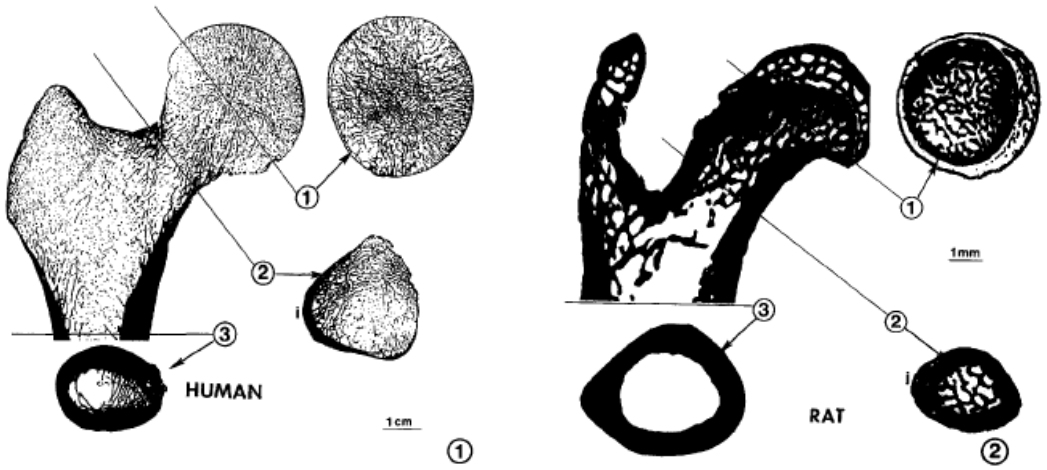

Figure 6. Diagram of Human and Rat Proximal Femur. [36]

The rat proximal tibia metaphysis better expresses the combination of cortical and cancellous bone that more closely mimics the human femoral neck, so this region was selected as the region of focus to analyze how the changes here could potentially affect the human femoral neck. While these comparisons are less than perfect, it has been shown that this is a good analog to humans because rat bone behavior at this site on the cellular and structural level mirrors human bone biology [37].

4.2. Experimental Design

The animals were block assigned to four groups based on body weight and total bone mineral density at the proximal tibia metaphysis in order to create equivalent baseline measurements across all groups. There were two control groups, an age-matched cage control (AC) and a hindlimb unloading control (HUC). There were also two drug treatment groups (ALN and RIS) that also underwent HU after receiving the drug pre-treatment.

The HU method follows a protocol modified from the Morey-Holton tail traction method [5]. A custom-made harness is affixed to the tail of the animal so that the hindlimbs no longer contact the cage bottom (Figure 7a). The rat is suspended at a 30° head-down tilt; the front limbs still retain full contact with the cage bottom. A hook at the end of the tail harness connects to a pulley and rod system in the cage (Figure 7b) so the animal has the ability to move about the cage to access food and water with only its front legs.

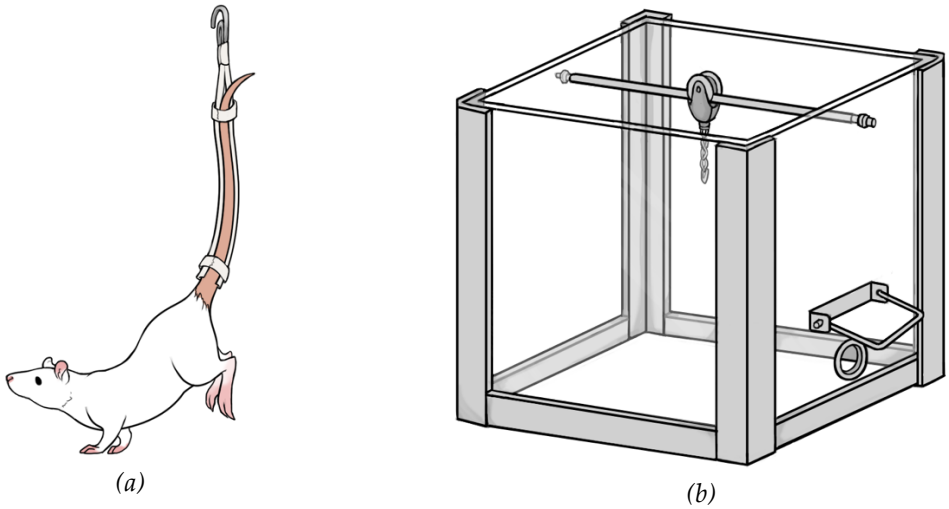

Figure 7. Rat Hindlimb Unloading Setup. (a) Rat in Hindlimb Unloading Harness (b) Hindlimb Unloading Cage.

The animals receive a health check twice daily during the 28-day HU period. After completing HU, the animals were given 56 days to recover. During recovery, the rats return to their pre-study regular ambulation and weight bearing. All rats were single housed throughout the duration of the study and were provided standard rodent chow

(Harlan Teklad 8604) and water ad-libitum, except where specified. When not undergoing HU, the rats were housed in the standard shoebox cages.

The study design was laid out in 28-day (1 month) increments. The first 28 days consisted of the drug pre-treatment. The drug treatment groups were given subcutaneous injections tri-weekly for four weeks. The ALN dosage was 2.4 μg/kg. The RIS dosage was 1.2 μg/kg. These doses correspond, respectively with 10 ng/d and 5 mg/d clinical does given to treat postmenopausal osteoporosis in humans [38]. Upon reaching the 28th day of the study, HU of the animals began.

There were four important time points in the study that were used to measure the effects of the treatments in excised bone as shown in Figure 8. Bone tissue was collected from separate groups of rats terminated at, baseline (day 0), the end of pre-treatment (day 28), the end of HU (day 56) and the end of recovery (day 112).

Figure 8. Bisphosphonate Pre-Treatment Study Design.

The termination plan of the study is shown in Table 1. Eight AC rats were terminated at each time point. The HUC animals there were 10 rats terminated, but only at days 56 and 112. To streamline the study design, no HUC animals were terminated at day 0 or 28, because no animals had undergone HU until after day 28. The two drug treatment groups had terminations of 15 animals per days 28, 56, and 112. The unbalanced design

was used as part of a larger experiment where both the HUC and AC groups will eventually be filled out to have 15 rats per time point. The time point size of 15 per group was chosen to provide enough power to accurately measure the treatment effects in mechanical testing.

Table 1. Complete Study Termination Plan.

	Baseline	End of Pre-Treatment	End of HU	End of Recovery
AC	6	8	8	8
HUC	-	10	10	10
ALN	-	15	15	15
RIS	-	15	15	15

4.2.1. Hindlimb Unloading

HU is the method used in this experiment to induce bone loss on a level similar to that of spaceflight. The model causes bone loss that matches the magnitude of bone loss in astronauts when minimal countermeasures are taken to combat spaceflight induced bone loss [19], [20]. New measures are always being tested to help astronauts improve bone health in space, and this model is widely used to understand new ways of tackling this problem.

The model correlates well to spaceflight because the lack of weight bearing causes the bone to modify itself to meet the new loading conditions. The model also produces effects on the cardiovascular, immune, renal, neural, metabolic and reproductive systems that mimic spaceflight [19]. The changes in loading due to HU mean that bone loss

occurs because the skeleton no longer carries the same mechanical load needed to support the body. These rapid changes are marked by a dramatic increase in resorption and a suppression of bone formation [19]. Not only is the HU model a well-established and accepted ground based model for simulating the effects of microgravity, but it other serious advantages over other methods of simulating microgravity. This model was chosen over onabotulinum toxin A, and other methods of disuse because of the feasibility of a rodent model. Human bed rest studies can be incredibly costly and astronaut studies of bisphosphonates have also been very limited in data collection due to small sample sizes. The model was also chosen because of the good correlation between HU and the wide variety of changes seen in astronauts.

4.3. Ex Vivo Peripheral Quantitative Computed Tomography of Tibia

Each left tibia was analyzed to assess the levels of mineralization, measure various geometrical parameters, and estimate strength indices of the bone using ex vivo peripheral Quantitative Computed Tomography (pQCT). The tibia was scanned using a Stratec XCT 3000 (XCT Research M Stratec; Norland Corp., Fort Atkinson, WI). Using a voxel size of 70 μm, four scan lines 0.5 mm thick were completed in the metaphysis region beginning 4.25 mm distal from the tibia plateau. This region was chosen to avoid the growth plate, which is not as responsive to hindlimb unloading, and focus on the region of cancellous bone tissue. The scan locations are shown in Figure 9, along with sample output images. An additional scan was taken at the mid-diaphysis of the bone, half of the length of the bone.

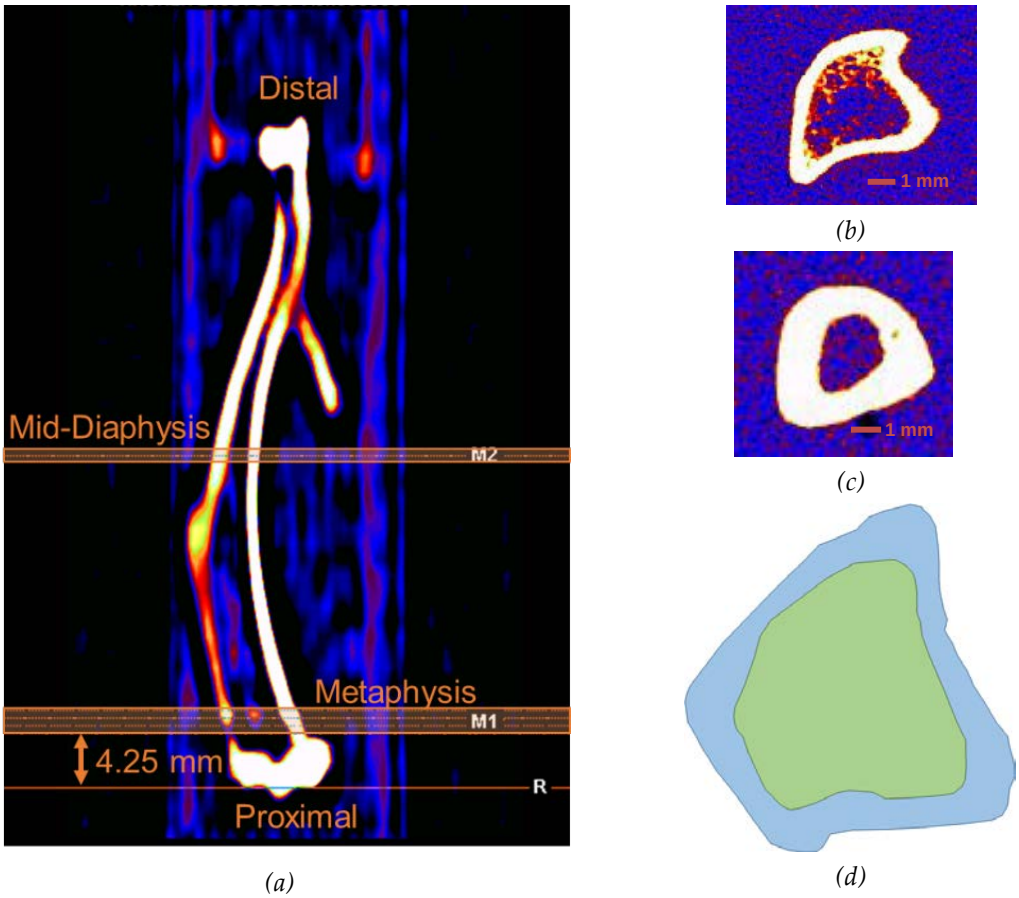

(a) *(b)* *(c)* *(d)*

Figure 9. Ex Vivo pQCT Location Information and Sample Scans. (a) Ex Vivo pQCT Scan Locations; Sample Image of pQCT at: (b) proximal tibia metaphysis (c) tibia mid-diaphysis (d) Regions of Analysis: Total Area (Blue + Green), Cortical (Blue), and Cancellous (Green).

In order to differentiate between cortical and cancellous bone contour and peel algorithms were used. These algorithms were provided by Stratec XCT software (v6.00, Norland Corp., Fort Atkinson, WI). The contour algorithm differentiates between density of cortical bone and surrounding fluid. The peel algorithm is used to delineate between the cortical and cancellous bone at the endocortical surface. The contour and

peel thresholds for the metaphysis were 450 g/mm^3 and 800 g/mm^3 respectively. The thresholds for the diaphysis were 650 g/mm^3 for both algorithms.

4.3.1. Peripheral Quantitative Computed Tomography Output Parameters

The parameters generated from this analysis method included the densitometric outcome variables bone mineral content (total, cortical, and cancellous) and bone mineral density (total, cortical, and cancellous). The pQCT data also included geometrical properties such as polar moment area of inertia (PAMOI), and cross-sectional areas (cortical, cancellous and total). Bone mineral content (BMC), volumetric bone mineral density (vBMD), and cross-sectional area were determined for each of the three regions of the cross-section (Figure 9d): cortical, cancellous, and total. The total region is sometimes referred to as integral for BMC and vBMD because they include contributions from both the cortical and cancellous regions.

In addition to geometric and mineral measurements, strength indices were derived using area and density properties. These indices are meant to be an estimated measure of mechanical strength. The bone strength index (BSI) was used to estimate the compressive strength of the tibia at the metaphysis. This is shown in Equation 1 and was compared to the results of the reduced platen compression test.

$$BSI = (total\ Area)(total\ vBMD)^2 \qquad \textbf{Equation 1 [3]}$$

The stress strain index (SSI) uses total bone mineral density as substitute for modulus and multiplies this value times the moment of inertia of the cross-section. This

value correlates roughly to the section modulus in beam theory (Equation 2). The SSI is given in Equation 3. The measurement made in this experiment is the polar SSI, which eliminates differences due to bone alignment in the scanning bed.

$$Z = \frac{I}{c}$$ **Equation 2**

$$SSI = \sum \frac{r_i^2 a_i \frac{CD_i}{ND}}{r_{max}}$$ **Equation 3 [39]**

The section modulus includes *I*, the moment of inertia, and *c*, the maximum distance from the bending axis to the outer edge of the beam. This parameter is meant to describe the bending stiffness. The SSI measurement (Equation 3) is a voxel-by-voxel summation used to estimate section modulus. In this measurement, r_i is the voxel distance from the center of mass, a_i is the voxel area, CD_i is the apparent voxel density, *ND* is the normal density of cortical bone (this is assumed to be a value of 1200 mg/cm^3), and r_{max} is the maximum distance between the density-weighted center of mass and the outermost voxel for the entire cross-section. The difference between this measurement and section modulus is that SSI is density weighted; however, they still reflect the same general principles. This value was taken at the diaphysis and compared to the results of the 3-point bend test.

4.4. Ex Vivo 3-Point Bend Test of Tibia

Upon completing ex vivo pQCT scans, a 3-point bend test was used to evaluate the mechanical properties of the left tibia mid-diaphysis. The bones were stored with saline and gauze and were thawed to room temperature. Prior to testing digital calipers were used to manually determine the anterior-posterior and medial-lateral periosteal diameters at the mid-diaphysis for each bone. The length of the bone and the midpoint were also recorded. This site is where the center of the bending load is placed, so that the pQCT data at the mid-diaphysis will correspond to the loading point. This is done so that the measurement of cross-sectional moment of inertia (CSMI) can be used to estimate intrinsic mechanical properties in addition to estimating whole bone extrinsic properties. The load was applied using an Instron 3345 Single Column Testing System (Norwood, MA). Each bone was positioned with the anterior side resting on two supports, each spaced 18 mm apart (Figure 10).

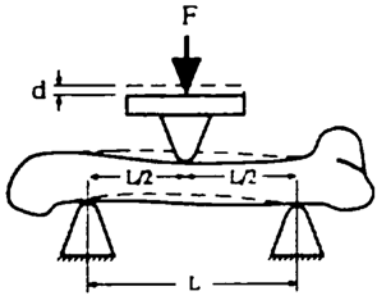

Figure 10. Left Tibia 3-Point Bending Experimental Setup (L = 18 mm). [40]

Once positioned, a preload of about 1 N was applied to the tibia. The crosshead then descended at a rate of 2.54 mm/min (0.1 in/min) and loaded the bones until failure.

Force and crosshead displacement were recorded at 50 Hz by Bluehill (version 2.35, Instron) using a 1kN Instron load cell (2519-105, Norwood, MA). Post hoc analysis was used to determine the intrinsic and extrinsic mechanical properties from the recorded force, displacement and bone CSMI data with a custom written MATLAB program (version 8.5, The MathWorks, Inc.).

4.4.1. 3-Point Bend Test Output Parameters

Extrinsic properties are recorded directly from the output of the 3-point bending test. Intrinsic properties are based on inherent properties specific to each material. The extrinsic properties reported from this test include maximum load (F_{ult}), stiffness (k), post-yield displacement and energy to fracture (E_f). These values were all calculated with post hoc analysis.

Intrinsic properties are derived using Equation 4-Equation 6 using half of the polar moment of inertia, (the CSMI, I) a property that varies between bones. These equations are based on classical beam theory for a beam with simple supports at two ends with a load applied in the middle. The intrinsic outcome variables of interest for this test were ultimate stress (σ_{ult}), elastic modulus (E), and pre-yield toughness (μ).

$$\sigma_{ult} = \frac{F_{ult} L c}{4I} \qquad \textbf{Equation 4}$$

$$E = \frac{k L^3}{48 I} \qquad \textbf{Equation 5}$$

$$\mu = \frac{E_f c^2}{L I} \qquad \textbf{Equation 6}$$

L is the span depth, c is the anterior-posterior diameter and I is the CSMI

It is important to note that, because of the nature of the assumptions used in the 3-point bend testing, these intrinsic properties are only estimates. The largest assumption involved in this analysis is that the location of the measurement of the CSMI is at the exact point of loading. Intrinsic properties are important to consider because they help answer the question of how important the geometry (i.e., CSMI) is to the structural integrity of the bone. There are also underlying assumptions to the analysis that the cross section is of uniform shape across the 18 mm region that is subjected to bending. These properties indicate changes of tissue quality that are independent of changes in bone mass or bone geometry.

4.5. Ex Vivo Reduced Platen Compression Test of Proximal Tibia Metaphysis

The other measure of mechanical strength, reduced platen compression (RPC) testing, was used to test the properties of the cancellous portion of the tibia metaphysis. This test is fairly complicated and requires machining specimens out of the proximal tibia metaphysis before testing. Once the machining is completed, the samples were analyzed to determine platen size required for the testing, and finally, the specimens were tested.

4.5.1. Specimen Preparation

Specimens were machined using a Well Precision Diamond Wire Saw model 3242 (Well Diamond Wire Saws, Inc., Norcross, GA). A 2 mm region 0.5 mm distal from the tibia lateral condyle was removed from the tibia for the RPC test, as shown in Figure 11a. This region is meant to roughly correspond to the region of interest from pQCT

measurements taken at the proximal tibia metaphysis. Prior to testing the specimen, photographs were taken of each of the specimens and Adobe Photoshop (Adobe Systems Incorporated, San Jose, CA), was used to determine platen size. Prior experience has demonstrated that platens should be sized to cover 70% of the diameter of the largest circle that can be inscribed into the endocortical perimeter (Figure 11b).

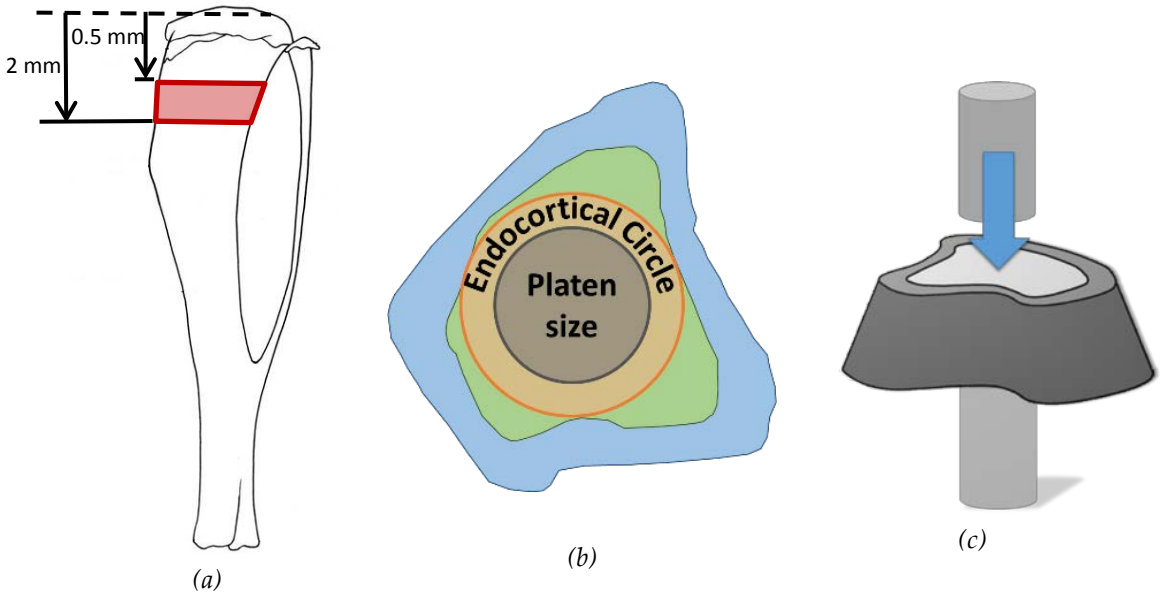

Figure 11. RPC Location, Sizing Methods, and Setup. (a) RPC Specimen Location (shown in red) (b) Platen Sizing Method (c) RPC Test Setup

4.5.2. Reduced Platen Compression Test Method

After preparation, the specimen was compressed between two platens using an Instron 3345 Single Column Testing System (Norwood, MA). Force and displacement data generated by a 100N Instron load cell (2519-103, Norwood, MA) were recorded using Bluehill (version 2.35, Instron) at 20 Hz. The most proximal end of the specimen

is placed on the bottom platen, while the most distal end of the specimen is loaded with the upper platen (Figure 11c). The specimens were loaded at a rate of 0.254 mm/min (0.01 in/min) and compressed. This test allowed the mechanical properties of proximal tibia metaphysis cancellous bone to be assessed, as it is the only region of direct loading in this test. Post hoc analysis was completed using the same custom written MATLAB program used for 3-point bending.

4.5.3. Reduced Platen Compression Test Output Parameters

The extrinsic variables of interest for this test were maximum force (F_{ult}) and stiffness (k). The intrinsic variables of interest for this test were ultimate stress (σ_{ult}) and elastic modulus (E) and strain at yield (ε). They are derived using the equations below (Equation 7-Equation 9). These equations calculate the material properties of an isolated cylinder in compression.

$$\sigma_{ult} = \frac{F_{ult}}{A_{platen}} \qquad \textbf{Equation 7}$$

$$\varepsilon = \frac{d}{t} \qquad \textbf{Equation 8}$$

$$E = \frac{\sigma}{\varepsilon} = \frac{dF_{yield}}{tA_{platen}} \qquad \textbf{Equation 9}$$

Where *d* is crosshead displacement and *t* is specimen thickness

4.6. Statistical Analysis

The data were evaluated for statistical relationships using R (The R Foundation). The statistical analysis of this data was done to compare differences between groups within each time point. No differences were tested between time points. Data were checked for normality using the Shapiro-Wilk test. Homoscedasticity was evaluated using a Brown-Forsythe Levene-type test. If the data were determined to be normally distributed, comparisons between groups were performed using a one-way ANOVA and a Tukey HSD post hoc test. If the Shapiro-Wilk and the Brown-Forsythe hypothesis were not rejected, then the comparisons were made using a Kurskal-Wallis rank sum test followed by a pairwise Dunn's Test for median difference. Differences were considered significant when $p < 0.05$.

5. RESULTS

The following plots for each of the four measures will show group means with bars representing standard deviations. The x-axis for each plot shows the time duration into the study at which each measurement occurred. Time is recorded in days and designated with a “d” preceding the numerical day. The gray region on each plot designated the period of HU. A solid blue line with a circle is used to represent the control group (AC). A short dashed, red line with triangles is used to represent the hindlimb unloading control (HUC). A purple, dot-dash line with diamonds is used to represent the alendronate group (ALN). Finally, a dashed green line with squares is used to represent the risedronate group (RIS). When comparing the time points it is important to note that different animals make up each of the reported means as the data was collected ex vivo. Due to specimen attrition throughout the study, the number of animals per group per time point vary slightly between measurements. The minimum number of animals per group is specified by measurement and given at the start of each measurement section. Additionally, a breakdown of the statistical analysis by time point for all measurements can be found in Appendix A. Appendix B includes additional measurements not included in the Results section.

The efficacy of the treatment is an important thing to mention before elaborating on the results of the actual data collection. Animals were weighed twice weekly and the body weights are shown in Figure 12.The animals lost some weight over HU but it was recovered by the end of the time period. AC animals were pair fed an average value of food eaten by the other groups over the period of HU. Several animals were lost over the

course of the study. Two ALN and two RIS animals were removed from HU due to health concerns. These were the only attritions during the course of treatment.

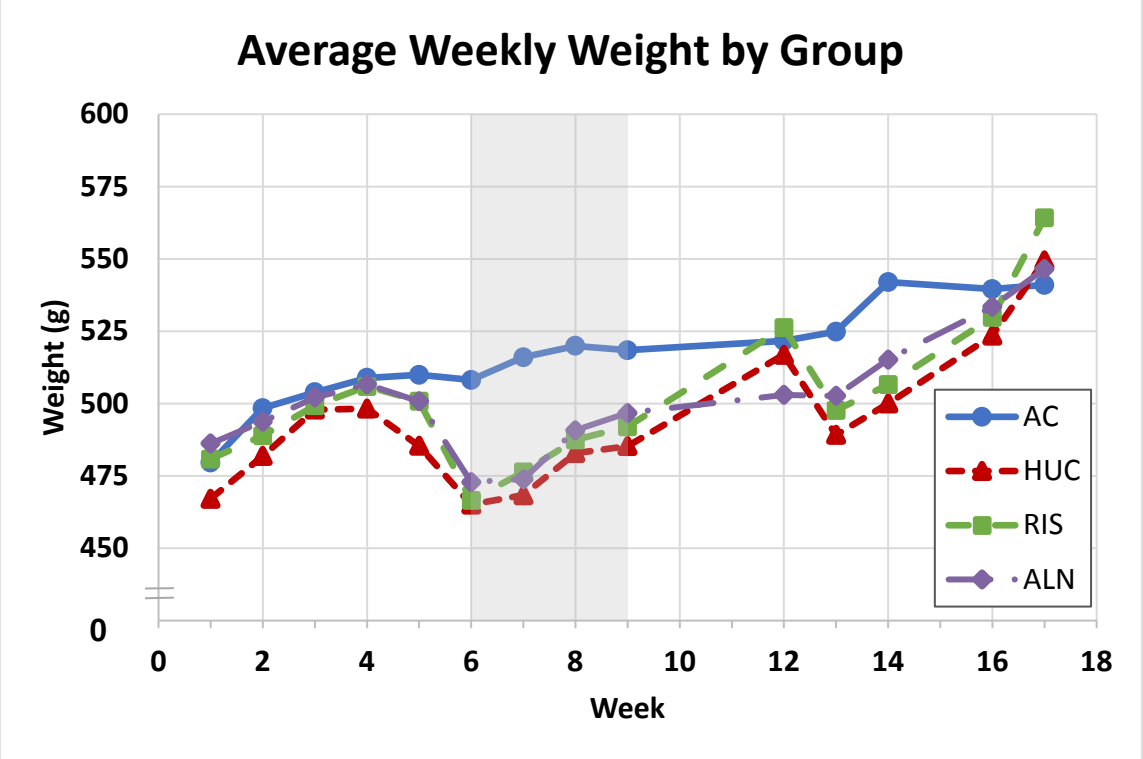

Figure 12. Average Weekly Body Weight by Group. Gray region represents HU.

5.1. Ex Vivo pQCT of the Left Tibia

Ex vivo pQCT scans were completed at the left tibia for each group at all time points. Four scans were taken at the proximal metaphysis and one scan was taken at the mid-diaphysis. For each time point there are at least 6 AC animals, 9 HUC animals, 11 RIS animals, and 13 ALN animals. Proximal Metaphysis Densitometric Properties

The values of proximal metaphysis densitometric properties are given in Table 2. BMC and vBMD were measured for the total, cortical and cancellous regions of the bone. All measures of bone mineral content (BMC) and bone mineral density (vBMD) are lower due to HU. Total BMC (Figure 13) for HUC was significantly lower than AC (10.3 mg/mm versus 12.8 mg/mm). There was also a significant difference between RIS (11.8 mg/mm) and ALN (11.7 mg/mm) versus HUC at the end of the HU period. RIS and ALN had a higher value than HUC, suggesting a mitigating effect of drug treatment. At the end of recovery these three groups were at level of AC. Total vBMD, in Figure 14, followed a similar trend but had no significant differences.

Cancellous BMC in Figure 15 also followed similar pattern to those of total BMC. The drug groups are not different from AC at day 56, but were much higher than the BMC of HUC. Cancellous vBMD (Figure 16) indicated that ALN and RIS, 236.6 mg/mm^3 and 252.9 mg/mm^3 respectively, were significantly higher than HUC, 170.5 mg/mm^3, at the end of HU, and HUC was significantly lower than AC (236.4 mg/mm^3). This lack of difference between ALN, RIS, and AC suggest that the pre-treatments mitigated HU losses. At the end of recovery, the drug pre-treatments still demonstrated a positive effect. ALN had a cancellous vBMD of 238.0 mg/mm^3 and RIS had a cancellous vBMD of 239.5 mg/mm^3, while AC had a cancellous vBMD of 197.93 mg/mm^3.

Cortical BMC (Figure 17) indicated that RIS, HUC, and ALN all had significantly lower BMC compared to AC after HU. ALN had a BMC of 8.83 mg/mm; RIS had a BMC of 8.85 mg/mm; HUC had a BMC of 8.32 mg/mm; and AC had a BMC of 9.90

mg/mm. BMC was gained over recovery to levels that are not statistically different from AC. In Figure 18, cortical vBMD had a difference from all other BMC and vBMD trends. The drug groups trended towards a gain in vBMD over pre-treatment. and then declined for the remainder of the study. For all intents and purposes, these values can be considered essentially constant as the largest change is about 3.5%.

Table 2. Densitometric Properties Measured at the Proximal Tibia Metaphysis.

	Total BMC		Total vBMD		Cancellous BMC		Cancellous vBMD		Cortical BMC		Cortical vBMD	
Baseline	**(mg)**		**(mg/cm³)**		**(mg)**		**(mg/cm³)**		**(mg)**		**(mg/cm³)**	
AC	13.07	(1.18)	599.7	(27.9)	3.38	(0.84)	259.4	(27.7)	9.69	(0.78)	1037.0	(40.2)
End of Pre-treatment (Day 28)												
AC	12.59	(0.96)	582.4	(32.9)	2.97	(0.98)	227.5	(34.0)	9.61	(0.65)	1040.1	(44.8)
ALN	12.29	(1.60)	616.0	(51.0)	2.63	(1.00)	229.0	(59.4)	9.66	(0.99)	1075.6	(39.2)
RIS	12.41	(0.90)	608.5	(28.8)	2.89	(0.65)	245.6	(43.9)	9.52	(0.45)	1059.1	(22.4)
End of Hindlimb Unloading (Day 56)												
AC	12.84	(1.23)	609.2	(46.2)	2.94	(1.02)	236.4	(38.4)	9.90	(0.45)	1061.2	(47.4)
HUC	10.26#	(0.82)	553.6	(55.2)	1.94	(0.64)	170.5#	(27.5)	8.32#	(0.79)	1059.1	(57.7)
ALN	11.69†	(1.17)	590.3	(35.3)	2.86	(0.97)	236.6†	(41.2)	8.83#	(0.61)	1058.9	(47.3)
RIS	11.83†	(1.31)	604.9	(47.0)	2.98	(0.89)	252.9†	(32.9)	8.85#	(0.88)	1057.8	(50.7)
End of Recovery (Day 112)												
AC	12.38	(1.15)	578.5	(26.8)	2.54	(0.97)	197.9	(43.2)	9.84	(0.62)	1070.3	(38.1)
HUC	11.94	(1.30)	578.38	(37.5)	2.40	(0.97)	192.7	(40.9)	9.54	(0.63)	1061.7	(41.0)
ALN	12.62	(1.39)	576.9	(38.8)	3.21	(1.03)	238.0	(39.5)	9.41	(0.82)	1043.4	(43.6)
RIS	12.47	(1.65)	599.3	(30.3)	3.03	(1.04)	239.5†	(45.3)	9.44	(0.89)	1059.2	(45.1)

Values presented as Mean and (Standard Deviation)
† - Indicates significant difference compared to HUC ($p < 0.05$)
 # - Indicates significant difference compared to AC ($p < 0.05$)

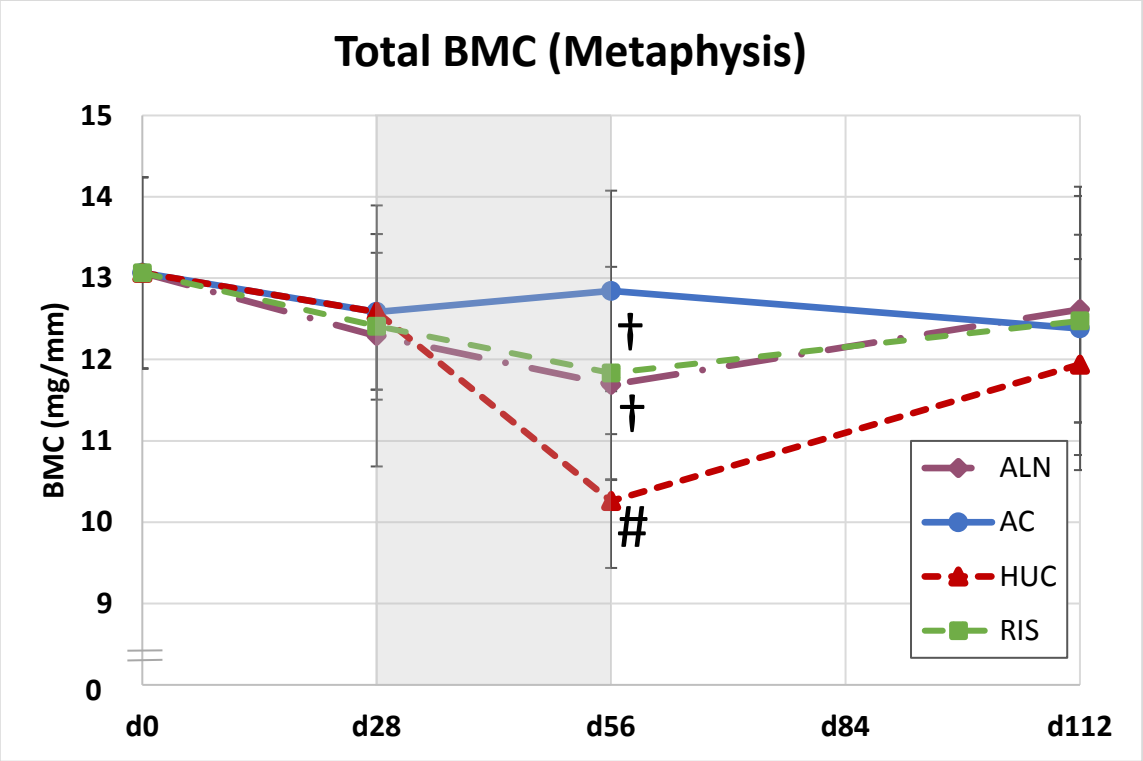

Figure 13. Total Bone Mineral Content for Tibia Metaphysis from Ex Vivo pQCT. Gray region represents HU. HUC is significantly lower than AC at day 56. Both drug treatments were lower than AC, but have significantly higher values than HUC at day 56. At both day 28 and day 112, there are no significant differences in the data. Values are presented as mean ± SD.

† - Indicates significant difference compared to HUC ($p < 0.05$)
 # - Indicates significant difference compared to AC ($p < 0.05$)

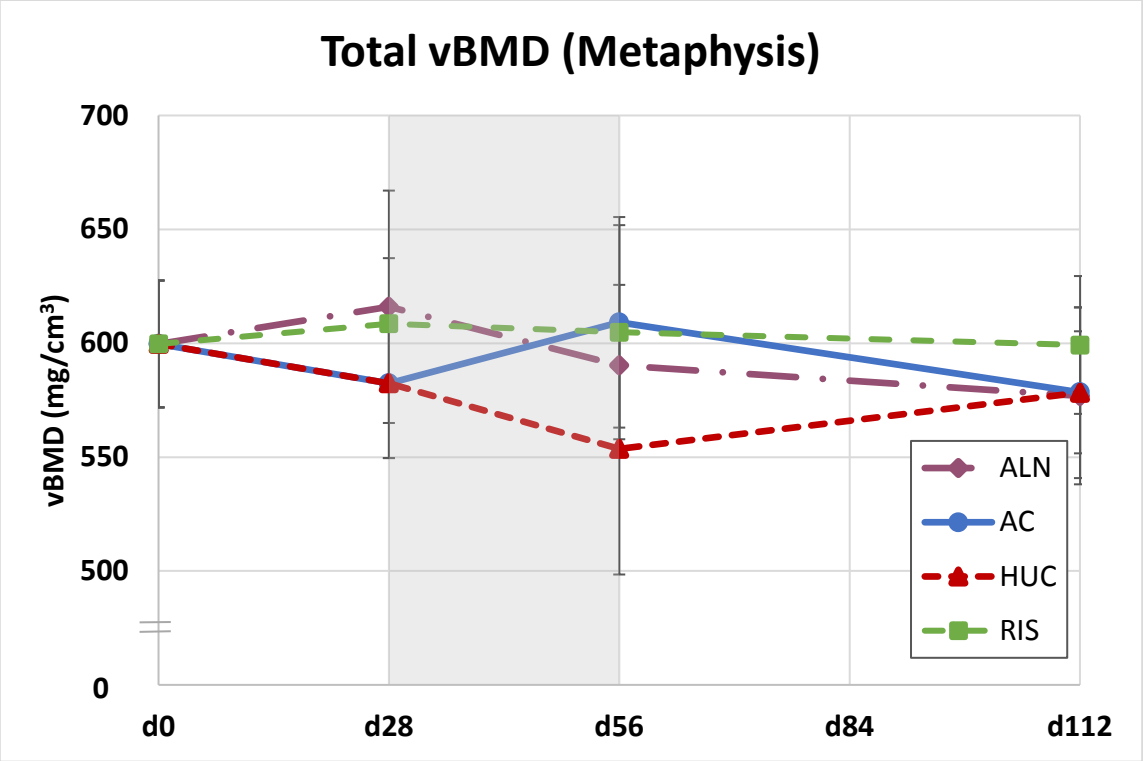

Figure 14. Total Bone Mineral Density for Tibia Metaphysis from Ex Vivo pQCT. Gray region represents HU. Total BMD was higher for AC compared to HUC, RIS, and ALN at day 56. Both RIS and ALN had higher values at day 28 than AC and HUC. By day 112, RIS had the highest BMD and the other groups had around the same BMD. There was no significance at day 28 or 112. Values are presented as mean ± SD.

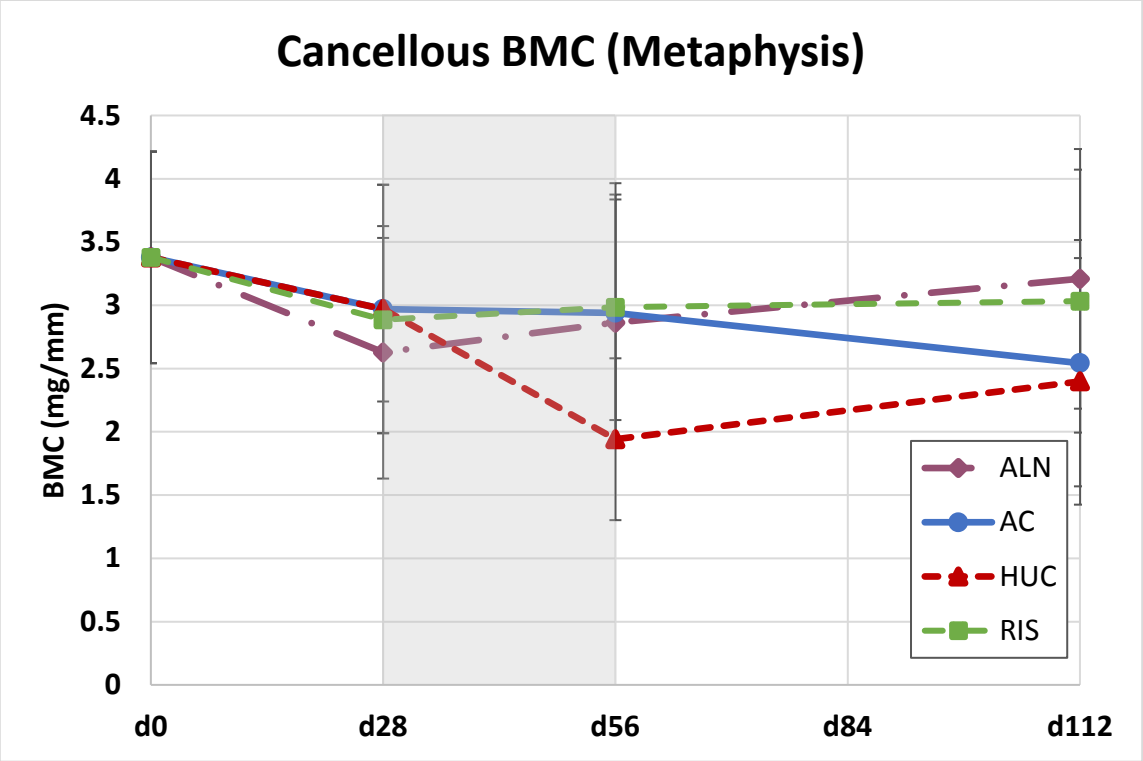

Figure 15. Cancellous Bone Mineral Content for Tibia Metaphysis from Ex Vivo pQCT.
Gray region represents HU. Both drug groups had relatively consistent BMC levels throughout the study with ALN finishing with a higher BMC at day 112. The HUC group was lower than the others at day 56. At the end of recovery there was not much difference between AC and HUC. Values are presented as mean ± SD.

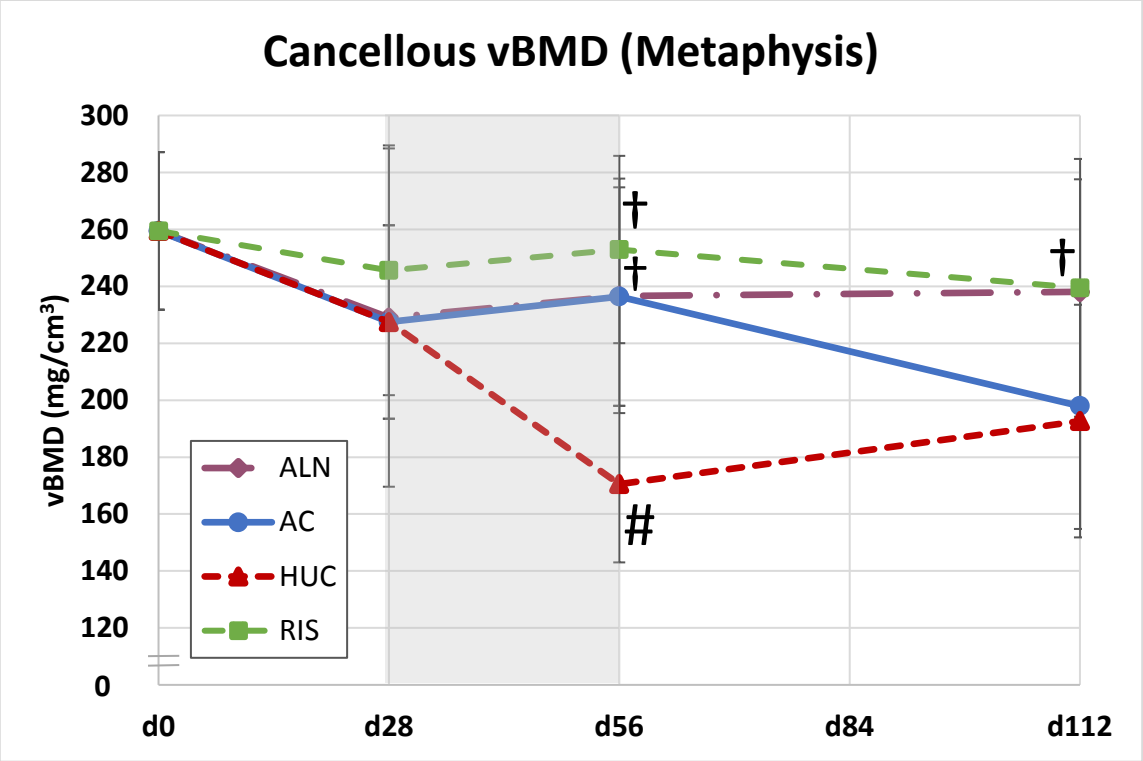

Figure 16. Cancellous Bone Mineral Density for Tibia Metaphysis from Ex Vivo pQCT.
Gray region represents HU. Both drug treatments prevented bone loss compared to HUC at day 56. The values of ALN and RIS were close to that of AC which was shown to be significantly higher from HUC. At day 112, ALN and RIS maintained the same level of BMD, while AC and HUC were at the same level, lower than the drug treatment groups. RIS was the only drug treatment that showed significance at day 112. Values are presented as mean ± SD.

† - Indicates significant difference compared to HUC ($p < 0.05$)
 # - Indicates significant difference compared to AC ($p < 0.05$)

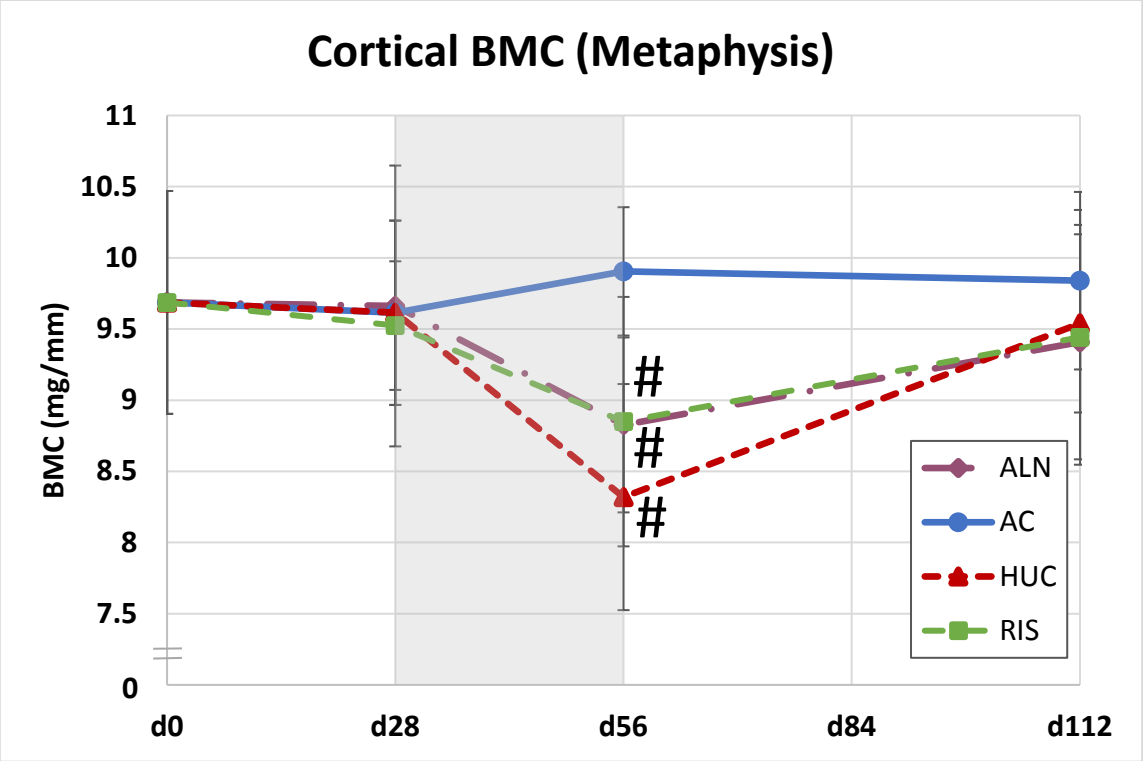

Figure 17. Cortical Bone Mineral Content for Tibia Metaphysis from Ex Vivo pQCT.
Gray region represents HU. All groups that were subjected to HU were significantly lower at day 56. Both drugs had about the same BMC, HUC had the lowest BMC. By day 112, ALN, RIS, and HUC had recovered these losses in BMC as they no longer showed a significant difference. Values are presented as mean ± SD.

 # - Indicates significant difference compared to AC ($p < 0.05$)

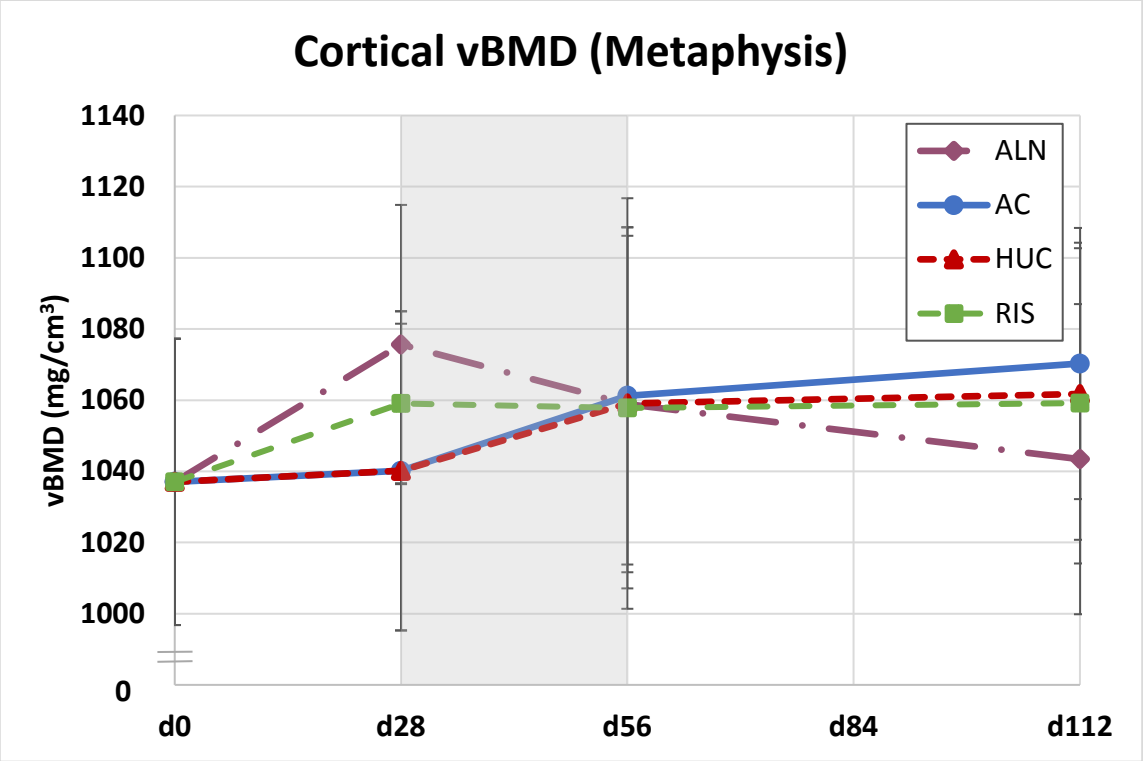

Figure 18. Cortical Bone Mineral Density for Tibia Metaphysis from Ex Vivo pQCT.
Gray region represents HU. There were no significant changes over time in cortical vBMD. The interesting result is that there was very little difference between groups at day 56. This is in spite of the significant losses shown in cortical BMC, Figure 23. Values are presented as mean ± SD.

5.1.1. Proximal Metaphysis Geometric Properties

The geometric properties as measured at the proximal metaphysis are given in Table 3. The reported parameters were area of the total, cortical and cancellous regions as well as the polar area moment of inertia. The total area of bone (Figure 19) was lower for all animals that underwent HU by day 56. HUC had the lowest total area but was not significantly lower than the other groups.

Cortical area (Figure 20) showed a trend that is similar to cortical BMC (Figure 17). The cortical area was measured to be significantly lower than AC for ALN, RIS and HUC at day 56. Cortical area were 9.38 mm^2 for AC, 7.87 mm^2 for HUC, 8.36 mm^2 for ALN, and 8.40 mm^2 for RIS. There is little difference between the drug groups at all time points.

Figure 21, endocortical area, did not show any significant differences in cancellous area over the duration of the study. Similarly, the same lack of significant differences was true for polar moment area of inertia (PAMOI), in Figure 22.

Table 3. Geometric Properties Measured at the Proximal Tibia Metaphysis

Baseline	Total Bone Area (mm^2)		Endocortical Area (mm^2)		Cortical Area (mm^2)		PAMOI (mm^4)	
AC	21.95	(2.8)	12.55	(2.14)	9.40	(0.84)	122.97	(89.38)
End of Pre-treatment (Day 28)								
AC	21.76	(2.3)	12.49	(2.10)	9.27	(0.58)	98.79	(28.79)
ALN	20.18	(3.4)	11.15	(2.38)	9.03	(1.12)	83.76	(27.61)
RIS	20.47	(1.7)	11.46	(1.32)	9.01	(0.48)	82.52	(13.12)
End of Hindlimb Unloading (Day 56)								
AC	21.35	(3.3)	11.97	(2.68)	9.38	(0.68)	95.79	(31.11)
HUC	18.79	(2.5)	10.92	(2.23)	7.87#	(0.6)	72.74	(18.04)
ALN	19.96	(2.6)	11.60	(2.22)	8.36#	(0.63)	80.76	(20.46)
RIS	19.79	(3.1)	11.39	(2.53)	8.40#	(0.88)	80.59	(24.92)
End of Recovery (Day 112)								
AC	21.53	(2.2)	12.30	(1.80)	9.22	(0.64)	95.08	(20.66)
HUC	20.86	(3.0)	11.84	(2.50)	9.02	(0.72)	89.67	(25.29)
ALN	22.06	(2.8)	13.00	(2.25)	9.05	(0.83)	100.04	(27.55)
RIS	20.99	(3.3)	12.03	(2.41)	8.96	(1.00)	91.14	(26.28)

Values presented as Mean and (Standard Deviation)
Note: PAMOI – Polar Moment Area of Inertia
 # - Indicates significant difference compared to AC ($p < 0.05$)

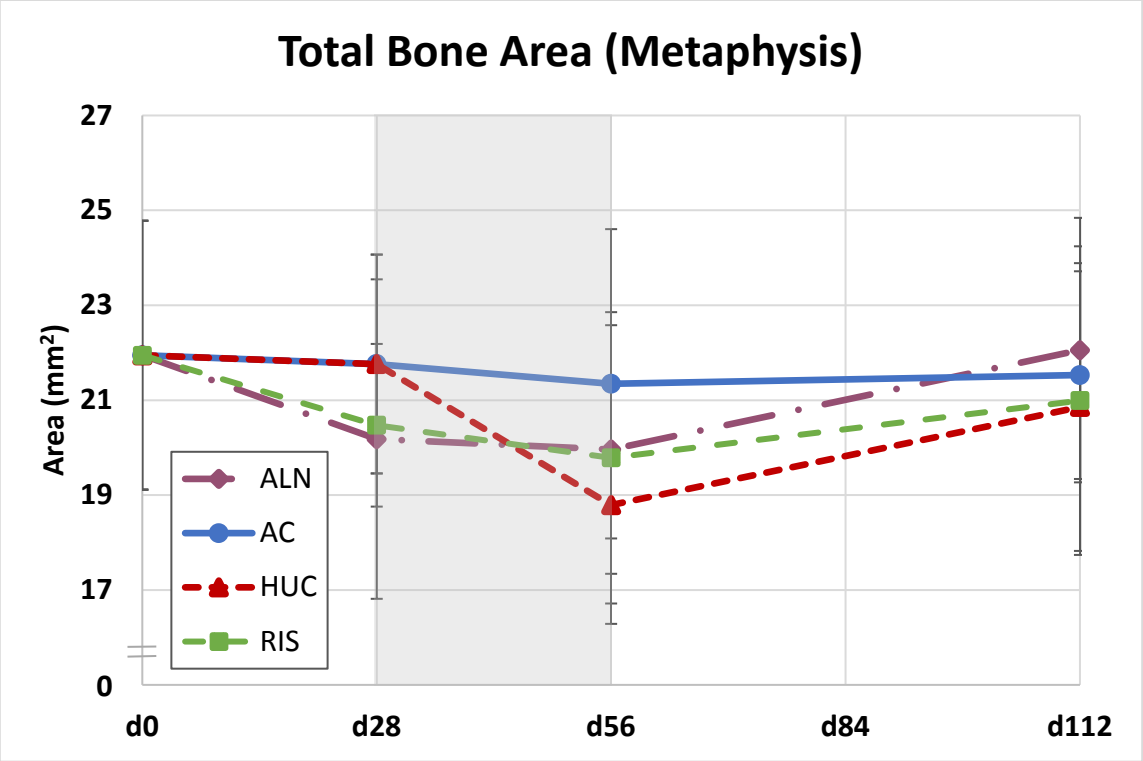

Figure 19. Total Bone Area for Tibia Metaphysis from Ex Vivo pQCT.
Gray region represents HU. There were no significant changes. ALN and RIS had higher areas than HUC at day 56. AC had the highest area at day 56; ALN had the highest area at day 112. Values are presented as mean ± SD.

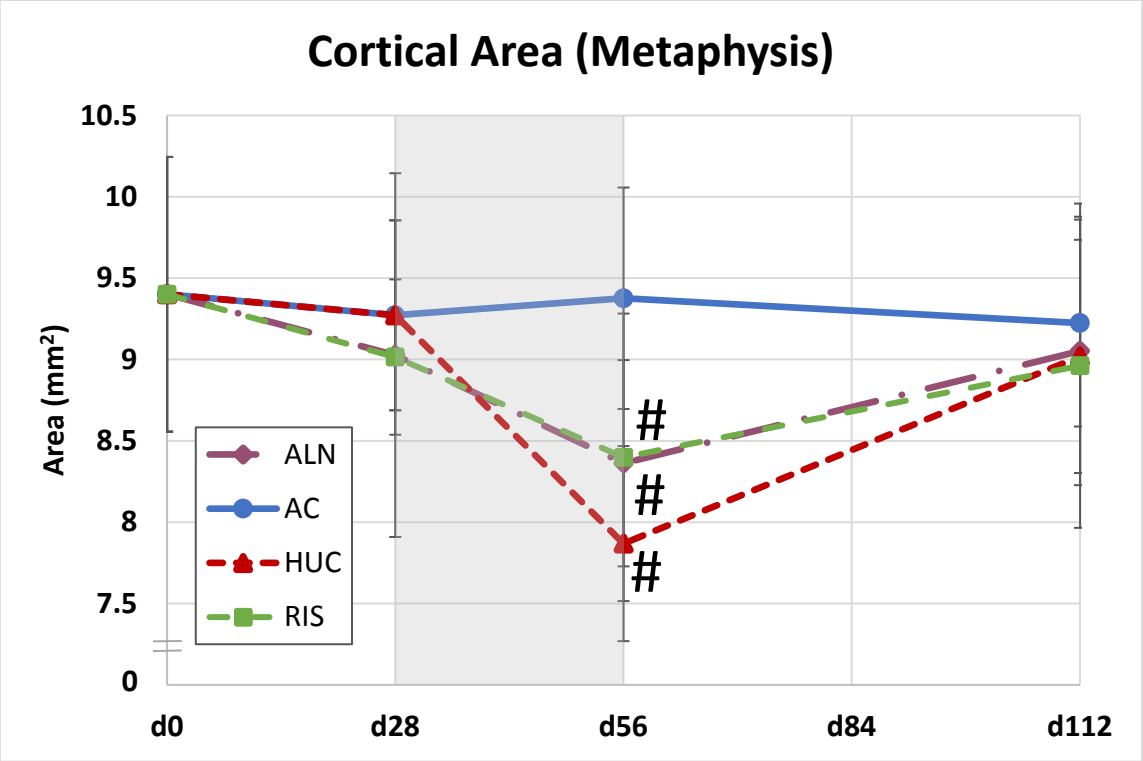

Figure 20. Cortical Bone Area for Tibia Metaphysis from Ex Vivo pQCT. Gray region represents HU. At day 56, HUC, ALN, and RIS all had significantly lower areas than AC. By day 112 there were no remaining significant differences between treatments. The HUC group faired worst at day 56, while ALN and RIS did not show any differences. Values are presented as mean ± SD.

 # - Indicates significant difference compared to AC ($p < 0.05$)

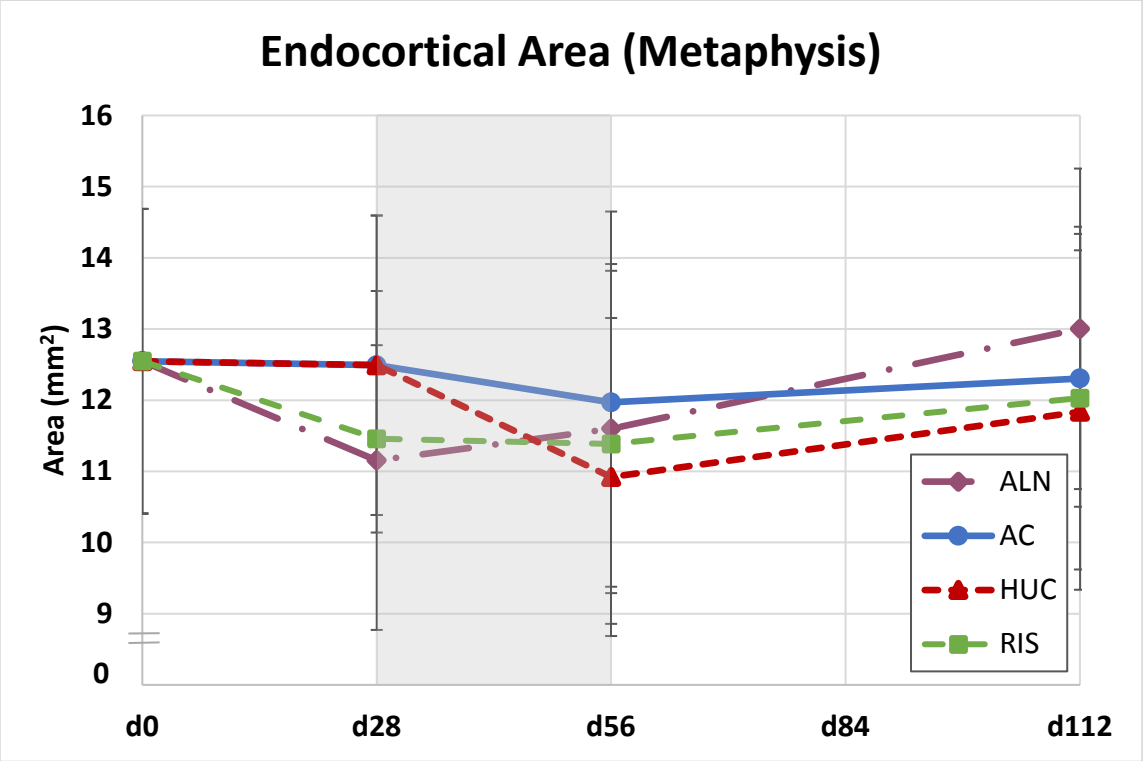

Figure 21. Endocortical Area for Tibia Metaphysis from Ex Vivo pQCT. Gray region represents HU. This area changed little when looking at each time point. There were no significant differences between groups. Values are presented as mean ± SD.

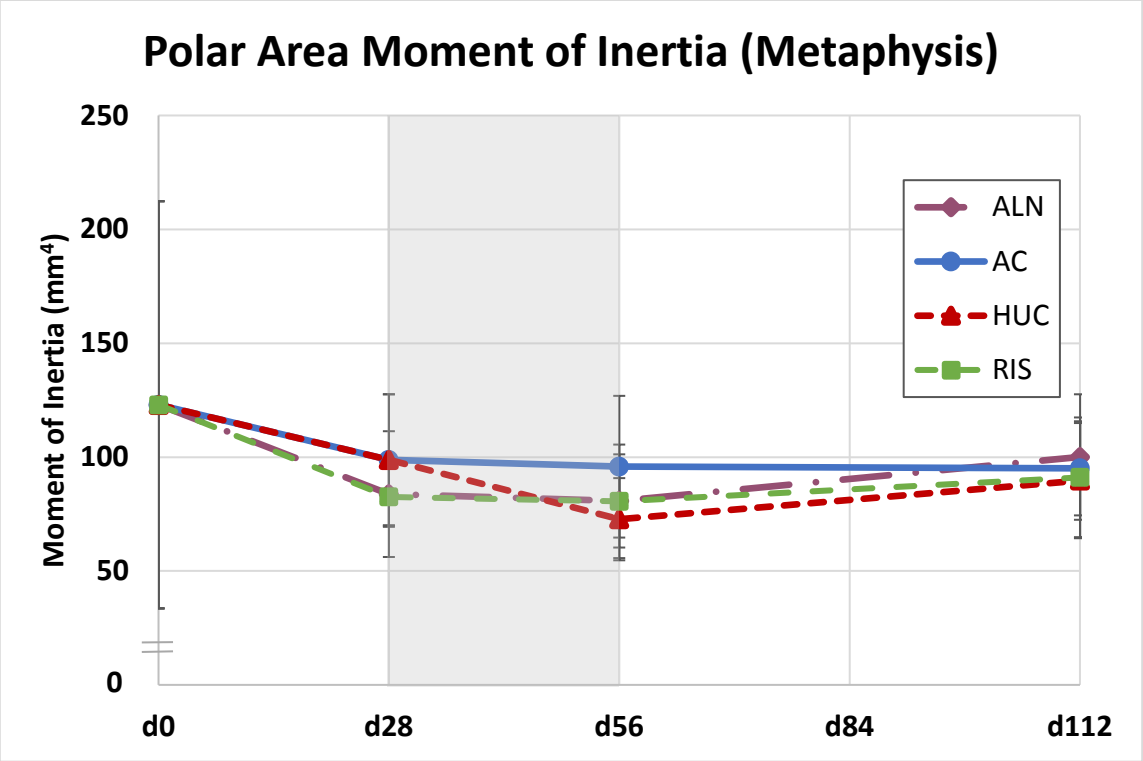

Figure 22. Polar Area Moment of Inertia for Tibia Metaphysis from Ex Vivo pQCT.
Gray region represents HU. PAMOI remained roughly constant between groups. The HUC group was lowest at day 56. Both drugs had around the same values for all time points. Values are presented as mean ± SD.

5.1.2. Mid-Diaphysis Densitometric Properties

At the mid-diaphysis of the tibia, no differences were found to be significant at all time points for both cortical BMC and cortical vBMD. The numerical results for both measures are shown in Table 4. Cortical BMC is plotted in Figure 23 and cortical vBMD is plotted in Figure 24. Cancellous measures of densitometry are not considered at this location because this is not a region where cancellous bone can be measured. Cancellous bone is not part of the structure at the mid diaphysis. There was a slight trend of increasing values over time, but again, there were no significant differences.

5.1.3. Mid-Diaphysis Geometric Properties

Geometric data from the pQCT scans at the mid-diaphysis included endocortical and cortical area, and polar area moment of inertia. Endocortical area is included because it indicates how the cavity at the interior of the mid-diaphysis changed during the study. The full geometric results are show in Table 5. Figure 25 – Figure 27 report the measured values of area for each of the time points. No statistical differences were found for any of the mid-diaphysis geometric properties.

Table 4. Densitometric Properties of the Tibia Mid-Diaphysis.

Baseline	Cortical BMC (mg)		Cortical vBMD (mg/cm^3)	
AC	8.26	(0.51)	1376.8	(9.18)
End of Pre-treatment (Day 28)				
AC	8.41	(0.43)	1382.1	(9.52)
ALN	8.59	(0.58)	1386.1	(15.7)
RIS	8.62	(0.55)	1384.3	(11.2)
End of Hindlimb Unloading (Day 56)				
AC	8.55	(0.73)	1398.9	(13.5)
HUC	8.39	(0.47)	1393.9	(16.2)
ALN	8.59	(0.71)	1389.9	(25.4)
RIS	8.79	(0.36)	1377.4	(31.2)
End of Recovery (Day 112)				
AC	9.04	(0.43)	1406.8	(12.8)
HUC	9.01	(0.64)	1394.1	(29.3)
ALN	9.01	(0.65)	1401.9	(9.53)
RIS	9.17	(0.59)	1401.3	(9.85)

Values presented as Mean (Standard Deviation)

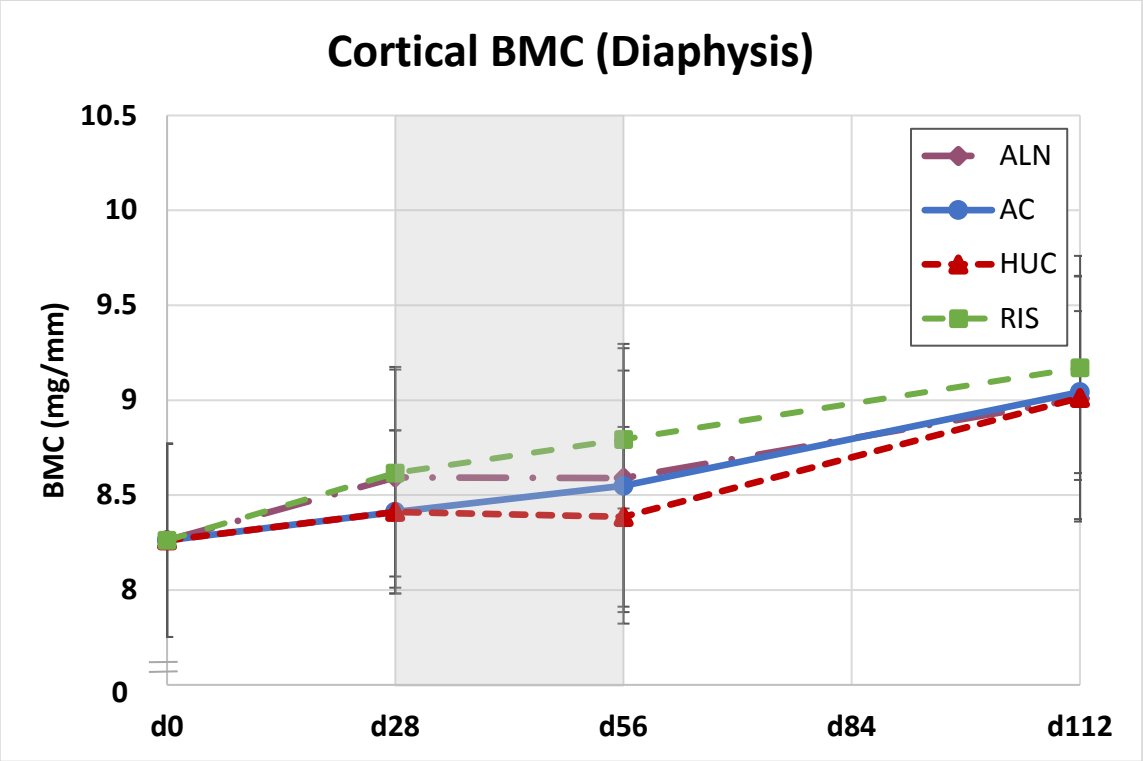

Figure 23. Cortical Bone Mineral Content for Tibia Diaphysis from Ex Vivo pQCT. Gray region represents HU. There were no significant differences at any time point. The data shows a general trend of increasing cortical BMC over time. Values are presented as mean ± SD.

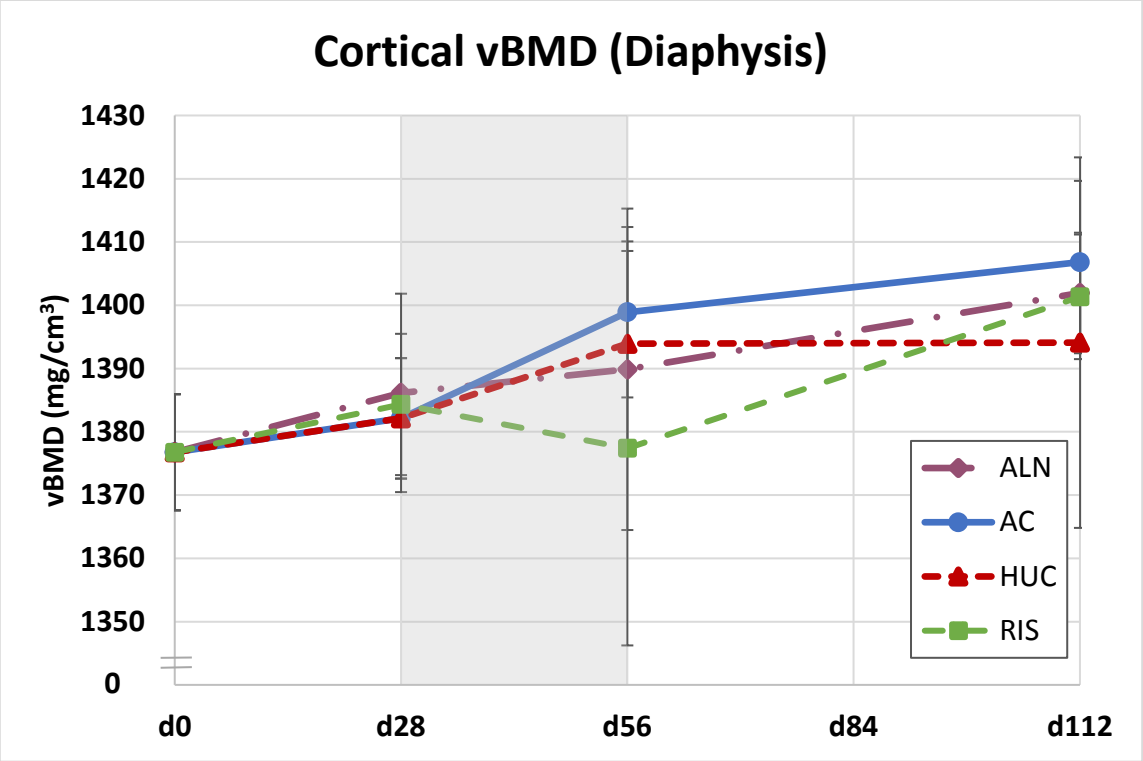

Figure 24. Cortical Bone Mineral Density for Tibia Diaphysis from Ex Vivo pQCT. Gray region represents HU. There were no significant differences. There is an increasing trend in cortical vBMD over time. Values are presented as mean ± SD.

Table 5. Geometric Properties of the Tibia Mid-Diaphysis

Baseline	Endocortical Area (mm^2)		Cortical Area (mm^2)		PAMOI (mm^4)	
AC	2.66	(0.34)	6.00	(0.37)	11.33	(1.47)
End of Pre-treatment (Day 28)						
AC	2.46	(0.23)	6.09	(0.31)	11.27	(1.16)
ALN	2.49	(0.38)	6.20	(0.42)	11.70	(1.8)
RIS	2.43	(0.29)	6.23	(0.42)	11.68	(1.69)
End of Hindlimb Unloading (Day 56)						
AC	2.56	(0.45)	6.11	(0.54)	11.65	(2.36)
HUC	2.35	(0.45)	6.01	(0.33)	10.85	(1.55)
ALN	2.35	(0.48)	6.18	(0.47)	11.53	(1.9)
RIS	2.40	(0.41)	6.39	(0.37)	12.40	(2.03)
End of Recovery (Day 112)						
AC	2.68	(0.26)	6.43	(0.30)	12.83	(0.93)
HUC	2.51	(0.50)	6.47	(0.46)	12.81	(2.26)
ALN	2.63	(0.32)	6.43	(0.45)	12.66	(1.79)
RIS	2.63	(0.36)	6.54	(0.41)	13.05	(1.75)

Values presented as Mean and (Standard Deviation)
Note: PAMOI – Polar Moment Area of Inertia

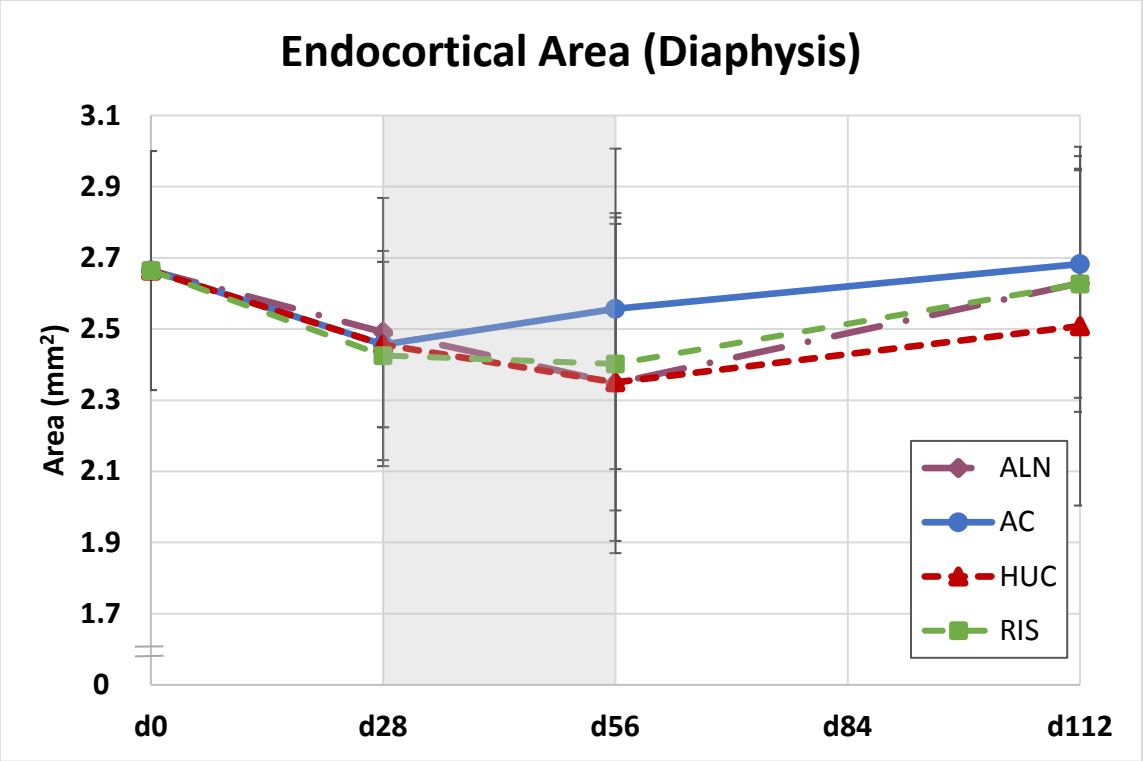

Figure 25. Endocortical Area for Tibia Diaphysis from Ex Vivo pQCT.
Gray region represents HU. There is no significance here. Values are presented as mean ± SD.

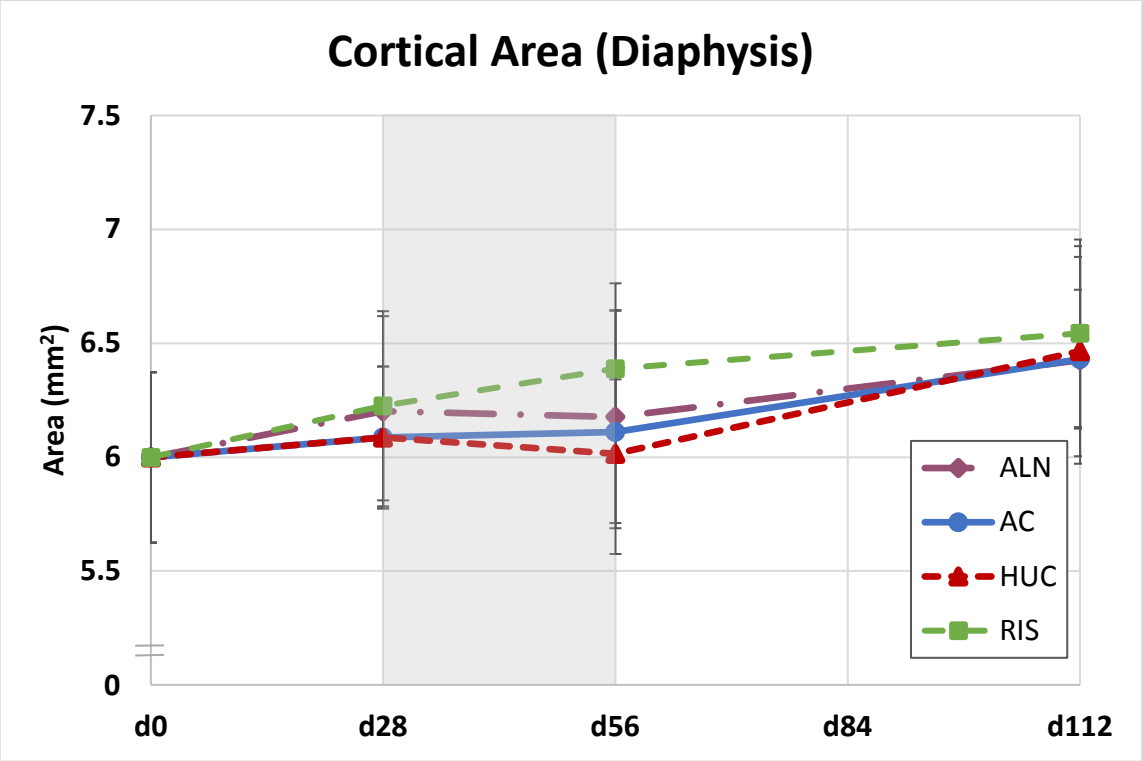

Figure 26. Cortical Bone Area for Tibia Diaphysis from Ex Vivo pQCT.
Gray region represents HU. The cortical area had no significant differences at any time point. Values are presented as mean ± SD.

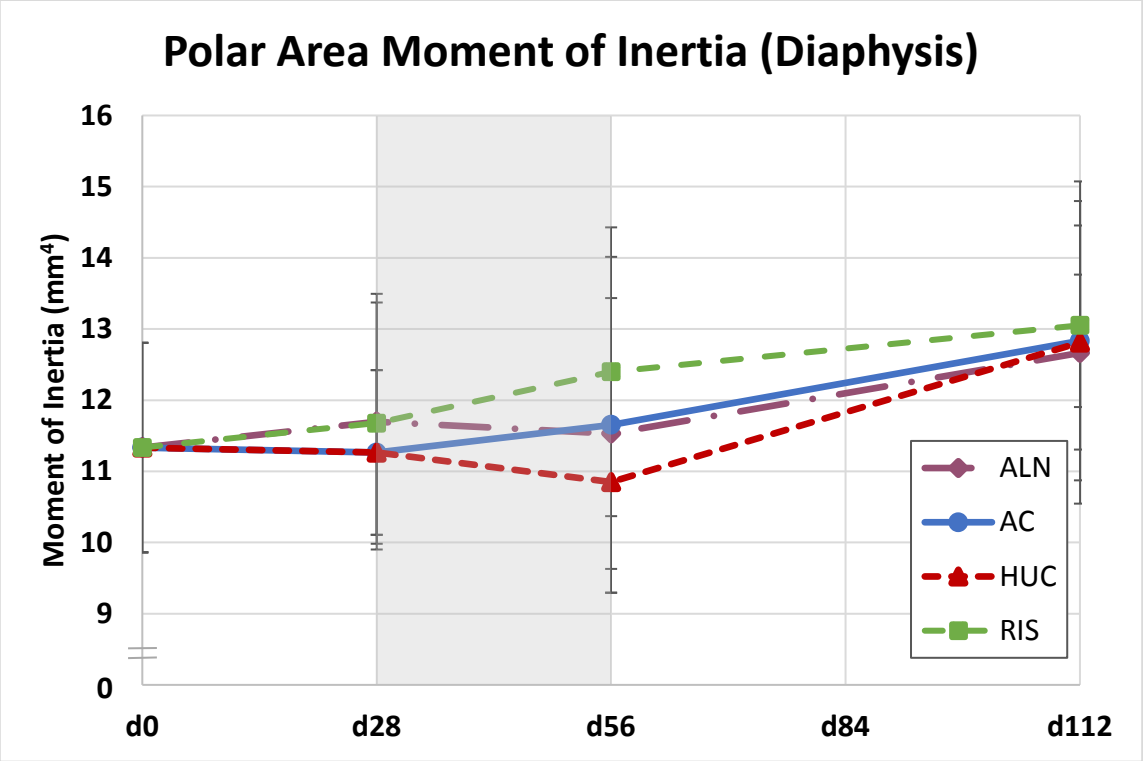

Figure 27. Polar Area Moment of Inertia for Tibia Diaphysis from Ex Vivo pQCT. Gray region represents HU. The PAMOI is the highest for RIS at every time point. HUC has the lowest value at the end of HU. There were no significant differences at any time point. Values are presented as mean ± SD.

5.1.4. Strength Indices

There were only two strength indices from the pQCT data that corresponded with the mechanical results and they are shown in Table 6. The first was bone strength index (BSI), shown in Figure 28, which corresponds to an estimation of compressive stiffness. This value was only considered at the metaphysis as it was the region that was mechanical tested under compression with the reduced platen compression test. At the end of HU, BSI was the lowest for HUC (5.66 mg^2/mm^4). This was much lower than the value of HUC at the beginning of HU (7.31 mg^2/mm^4). The BSI for HUC at the end of HU was significantly lower than AC. Both RIS and ALN had a significantly higher BSI than HUC at the same time point. RIS had a BSI of 7.13 mg^2/mm^4. ALN had a BSI of 6.88 mg^2/mm^4.This combination of statistical significances suggest that both bisphosphonate pre-treatments were able to mitigate the effects of HU. There were no significant differences between groups at day 112.

The second strength index, stress-strain index (SSI), corresponds to an estimated bending strength (Figure 29). This measure was only considered at the mid-diaphysis as it was the only location that was subjected to a bending test, the 3-point bending test. There was no significance in SSI at any time point.

Table 6. Strength Indices from Tibia pQCT Data.

	BSI		SSI	
Baseline	**(mg^2/mm^4)**		**(mm^3)**	
AC	7.80	(0.5)	6.25	(0.61)
End of Pre-treatment (Day 28)				
AC	7.31	(0.6)	6.14	(0.52)
ALN	7.53	(1.0)	6.34	(0.70)
RIS	7.54	(0.7)	6.32	(0.75)
End of Hindlimb Unloading (Day 56)				
AC	7.78	(0.6)	6.29	(0.93)
HUC	5.66#	(0.7)	6.02	(0.65)
ALN	6.88†	(0.7)	6.22	(0.85)
RIS	7.13†	(0.8)	6.45	(0.66)
End of Recovery (Day 112)				
AC	7.14	(0.8)	6.74	(0.38)
HUC	6.88	(0.8)	6.75	(0.93)
ALN	7.26	(0.9)	6.75	(0.74)
RIS	7.44	(0.9)	6.90	(0.74)

Values presented as Mean and (Standard Deviation)
† - Indicates significant difference compared to HUC ($p < 0.05$)
 # - Indicates significant difference compared to AC ($p < 0.05$)

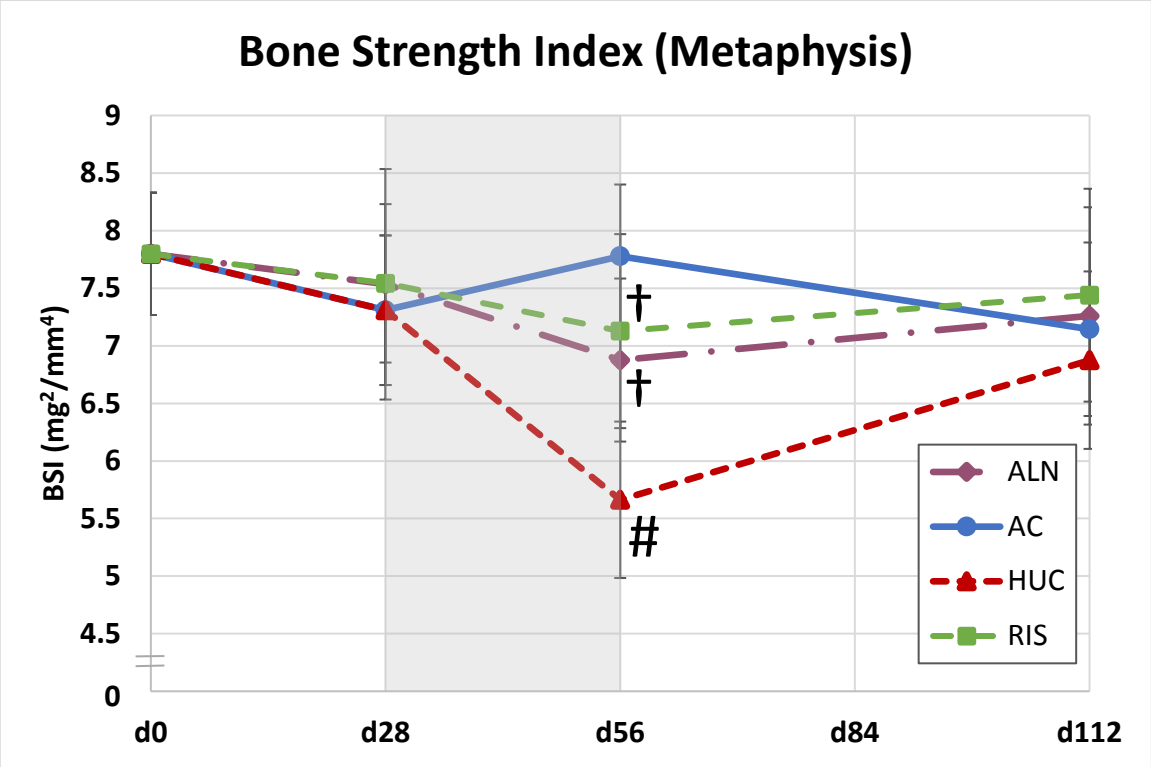

Figure 28. Bone Strength Index for Tibia Metaphysis from Ex Vivo pQCT. Gray region represents HU. Day 56 shows a drastic decline in BSI for HUC. ALN and RIS have a slight decline that returns to the pre-HU value by the end of recovery. AC shows a decrease from day 56 to day 112. HUC does not fully recover BSI. Values are presented as mean ± SD.

† - Indicates significant difference compared to HUC ($p < 0.05$)
 # - Indicates significant difference compared to AC ($p < 0.05$)

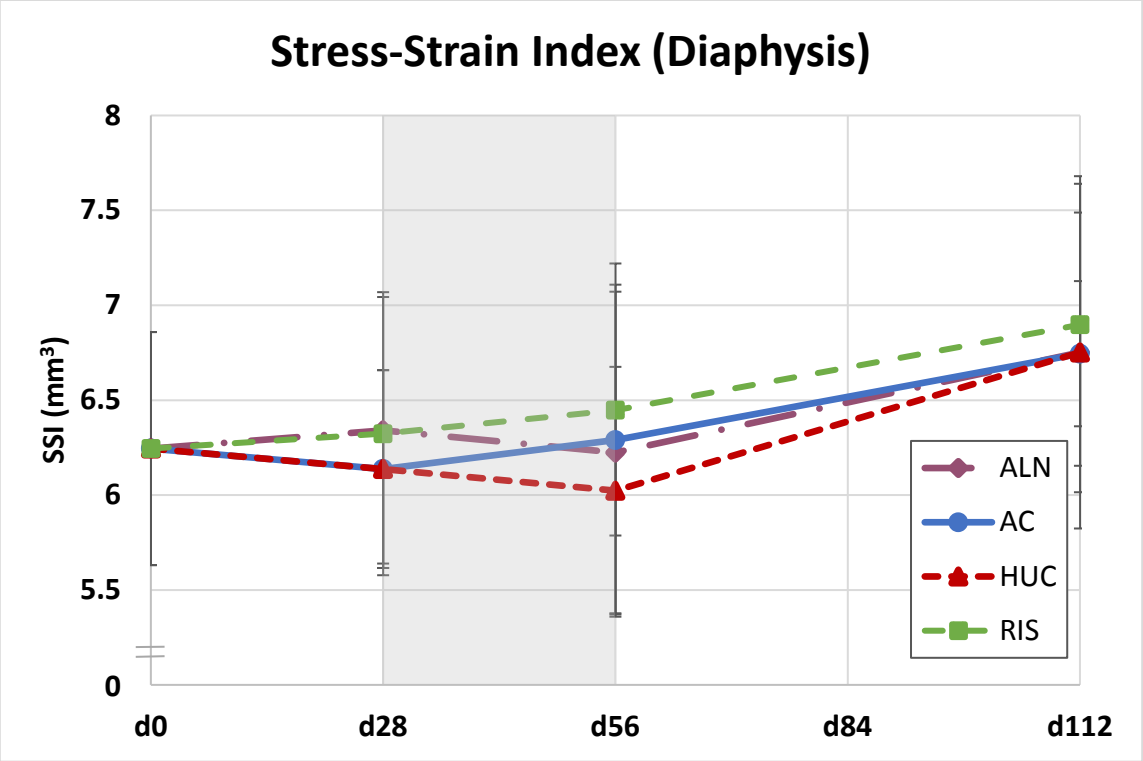

Figure 29. Stress-Strain Index for Tibia Diaphysis from Ex Vivo pQCT.
Gray region represents HU. HUC has the lowest SSI for every time point. The SSI for RIS is the highest at each time point. There were no significant differences. Values are presented as mean ± SD.

5.2. Ex Vivo 3-Point Bend Test of the Left Tibia

Each tibia was subjected to a 3-point bending test. The applied load was located roughly at the middle of the bone and meant to correspond with the pQCT scans taken at the mid-diaphysis. Two sets of measurements were taken from this mechanical testing data. Extrinsic properties were measured directly from the force and displacement outputs and represent the mechanical behavior of the tibia at the structural level. Intrinsic properties were measured using equations from beam theory (Equation 4 – Equation 6) and the measured force and displacement data. The intrinsic properties are estimates of the material behavior of the bone.

5.2.1. Extrinsic Mechanical Properties from 3-Point Bending

The extrinsic mechanical properties were derived directly from the load-displacement from the 3-point bend test and it included maximum force, stiffness, post-yield displacement, and energy to fracture. The values for these measurements are given in Table 7. Each of these output variables can be found in Figure 30 – Figure 34. There were no statistical differences were not found between groups at each time point.

5.2.2. Intrinsic Mechanical Properties from 3-Point Bending

The intrinsic mechanical properties were calculated at all time points for all of the collected 3-point bending data were ultimate stress, elastic modulus, and pre-yield toughness and they are shown in Table 8. The intrinsic mechanical properties mirrored the results from the extrinsic mechanical properties. Each of the intrinsic mechanical properties are plotted in Figure 35 – Figure 37. There were no significant differences found between groups at any time point for these measurements.

Table 7. Extrinsic Mechanical Properties from Tibia 3-Point Bending.

Baseline	Maximum Force (N)		Stiffness (N/mm)		Energy to Fracture (mJ)		Displacement at Fracture (mm)		Post-Yield Displacement (mm)	
AC	120.8	(16.6)	327.4	(51.8)	59.0	(36.4)	0.71	(0.37)	0.39	(0.35)
End of Pre-treatment (Day 28)										
ALN	113.8	(20.0)	364.3	(31.4)	47.6	(31.0)	0.58	(0.27)	0.34	(0.26)
AC	119.0	(19.6)	363.5	(25.6)	54.8	(41.4)	0.62	(0.34)	0.37	(0.33)
RIS	129.2	(6.93)	373.0	(30.7)	63.7	(32.0)	0.71	(0.30)	0.44	(0.30)
End of Hindlimb Unloading (Day 56)										
AC	125.1	(21.1)	362.9	(64.6)	46.1	(23.7)	0.56	(0.20)	0.31	(0.21)
HUC	135.8	(11.3)	385.0	(48.5)	64.1	(17.3)	0.69	(0.16)	0.41	(0.18)
ALN	132.6	(19.6)	348.7	(69.4)	66.2	(22.2)	0.74	(0.21)	0.47	(0.22)
RIS	135.5	(15.0)	396.6	(50.0)	61.9	(28.4)	0.66	(0.26)	0.38	(0.25)
End of Recovery (Day 112)										
AC	121.8	(25.7)	413.6	(23.2)	43.0	(31.7)	0.49	(0.25)	0.25	(0.24)
HUC	119.3	(22.8)	408.3	(33.6)	32.8	(19.7)	0.41	(0.14)	0.17	(0.13)
ALN	113.4	(32.5)	401.4	(42.2)	38.4	(38.6)	0.45	(0.29)	0.22	(0.26)
RIS	134.5	(21.5)	407.3	(43.2)	58.8	(40.4)	0.62	(0.31)	0.36	(0.30)

Values presented as Mean and (Standard Deviation)

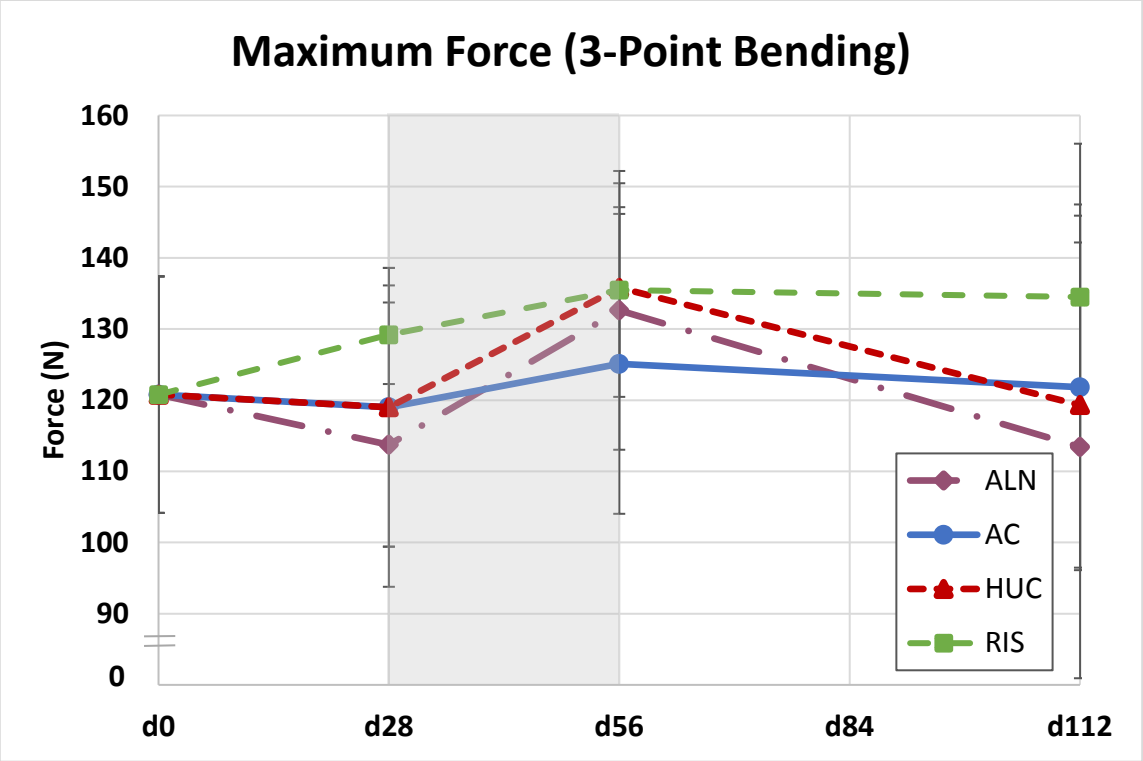

Figure 30. Maximum Force for Tibia in 3-Point Bend Test.
Gray region represents HU. Max force of all groups peaks at day 56. RIS has the highest value at day 56. AC has the lowest value at day 56. ALN has the lowest max force at d112. There were no significant differences. Values are presented as mean ± SD.

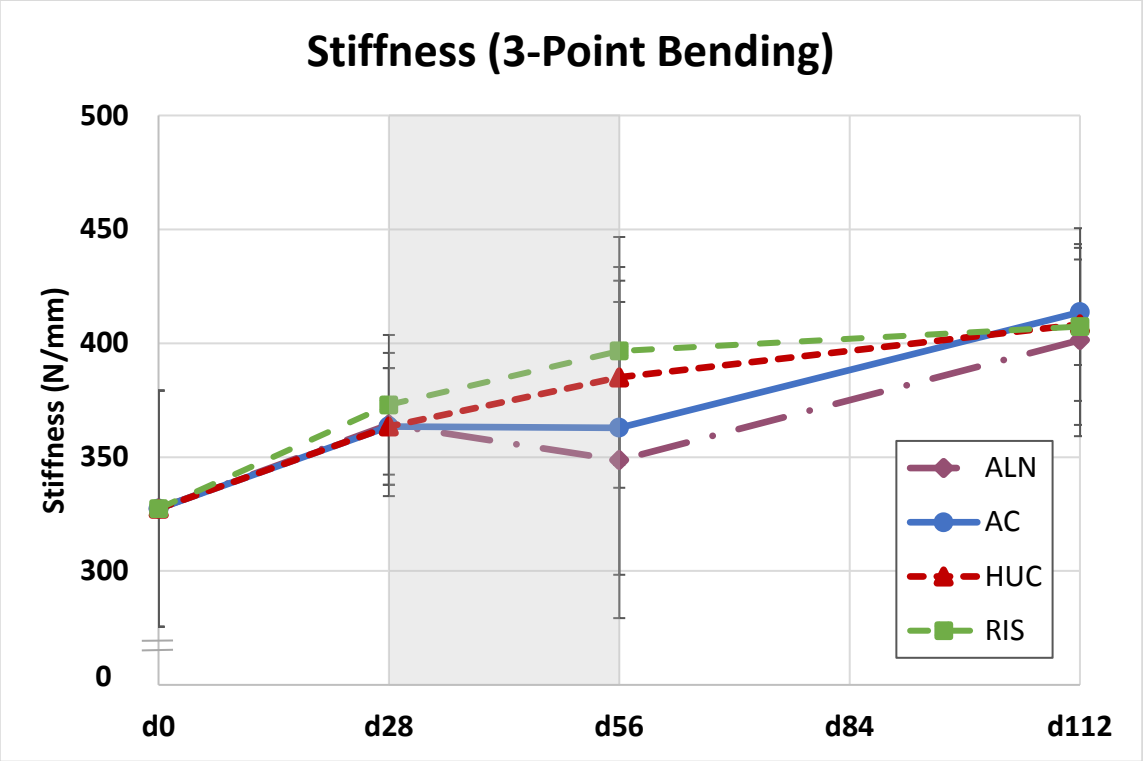

Figure 31. Stiffness for Tibia in 3-Point Bend Test.
Gray region represents HU. There were no significant differences. Values are presented as mean ± SD.

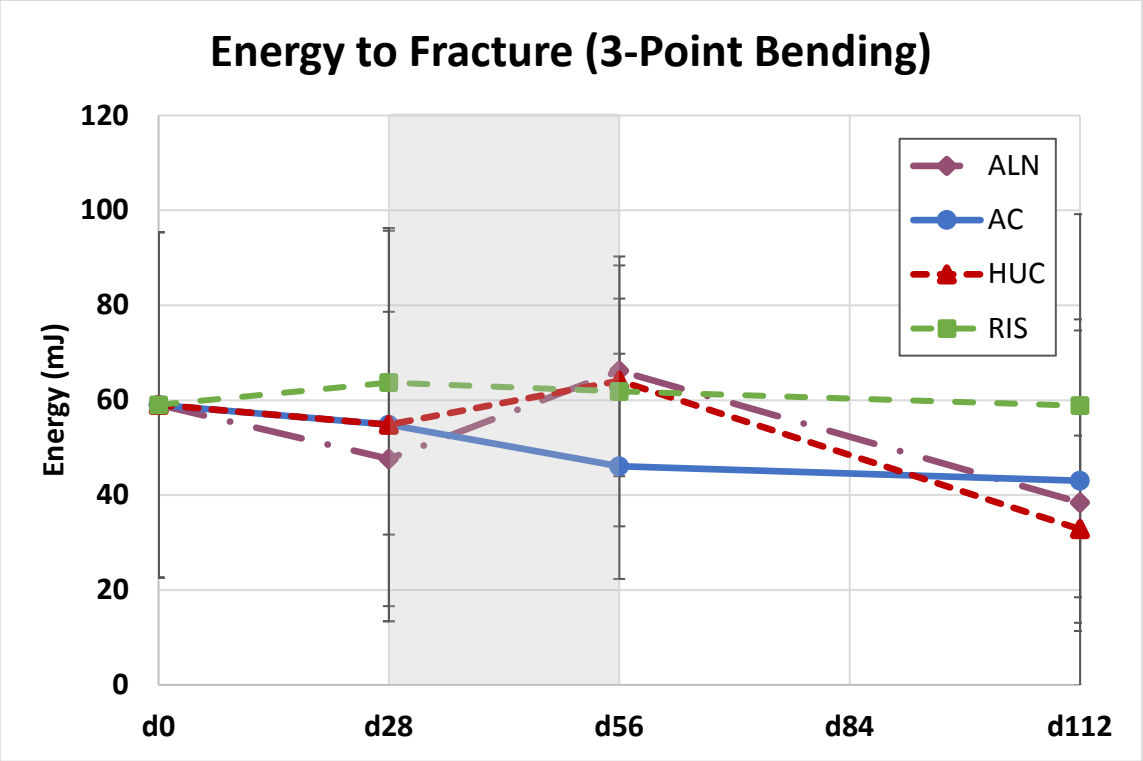

Figure 32. Energy to Fracture for Tibia in 3-Point Bend Test.
Gray region represents HU. RIS has the highest energy at day 28 and day 112. ALN has the highest value at day 56. There were no significant differences. Values are presented as mean ± SD.

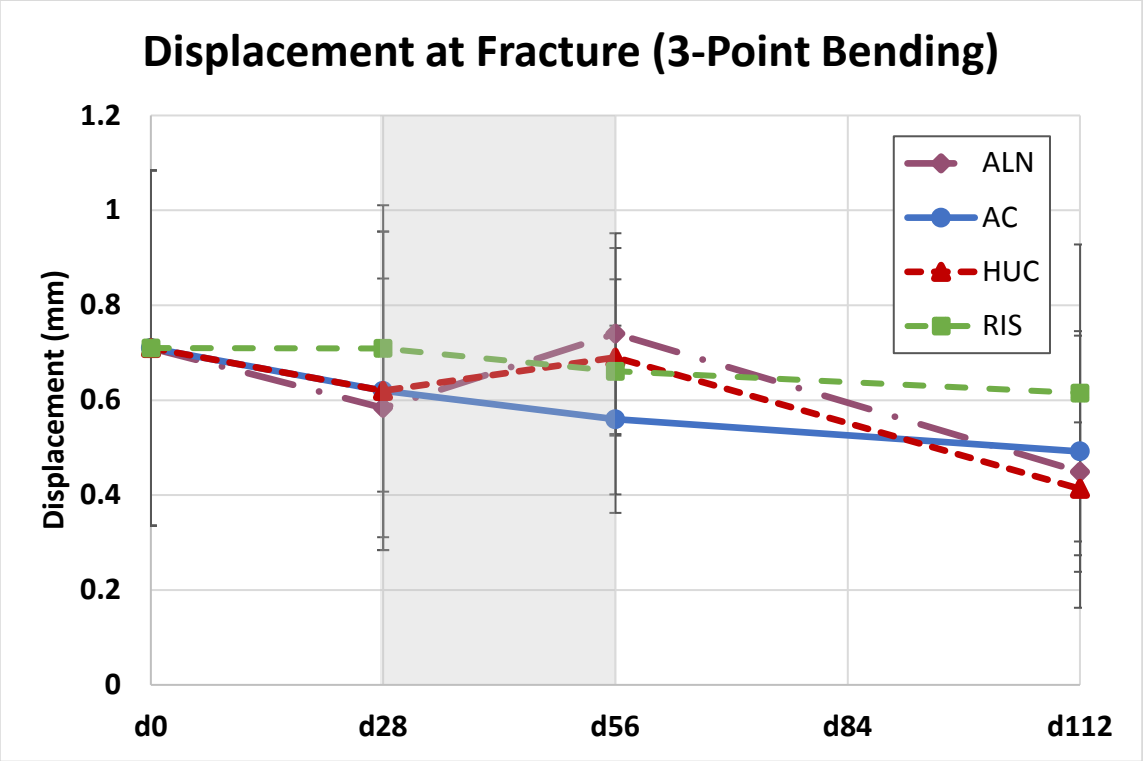

Figure 33. Displacement at Fracture for Tibia in 3-Point Bend Test.
Gray region represents HU. No significant differences. Values are presented as mean ± SD.

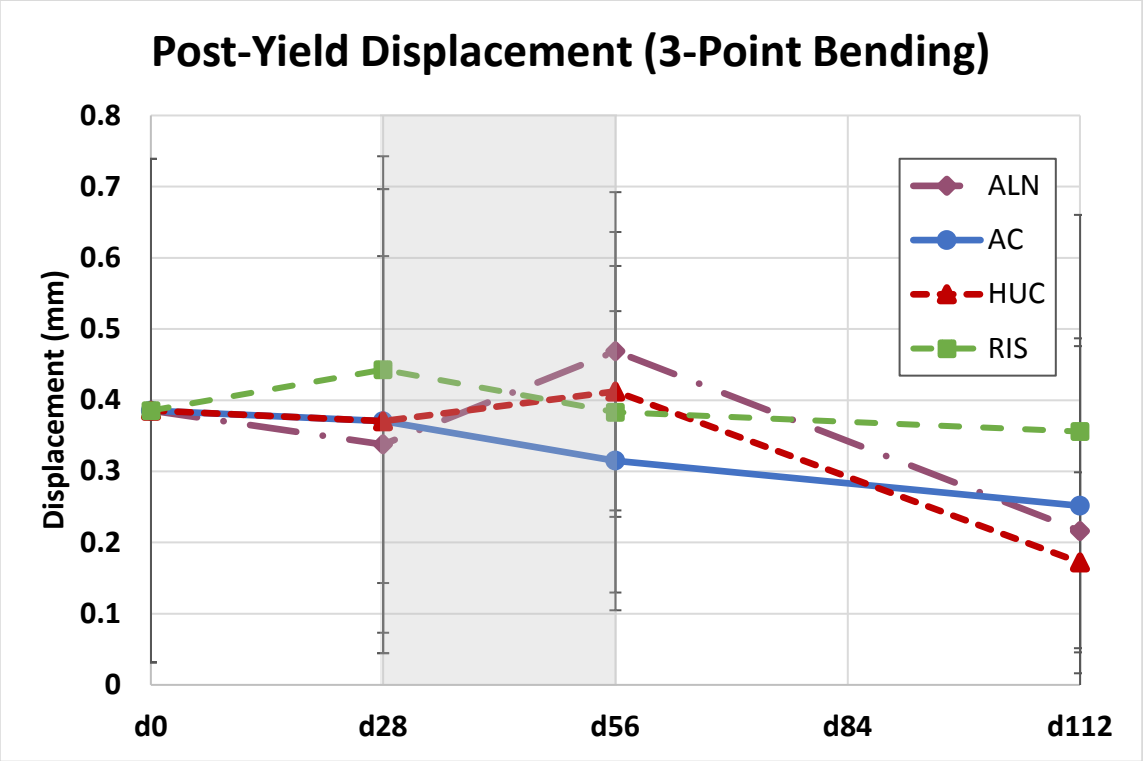

Figure 34. Post-Yield Displacement for Tibia in 3-Point Bend Test.
Gray region represents HU. RIS has the highest displacement at day 28 and day 112. ALN has the highest displacement at day 56. HUC has the lowest displacement at day 112 and AC has the lowest at day 56. Values are presented as mean ± SD.

Table 8. Intrinsic Mechanical Properties from Tibia 3-Point Bending.

Baseline	Ultimate Stress (MPa)		Modulus (MPa)		Pre-Yield Toughness (mJ/mm^3)	
AC	184.1	(30.6)	7.11	(1.28)	2.32	(1.76)
End of Pre-treatment (Day 28)						
AC	179.1	(25.9)	7.88	(0.57)	1.42	(0.24)
ALN	173.5	(34.6)	7.69	(1.01)	1.49	(0.38)
RIS	192.6	(17.7)	7.85	(0.77)	1.72	(0.57)
End of Hindlimb Unloading (Day 56)						
AC	194.0	(24.3)	7.72	(1.60)	1.52	(0.40)
HUC	215.8	(21.4)	8.66	(0.57)	1.99	(0.43)
ALN	204.6	(28.9)	7.37	(1.24)	1.80	(0.72)
RIS	198.1	(27.9)	7.92	(1.32)	2.06	(0.91)
End of Recovery (Day 112)						
AC	170.4	(36.2)	7.85	(0.47)	1.50	(0.47)
HUC	168.7	(33.9)	7.84	(0.91)	1.56	(0.68)
ALN	159.2	(49.3)	7.77	(0.72)	1.37	(0.55)
RIS	187.3	(30.1)	7.68	(0.73)	1.72	(0.43)

Values presented as Mean and (Standard Deviation)

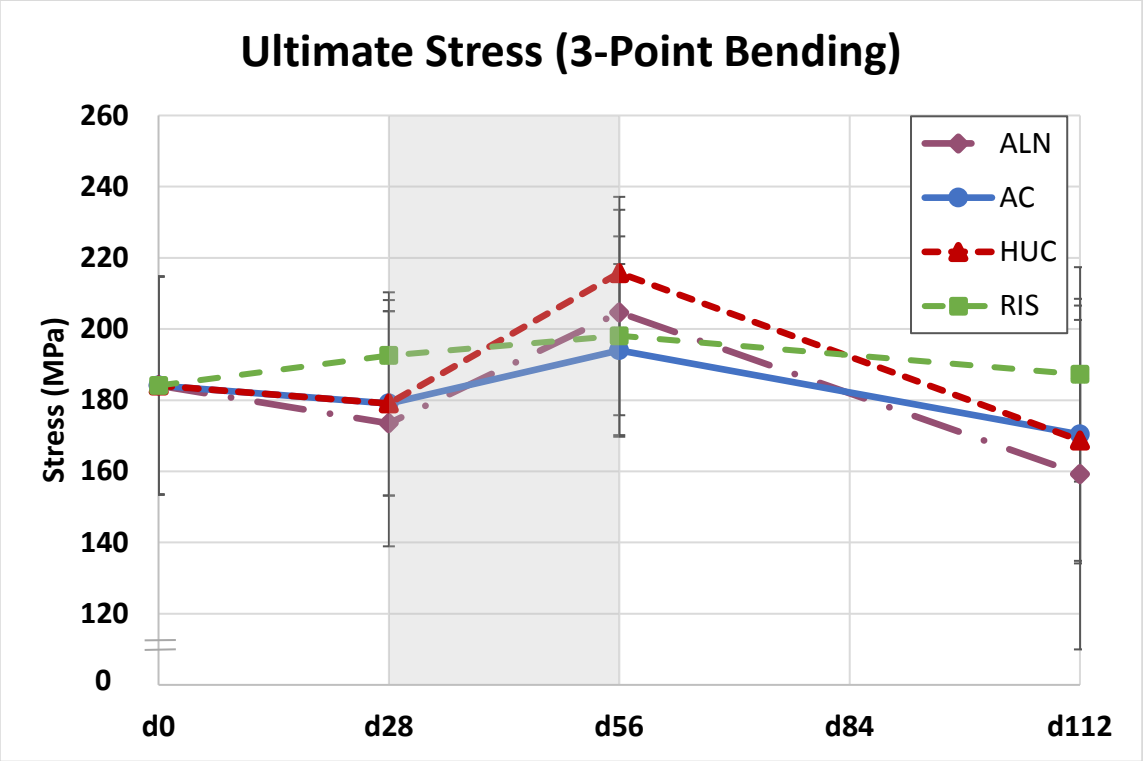

Figure 35. Ultimate Stress for Tibia in 3-Point Bend Test.
Gray region represents HU. RIS has the highest stress at day 28 and day 112. HUC and ALN are higher than RIS at day 56 and ALN has the lowest value at day 112. Values are presented as mean ± SD.

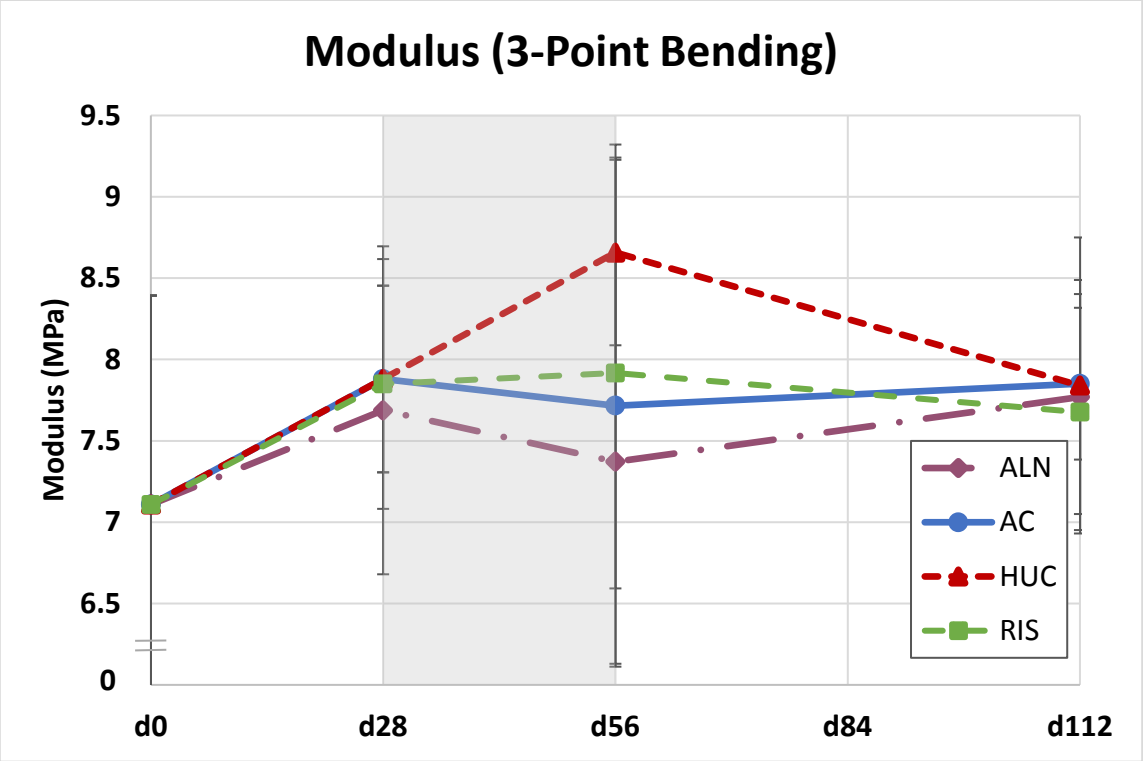

Figure 36. Modulus for Tibia in 3-Point Bend Test.
Gray region represents HU. The most prominent feature to this plot is that HUC has a larger modulus that the other groups at day 56. At day 28 and day 112, there are no large differences between groups. Values are presented as mean ± SD.

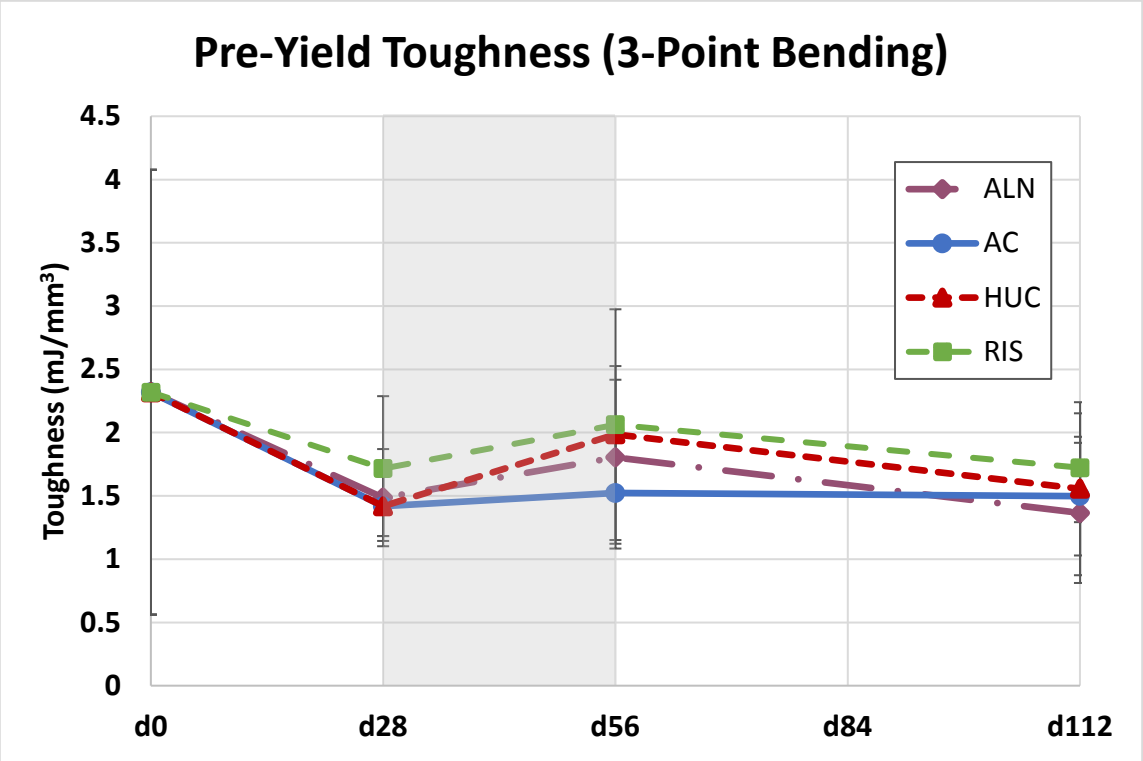

Figure 37. Pre-Yield Toughness for Tibia in 3-Point Bend Test.
Gray region represents HU. RIS has the highest pre-yield toughness throughout the study. ALN has the lowest values at day 112 and AC has the lowest toughness at day 56. HUC outperforms ALN at all time points. Values are presented as mean ± SD.

5.3. Ex Vivo Reduced Platen Compression Test of the Left Tibia

The reduced platen compression test was completed using machined specimens and platens sized to 70% of the largest circle that could be inscribed into the endocortical perimeter. For each time point there were at least 5 AC animals, 8 HUC animals, 12 ALN animals, and 8 RIS animals. For this test, intrinsic properties were calculated using platen area according to the equations described in Section 4.5.3.

5.3.1. Extrinsic Mechanical Properties from RPC Test

The extrinsic properties reported from this test were maximum force and stiffness; the values for each of these are in Table 9. Maximum force (Figure 38) at day 56 for ALN (4.0 N) and RIS (5.6 N) were both significantly higher than HUC (1.6 N). HUC was significantly lower than AC (6.0 N). Additionally, RIS was significantly higher than ALN, and ALN was significantly lower than AC.

Stiffness, as shown in Figure 39, did not differ much between groups except for day 56. At the end of HU, RIS, had a stiffness of 57.6 N/mm, and was significantly higher than both ALN (stiffness of 33.7 N/mm) and HUC (stiffness of 17.8 N/mm). HUC was also significantly lower than the stiffness of AC, 60.4 N/mm.

Table 9. Extrinsic Mechanical Properties from Tibia RPC.

	Max Force (N)		Stiffness (N/mm)	
Baseline				
AC	8.15	(7.97)	60.2	(71.9)
End of Pre-treatment (Day 28)				
AC	4.21	(2.64)	33.6	(20.6)
ALN	4.68	(4.06)	42.3	(37.4)
RIS	5.11	(3.47)	40.6	(31.0)
End of Hindlimb Unloading (Day 56)				
AC	5.98	(3.40)	60.4	(35.5)
HUC	1.76$^{\#}$	(1.25)	17.8$^{\#}$	(14.5)
ALN	4.01$^{\dagger\#}$	(4.28)	33.7	(31.0)
RIS	5.60$^{\dagger *}$	(2.32)	57.6$^{\dagger *}$	(28.4)
End of Recovery (Day 112)				
AC	2.28	(1.38)	20.4	(13.8)
HUC	2.42	(2.87)	19.4	(16.2)
ALN	3.72	(2.77)	36.8	(40.6)
RIS	2.38	(1.41)	27.1	(14.0)

Values presented as Mean and (Standard Deviation)
† - Indicates significant difference compared to HUC ($p < 0.05$)
 # - Indicates significant difference compared to AC ($p < 0.05$)
*** - Indicates significant difference compared to ALN ($p < 0.05$)**

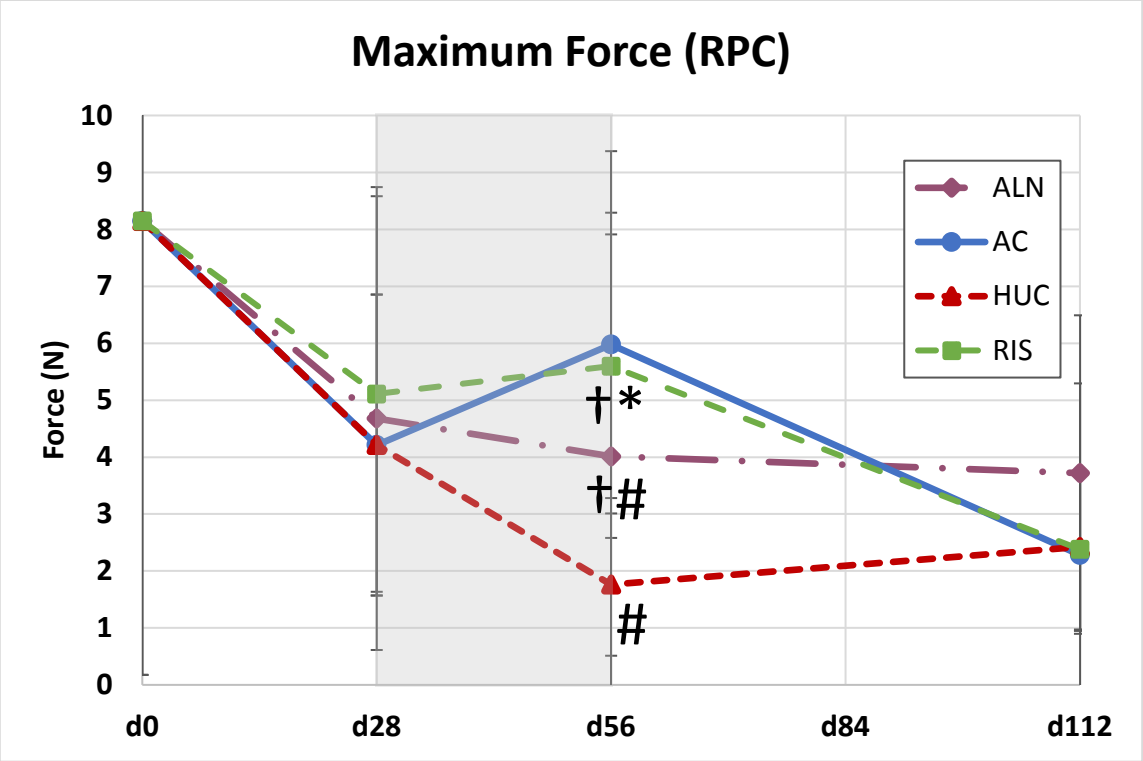

Figure 38. Maximum Force for Tibia Metaphysis in RPC Test.
Gray region represents HU. The maximum force peaked for RIS and AC at day 56. RIS and ALN were significantly higher values than HUC at the end of HU. HUC had significantly lower values than AC at the same time point. By day 112, there were no significant differences between groups. Values are presented as mean ± SD.

† - Indicates significant difference compared to HUC ($p < 0.05$)
 # - Indicates significant difference compared to AC ($p < 0.05$)
*** - Indicates significant difference compared to ALN ($p < 0.05$)**

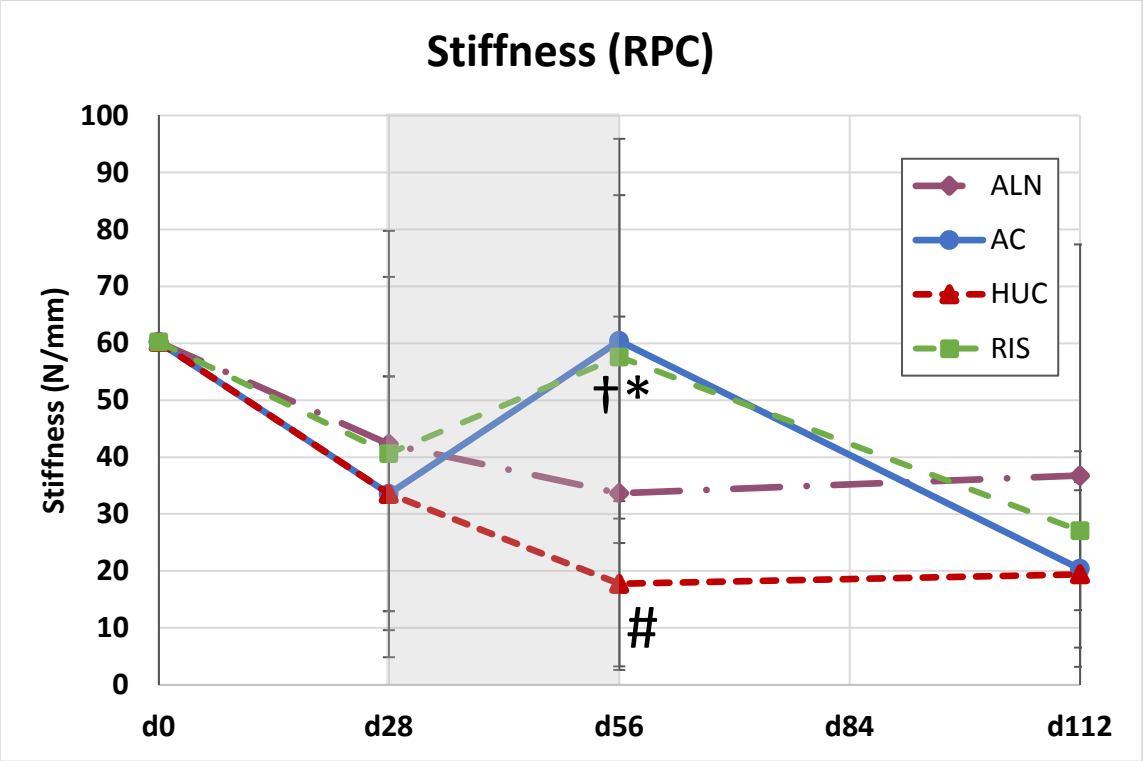

Figure 39. Stiffness for Tibia Metaphysis in RPC Test.
Gray region represents HU. RIS was significantly higher stiffness than HUC and ALN. HUC had significantly lower stiffness than AC. Day 112 had no significant differences. Values are presented as mean ± SD.

† - Indicates significant difference compared to HUC ($p < 0.05$)
 # - Indicates significant difference compared to AC ($p < 0.05$)
*** - Indicates significant difference compared to ALN ($p < 0.05$)**

5.3.2. Intrinsic Mechanical Properties from RPC Test

The intrinsic properties recorded from this test were ultimate stress, modulus and strain at yield. These can be found in Table 10. For ultimate stress (Figure 40), RIS and ALN were both significantly higher than HUC at day 56, but they were not significantly different from each other or AC. AC had the highest ultimate stress of 1.7 MPa at day 56 followed by RIS at 1.5 MPa. ALN had an ultimate stress of 1.0 MPa and HUC an ultimate stress of 0.5 MPa. There were no significant differences at the end of recovery.

Modulus, in Figure 41, followed similar trends to the measurements of ultimate stress. The only significant differences occurred at day 56. At this time point, both drug groups had a significantly higher modulus than HUC, 36.2 MPa for ALN and 27.8 MPa for RIS versus 9.65 MPa for HUC. HUC was significantly lower than AC (18.2 MPa). Day 28 and day 112 did not have any significant differences.

Table 10. Intrinsic Mechanical Properties from Tibia RPC.

Baseline	Ultimate Stress (MPa)		Modulus (MPa)		Strain at Yield (mm/mm)	
AC	2.02	(1.76)	28.6	(31.5)	0.03	(0.02)
End of Pre-treatment (Day 28)						
AC	1.10	(0.72)	17.6	(11.1)	0.05	(0.01)
ALN	1.35	(1.27)	23.3	(23.06)	0.04	(0.02)
RIS	1.34	(0.94)	20.7	(15.7)	0.05	(0.02)
End of Hindlimb Unloading (Day 56)						
AC	1.73	(0.96)	36.2	(28.1)	0.04	(0.01)
HUC	0.50#	(0.30)	9.7#	(5.78)	0.03	(0.01)
ALN	1.04†	(0.79)	18.2†	(10.7)	0.04	(0.02)
RIS	1.48†	(0.77)	27.8†	(15.2)	0.04	(0.02)
End of Recovery						
AC	0.66	(0.36)	10.9	(6.23)	0.04	(0.02)
HUC	0.68	(0.69)	10.5	(7.29)	0.03	(0.01)
ALN	0.98	(0.71)	18.9	(20.4)	0.04	(0.02)
RIS	0.67	(0.34)	14.3	(6.58)	0.03	(0.01)

Values presented as Mean and (Standard Deviation)
† - Indicates significant difference compared to HUC ($p < 0.05$)
 # - Indicates significant difference compared to AC ($p < 0.05$)

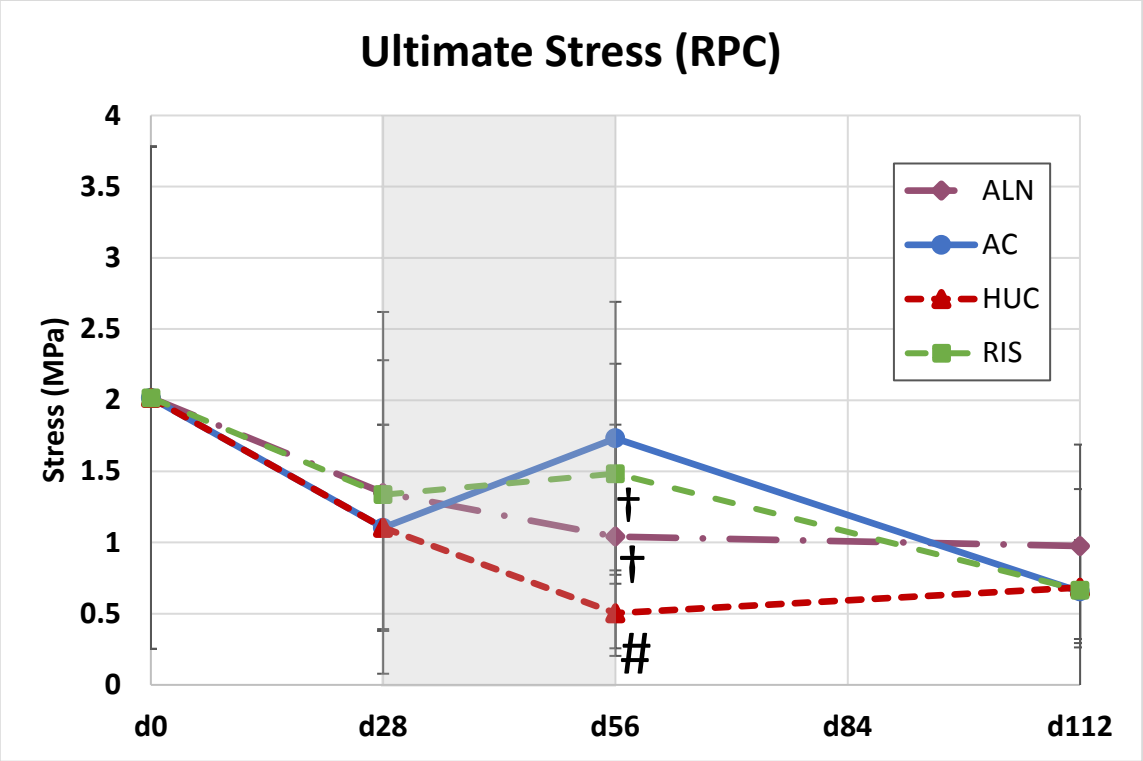

Figure 40. Ultimate Stress for Tibia Metaphysis in RPC Test.
Gray region represents HU. Ultimate stress showed that AC had the highest ultimate stress, but was not significantly different from the drug pre-treatment groups. ALN and RIS were significantly higher than HUC. HUC was significantly lower than AC. By the end of recovery there were no more significant differences between groups. Values are presented as mean ± SD.

† - Indicates significant difference compared to HUC ($p < 0.05$)
 # - Indicates significant difference compared to AC ($p < 0.05$)

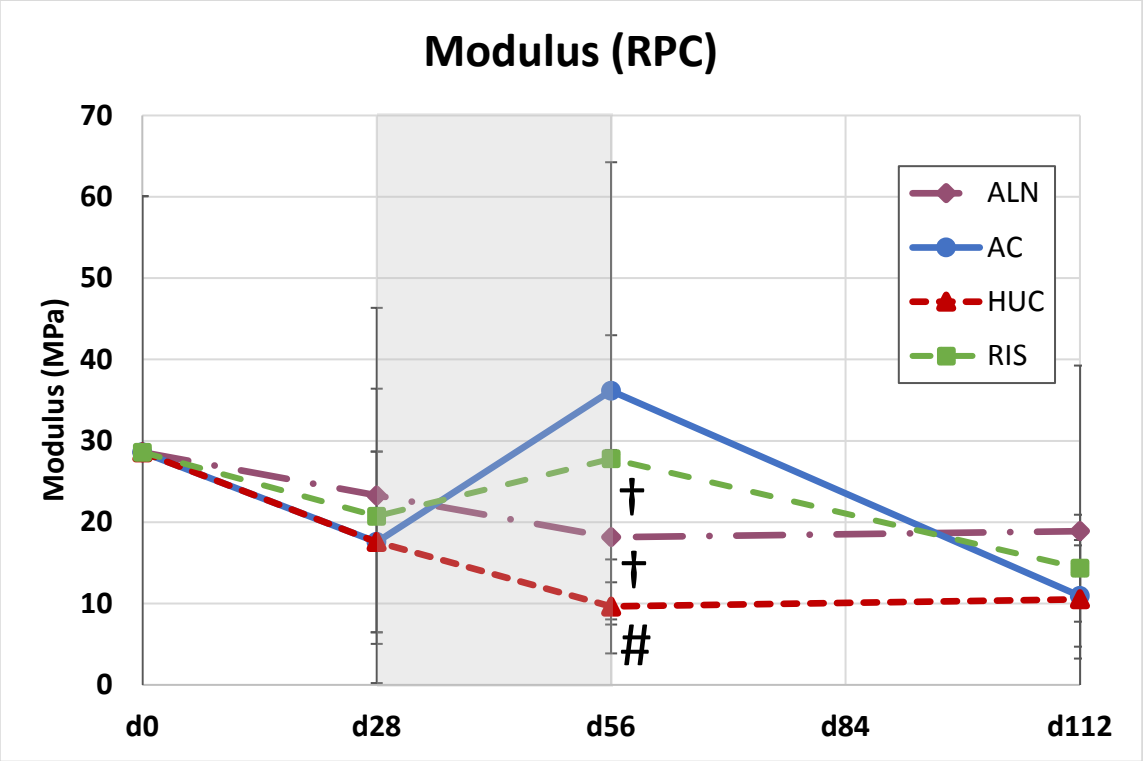

Figure 41. Modulus for Tibia Metaphysis in RPC Test.
Gray region represents HU. The AC animals had the highest modulus at day 56. RIS and ALN were lower than AC, but only significantly different (higher) than HUC. HUC was significantly lower than AC. At the end of recovery, there were no more significant differences between groups. Values are presented as mean ± SD.

† - Indicates significant difference compared to HUC ($p < 0.05$)
 # - Indicates significant difference compared to AC ($p < 0.05$)

6. DISCUSSION

The overall trend in the data across all variety of measures shows that the two bisphosphonates, alendronate and risedronate, were effective in limiting the detrimental effects of hindlimb unloading (HU) when administered as a pre-treatment.

Bisphosphonate treatments are typically administered concurrently with bedrest, spaceflight, or HU as a countermeasure to the unloading of actual or simulated microgravity. The unique discovery in this study is that it shows they have been effective when given prior to the unloading. This study showed, across a variety of metrics, that the drugs effectively prevent the levels of bone deterioration that were seen in the hindlimb unloading control (HUC) animals. This effect of the pre-treatment is despite the fact that the effect of the drugs is somewhat reduced compared to treatment concurrent with HU. The following sections will expand upon how these trends were apparent or unapparent in each of the measurements made on the tibia.

6.1. Comparison of pQCT Results

The pQCT measurements in the metaphysis show the greatest amount of difference between the different treatment groups. For the majority of the pQCT results, there were no differences at any time point other than the end of HU. At the mid-diaphysis, there were no differences shown between groups across any of the time points.

6.1.1. Densitometric Measurements at the Proximal Tibia Metaphysis

Densitometric measurements of BMC and vBMD across all compartments (total, cancellous, and cortical) at the proximal tibia metaphysis provide insight into how bone mineral changed at each time point. Cortical bone had significantly lower BMC for

ALN, RIS, and HUC compared to AC at the end of HU on day 56. This suggests that the drugs were unable to maintain cortical bone at the same level as AC. Cortical vBMD had no significant differences. This measurement is a normalization of cortical BMC by cortical volume (area times scan slice thickness) and suggests that changes in area caused the significantly lower values of cortical BMC. Unlike the cortical region, the cancellous region had significant differences for vBMD only. Cancellous vBMD was significantly lower for HUC compared to AC, ALN, and RIS at the end of HU. ALN and RIS were not statistically different than AC. This suggests that the drugs were able to prevent losses in cancellous vBMD and maintain them at levels similar to control.

When both the cortical and cancellous regions are considered together in total BMC and total vBMD, the only significant differences observed were in the measurement of total BMC. The values of total BMC were significantly higher than HUC for both bisphosphonates and for AC. There was no significant difference between AC and the drug groups. This lack of significance was in spite of the fact that there were significant losses in these groups in cortical BMC, a component of total BMC, compared to AC. These results suggest that both drugs were effective in preventing losses due to HU for total BMC. This highlights an important difference between cortical and total BMC as cortical BMC showed the drug treatments were significantly lower than AC at day 56, unlike total BMC.

Considering the cortical and cancellous densitometry measures in conjunction with the results from the total metaphysis cross-section, they suggest that the drugs were most effective in the cancellous compartment. While there was not a statistically significant

effect of HU in cancellous BMC for HUC, the measured values at day 56 for both ALN and RIS were almost equivalent to AC. Although cortical BMC loss could not be prevented by the drugs, the maintenance of cancellous BMC was able to mitigate the reductions in total BMC due to HU. The results from vBMD further support the notion that the cancellous compartment experienced the main effect of the bisphosphonate pre-treatment.

The data presented here echo the results of other studies that have shown that bisphosphonate treated animals were able to totally or partially avoid the bone loss seen in HUC. In rats of the same age, receiving a higher dose (30 μg/kg) of alendronate given concurrently to 28 days of HU, the drug was observed to have significant beneficial effects [42]. In this study, Swift et al. found that HU decreased total vBMD, total BMC and cancellous vBMD. On the other hand, the current study showed significantly lower values between HUC and AC for only total BMC and cancellous vBMD, but not for total vBMD. Nevertheless, the effects of both bisphosphonate pre-treatments on total BMC and cancellous vBMD in the current study were essentially the same as the effects of a concurrent alendronate treatment as measured by Swift et al. [42]. Both the current study and Swift et al. showed that alendronate mitigated the losses due to HU for total BMC [42]. These values for the drug treated animals were lower than AC but significantly higher than HUC. For cancellous vBMD, both studies showed fully protective effects, with the drug treated animals having essentially the same values as controls after 28 days of HU.

In other disuse models, both risedronate and alendronate have been shown to significantly protect against bone loss (BMD) in the tibia metaphysis. Mosekilde et al. showed that in 4 month old female rats both alendronate and risedronate were able to prevent losses in DXA measurements of aBMD in the proximal tibia metaphysis [43]. Unloading was achieved in this model by taping one hindlimb to the abdomen for a 28 day period of unloading. Untreated animals lost 9.5 % aBMD in the proximal tibia over the immobilization period while both bisphosphonates demonstrated positive effects for at least the two highest out of the three doses studied [43]. Risedronate was dosed at 0.1, 0.2 and 1.0 mg/kg and yielded significantly higher aBMD than HUC for the two higher doses (6% and 9 %, respectively) [43]. Alendronate was dosed at 0.2, 1.0, and 2.0 mg/kg and showed slightly milder beneficial effects, with aBMD significantly higher than HUC for the two higher doses (6% and 6.6%, respectively) [43]. In the current study, total vBMD for HUC was 9.3% lower than AC at the end of unloading, but not statistically significant. However, when considering total BMC and cancellous vBMD, the drug treatments were similarly effective. Both alendronate and risedronate protected against losses from HU. Further, mean values for RIS for both total BMC and cancellous vBMD were slightly higher at the end of HU when compared to ALN pre-treated animals, which is also consistent with the study by Mosekilde et al. [43]. Both Mosekilde et al. and the current study did not show any major statistical significant differences between either of these two drugs.

Additionally, other studies with alendronate, in concordance with this study, showed that treatment to counteract HU helped maintain bone density in the proximal tibia

metaphysis across all compartments [13], [14]. These two studies both used rats that started at a younger age, but the effect of alendronate is still clear. The concurrent treatment showed ALN had a significantly higher tibia aBMD at the end of 28 days of HU (25 % greater than HUC) [13]. Apseloff et al. pre-treated animals 2 days before unloading [13]. The results showed that ALN had a significantly higher tibia aBMD than HUC (45% greater) [14]. These two studies have different designs than the current study, so direct comparisons are problematic. The general finding is that alendronate is consistently protective against the negative effects of HU. Furthermore, comparing the results to those of similar studies [13], [14], [42], [43], emphasizes the noteworthy finding of the current study that bisphosphonates, given as a pre-treatment prior to HU, still result beneficial effects generally as effective as concurrent administration.

Previous human spaceflight studies also offer another comparison to the current rat model in this study. The use of alendronate, in addition to exercise, was shown to improve densitometric measurements at multiple anatomic sites when compared to untreated crew members of the International Space Station (ISS) [8]. LeBlanc et al. studied 7 ISS crew members who took alendronate during 4-6 months of spaceflight. They showed that the alendronate treatment was able to mitigate losses in cortical, cancellous and total aBMD and BMC at the femoral neck seen in the non-drug treated crew members [8]. These changes are measured over time by comparing pre- and post-flight in vivo scan measurements. The results for cancellous aBMD are most comparable to the cancellous vBMD in the current study, and the effects of the drug treatments are similar. That is, the HUC animals at the end of HU had significantly lower cancellous

vBMD than both drug treatments suggesting that the drug treatments mitigated losses over HU. LeBlanc et al. also showed the most prominent effects in the cancellous compartment (of the femoral neck in their case). They report actual increases in cancellous vBMD (+6.5%) and cancellous BMC (+20.9%) over the duration of the spaceflight mission on the ISS [8]. Leblanc et al. found similar significance to the HU results in total BMC as well. The one major difference between the results of the two studies is that the astronauts experienced a mitigating effect of alendronate in the cortical BMC of the femoral neck, while ALN, RIS, and HUC all lost cortical BMC with no differences between these groups in the current study. Overall, however, there are considerable similarities in the effects of bisphosphonates on the response of the skeleton to mechanical unloading.

The current study was unable to show any significant differences at the end of recovery except for in cancellous vBMD. This difference was could be suggesting a prevention of age related decline. The combination of significance in the cancellous vBMD and the lack of significant differences elsewhere suggests that the drugs do not hinder recovery during return to weight bearing. In fact, they may actually be better off during recovery because of this potential prevention of age related decline. While there are few studies that examine the effects of recovery, the observed differences at the end of recovery in the proximal tibia metaphysis shown in this study are comparable to other results [22], [44]. All of these studies showed that there were no differences at the end of recovery in any BMC or BMD measurements when comparing hindlimb unloaded controls to age matched control animals. Comparable changes during recovery in human

models follow the trends in these other rat HU studies. The same effects of recovery have been observed in both bed rest [45] and spaceflight reambulation [46]. Both of these studies showed an eventual complete recovery that was not statistically different from pre-disuse values.

In a related study observing treatments of alendronate and risedronate on ovariectomized rats, the effect of both drugs were shown to persist through a period twice as long as the treatment period [38]. This is corroborated by data that showed a significantly higher cancellous vBMD for RIS at day 112 compared to AC. With the knowledge that the drugs were found to still have an effect on the tibia at day 112, it is reasonable to say that they did not show any evidence of a negative effect during the recovery period. This finding was contrary to the expectation that differences between both bisphosphonates would be evident in the recovery of the animals from HU.

6.1.2. Comparing the Metaphysis and the Mid-Diaphysis

Due to the lack of significance in the mid-diaphysis, the changes in treatment between groups did not translate to all parts of the tibia. The effects of both the bisphosphonates and HU seem to be site specific and not causing the same effects for both of the regions of the tibia. For the metaphysis, it is clear that the bisphosphonates are not able to prevent losses in the cortical region, but were able to maintain bone in the cancellous region. Cancellous bone has a much higher surface area than cortical bone, due to the porous network that makes up cancellous bone. This is why the effect is much more pronounced in proximal tibia metaphysis than the mid-diaphysis. The drugs were unable to significantly affect the mid-diaphysis cortical BMC because there was a

significantly reduced surface area available for binding. This is not a major factor, however, because no effects of HU are typically observed at the tibia diaphysis anyway.

6.1.3. Geometric Measurements at the Proximal Tibia Metaphysis

For the geometric measurements at the metaphysis, there were significant changes in cortical area only. The cortical areas of ALN, RIS, and HUC were significantly lower than AC. The measurements of total bone area, endocortical area and PAMOI did not show any significant changes at any time point. Since endocortical area was largely constant, but larger than the cortical area, significant changes in cortical area are not reflected as significant changes in the total area. In other words, because endocortical area a much greater proportion of the total cross-section, the total area results do not show any significant differences even though cortical area results do show significant differences.

This may be one possible explanation for the reduction in BMC seen in the cortical metaphysis and not in the cortical mid-diaphysis. The cortical BMC changes occur in the metaphysis because bone is being removed from the cortical region causing a reduction in area. BMC is based on the amount of mineral present, and does not normalize for the total volume scanned like vBMD. The vBMD measurements do not show any difference in the cortical region for both the mid-diaphysis and metaphysis.

6.2. Comparison of 3-Point Bend Results

The 3-point bending at the mid-diaphysis did not offer any significant differences in the effects of HU or bisphosphonate drug treatments. Also, the 3-point bending stiffness and SSI results both had no significance.

The lack of an effect of HU in the mid-diaphysis is consistent with the findings of other studies. That is, 28 days of hindlimb unloading in adult male rats does not typically result in any significant changes in the tibia mid-diaphysis for either extrinsic or intrinsic mechanical properties from 3-point bending. The findings of Shirazi et al. found a lack of significant differences between HU animals and regular control animals across the reported measures of extrinsic and intrinsic properties [22]. In this study, energy to fracture, pre-yield toughness, and displacement at fracture were reported in addition to the mechanical properties measured by Shirazi et al [22]. These additional mechanical properties, included in this study, in the showed no significance. Bloomfield et al. reported no differences in measured extrinsic or intrinsic results compared to age matched controls at day 56 in similarly aged animals [20]. Post-yield displacement, energy to fracture, displacement at fracture, and pre-yield toughness were not reported. These results corroborate the findings of Shirazi et al. and the current study [22].

When comparing the mechanical properties measured for alendronate and risedronate to other studies of skeletally mature animals show similar results across 3-point bending mechanical properties. In a study of ovariectomized baboons, the results of femoral 3-point bending did not show significant differences in maximum force or stiffness compared to control animals [50]. In a study of ovariectomized female beagles, significant differences were not shown in tibia 3-point bending mechanical properties for equivalent doses of either risedronate or alendronate compared to control [51]. In a study of female ovariectomized rats, the 3-point bending measures of maximum force and stiffness again showed no significant effect of alendronate compared to age matched

control animals at the same time point [52]. These three studies support the findings of this study; neither bisphosphonate was able to significantly improve the performance of bone at day 56. The HU procedure significantly reduced bone mineral content of the HUC group and the effect of the bisphosphonates counteracted that loss.

6.3. Comparison of RPC Results

The RPC test results showed a significant difference between groups at the end of HU. Both ultimate stress and modulus support the conclusion that bisphosphonates protect cancellous bone against losses in HU. Comparing to previous RPC results, the modulus and ultimate stress were almost the same as the baseline animals between the current study and that of Shirazi et al [47]. Shirazi et al. showed a significant reduction in ultimate stress for HUC versus AC after 28 days of unloading. There were no differences in modulus after HU [47]. Unlike Shirazi et al, the current study found significantly lower values of both ultimate stress and modulus at the end of HU in HUC compared to AC. Additionally, ALN and RIS were able to mitigate the effect of HU at day 56 and were both significantly higher than HUC.

Overall, these results are similar to those of the metaphysis pQCT data. They show that the mechanical strength of cancellous bone at day 56 is higher than HUC for both drug treated groups, and that mechanical strength was lower due to HU. Table 11 shows that the differences between various pQCT and RPC measurements and their relative percent differences compared to AC. These results show that the differences in mean values were for RPC properties than for densitometric variables. There are no differences in the statistically significant differences between these two measurements,

but the percent differences in the table suggest that smaller, yet still statistically significant changes in densitometric variables may have a much larger impact on mechanical properties. A comparison of cancellous vBMD and RPC ultimate stress suggests that both the negative effects of HU and the beneficial effects of the drug pre-treatments could be underestimated by pQCT measurements.

Table 11. Comparison of Percent Differences in Means from AC at the End of Hindlimb Unloading for pQCT and RPC Measurements.

Comparison	Total BMC	Cancellous vBMD	BSI	RPC Ultimate Stress	RPC Modulus
RIS to AC	-7.9% †	7.0% †	-8.4% †	-14.4% †	-23.1% †
ALN to AC	-9.0% †	0.1% †	-11.6% †	-39.8% †	-49.8% †
HUC to AC	-20.1% #	-27.9% #	-27.2% #	-70.9% #	-73.3% #

† - Indicates significant difference compared to HUC ($p < 0.05$)
 # - Indicates significant difference compared to AC ($p < 0.05$)

6.4. Overall Conclusions

Measurements at the metaphysis showed that the drugs were able to counteract the effects of HU by maintaining bone at levels of age-matched control (AC). This was shown significantly in total BMC and cancellous vBMD. Cortical BMC was unable to be maintained at levels of AC; however, the changes in cancellous bone were enough to counteract the changes in cortical bone over HU. This prevented significant losses in total BMC compared to AC. Over recovery, cortical bone was recovered to nearly the same values as AC. The drugs did not hinder the ability of bone to recover, and were able to combat the effect of age related decline in HUC and AC over recovery. The mid-

diaphysis did not show any significant change in BMC or vBMD, suggesting that the changes in BMC and vBMD were limited to the metaphysis.

Geometric measurements of the metaphysis showed decreases over HU and increases over recovery to correspond with the densitometric results. The significant decrease in cortical area, in conjunction with the significant decrease in cortical BMC (both compared to AC), means that HU caused bone to be removed from the cortical region. The drugs were unable to significantly alter this effect of HU. The mid-diaphysis showed an increase in area and moment of inertia across the course of the study. This was in line with age related change and was not influenced significantly by either the bisphosphonates or HU.

Mechanical strength of the mid-diaphysis was evaluated using a 3-point bend test. No significant differences were found in the bending results. In spite of this, it seems that a difference in the energy to fracture may exist between the drugs. There is research that suggests that alendronate may increase the brittleness of bone. The head-to-head comparison of energy to fracture for risedronate and alendronate at day 112 suggests that this might be slowly occurring. Additionally, the modulus shows a large rise for HUC at the end of HU. This was caused by a decrease in cross-sectional moment of inertia. The decrease was not significant for HUC, but this decrease was larger than the decrease in the drug groups. That kept the modulus closer to the value of AC. A comparison of the 3-point bending results to an estimated bending strength index from pQCT data did not show much similarity. This was because the mechanical testing results and the pQCT did not follow the same trends.

7. LIMITATIONS

The rat hindlimb unloaded model has various limitations. The most obvious of these is that rats are quadrupeds while humans are not. Rat bone also lacks the same intracortial bone structure as humans. With this study in particular, there were other imperfections worth noting. Some of the alendronate animals did not receive the correct dosing; it was lower than was listed in the method. This did not seem to affect the results. There were no explicit significant differences observed between the drugs as this was supported by the findings in other published studies. There were also concerns about differences in cohort size that may have caused additionally variability. One cohort was much smaller than the other two. Again, the design of the study called for multiple animals at each time point from each cohort so this distribution was still done randomly.

For ex vivo testing, there are limitations to the RPC test. There are concerns when placing the bone specimen on the platens so only the cancellous bone experiences direct contact. Additionally, the largest assumption in the test is that the cancellous bone is homogenously distributed throughout the entire cross-section. Unfortunately, this is not always the case. The test was completed with as many bones as possible, but some were omitted because there were not enough trabeculae to constitute even an imperfect mechanical test. That is, the central region of the specimen was mostly devoid of cancellous bone. This is why the mechanical properties measured are estimates as they were subjected to local variations in structure. The analysis was done carefully and systematically to ensure that the results were as valid as possible, but it is impossible to avoid some level of variability or imperfection.

8. FUTURE WORK

This study is a part of a larger experiment that compares the effect of these two anti-catabolic (bisphosphonate) pre-treatments with two anabolic pre-treatments. The anabolic treatments utilize an anti-sclerostin antibody and a jumping resistance exercise meant to mimic strength training. The resulting comparison will shed light on how different methods of pre-treatment compare to one another.

For the study of the bisphosphonate pre-treatment focused on in this thesis, forthcoming data includes histology of the tibia at various locations and a full battery of tests for the femur. The femur data will include pQCT scans of the femoral neck, mid-diaphysis and distal metaphysis. RPC testing of the distal metaphysis, 3-point bending and femoral neck testing will all additionally be completed. These measures will also assess how the effects of the bisphosphonate treatment will be extend beyond the left tibia to other bones in the body.

The left tibia metaphysis, included in this thesis, will also undergo μCT to analyze the changes in microarchitecture in the cancellous bone. To better understand some of the effects of the bisphosphonates, it could beneficial to complete a future study that extends the recovery time of the animals in HU. This modification may be able to better understand how differences in binding affinity affect recovery. The period of recovery used in this study is enough to capture the changes that occur directly after spaceflight, but bone is constantly changing. There could be effects that occur slowly and appear beyond the two month recovery investigated in this study.

9. CONCLUSIONS

This study sought to determine if a bisphosphonate treatment could effectively combat the bone loss of hindlimb unloading (HU) when given as a treatment prior to unloading rather than concurrently. HU is an effective rat model of human spaceflight and was used to understand how the changes in rat bone might reflect changes in human bone in microgravity. The aim of this type of study is to better understand the countermeasures for treating patients in space and those on earth with conditions that cause detrimental bone loss.

More specifically, this study examined the effects of two different bisphosphonate pre-treatments administered prior to a period of HU. The pre-treatment and bout of HU were both 28 day long period that were followed by 56 days of recovery, a return to normal ambulation. Two bisphosphonates were used in this study to understand how differences in binding affinity might affect the effectiveness of treatment. Alendronate, a high affinity drug, and risedronate, a lower affinity drug, were the two bisphosphonates chosen for this study. The effects of HU were assessed with pQCT scans of the tibia metaphysis and mid-diaphysis. Measurements of mechanical strength were also made at each location.

The results from this study are not a direct assessment of how human bone would behave under the same situations, but they offer a prediction of what could be expected. The tibia metaphysis is selected as a region of interest because the composition of the site is comparable to the composition of the human femoral neck. By making this comparison, the results of this study suggest that, at the very least, the use of a

bisphosphonate pre-treatment would reduce fracture risk upon return from space, and would also not hinder the recovery of bone post-spaceflight. It is also reasonable to assume that the bisphosphonate chosen will still be able to combat age related bone loss over the recovery period. The results also show that the binding affinity of the drug will not significantly change how well the drug works to counter HU induced bone loss. There was not a noticeable effect of changing the resorption activity of the bone that caused a change the brittleness of the bone.

Broadly speaking, the results of this study show that both bisphosphonates were effective countermeasures even though they were given before and not during HU. The beneficial effects of the pre-treatments were concentrated in the cancellous compartment of the proximal tibia metaphysis. This was found in both densitometric variables and mechanical properties. No beneficial effects were observed for the tibia mid-diaphysis; however, no detrimental effects of HU were observed at this location in this study and other rat studies. In addition, the results from this study showed that neither bisphosphonate pre-treatment had a negative effect on the 56 days of reambulation recovery that followed HU. Consequently, this study suggests a pre-treatment protocol might be effective for bisphosphonates used as countermeasures in human space flight scenarios. Finally, no significant differences in relative effectiveness were observed in this study between alendronate and risedronate.

REFERENCES

[1] A. Leblanc, V. Schneider, L. Shackelford, S. West, V. Oganov, A. Bakulin, L. Voronin, Bone Mineral and Lean Tissue Loss After Long-Duration Spaceflight, Journal of Musculoskeletal Neuronal Interaction, 1 (2000) 157-160.

[2] P. Collet, D. Uebelhart, L. Vico, L. Moro, D. Hartmann, M. Roth, C. Alexandre, Effects of 1- and 6-Month Spaceflight on Bone Mass and Biochemistry in Two Humans, Bone, 20 (1997) 547-551.

[3] T. Lang, A. Leblanc, H. Evans, Y. Lu, H. Genant, A. Yu, Cortical and Trabecular Bone Mineral Loss from the Spine and Hip in Long-Duration Spaceflight, Journal of Bone and Mineral Research, 19 (2004) 1006-1012.

[4] T. P. Stein, Weight, Muscle and Bone Loss During Space Flight: Another Perspective, European Journal of Applied Physiology, 113 (2012) 2171-2181.

[5] E. Morey, D. Baylink, Inhibition of Bone Formation During Space Flight, Science, 201 (1978) 1138-1141.

[6] J. Iwamoto, T. Takeda, Y. Sato, Interventions to Prevent Bone Loss in Astronauts During Space Flight, Keio Journal of Medicine, 54 (2005) 55-59.

[7] P. Cavanagh, A. Licata, A. Rice, Exercise and Pharmacological Countermeasures for Bone Loss During Long-Duration Space Flight, Gravitational Space Biology, 18 (2005) 39-58.

[8] A. Leblanc, T. Matsumoto, J. Jones, J. Shapiro, T. Lang, L. Shackelford, S. M. Smith, H. Evans, E. Spector, R. Ploutz-Snyder, J. Sibonga, J. Keyak, T. Nakamura, K. Kohri, H. Ohshima, Bisphosphonates as a Supplement to Exercise to Protect Bone During Long-Duration Spaceflight, Osteoporosis International, 24 (2013) 2105-2114.

[9] L. C. Shackelford, Resistance Exercise as a Countermeasure to Disuse-Induced Bone Loss, Journal of Applied Physiology, 97 (2004) 119-129.

[10] E. S. Orwoll, R. A. Adler, S. Amin, N. Binkley, E. M. Lewiecki, S. M. Petak, S. A. Shapses, M. Sinaki, N. B. Watts, J. D. Sibonga, Skeletal Health in Long-Duration Astronauts: Nature, Assessment, and Management Recommendations from the NASA Bone Summit, Journal of Bone and Mineral Research, 28 (2013) 1243-1255.

[11] M. F. Holick, Perspective on the Impact of Weightlessness on Calcium and Bone Metabolism, Bone, 22 (1998) 105-111.

[12] Y. Watanabe, H. Ohshima, K. Mizuno, C. Sekiguchi, M. Fukunaga, K. Kohri, J. Rittweger, D. Felsenberg, T. Matsumoto, T. Nakamura, Intravenous Pamidronate Prevents Femoral Bone Loss and Renal Stone Formation During 90-Day Bed Rest, Journal of Bone and Mineral Research, 19 (2004) 1771-1778.

[13] G. Apseloff, B. Girten, S. E. Weisbrode, M. Walker, L. S. Stern, M. E. Krecic, N. Gerber, Effects of Aminohydroxybutane Bisphosphonate on Bone Growth when Administered After Hind-Limb Bone Loss in Tail-Suspended Rats, Journal of Pharmacology and Experimental Therapeutics, 267 (1993) 515-521.

[14] G. Apseloff, B. Girten, M. Walker, D. R. Shepard, M. E. Krecic, L. S. Stern, N. Gerber, Aminohydroxybutane Bisphosphonate and Clenbuterol Prevent Bone Changes and Retard Muscle Atrophy Respectively in Tail Suspended Rats, Journal of Pharmacology and Experimental Therapeutics, 264 (1992) 1071-1078.

[15] E. S. Siris, S. T. Harris, C. J. Rosen, C. E. Barr, J. N. Arvesen, T. A. Abbott, S. Silverman, Adherence to Bisphosphonate Therapy and Fracture Rates in Osteoporotic Women: Relationship to Vertebral and Nonvertebral Fractures from 2 US Claims Databases, Mayo Clinic Proceedings, 81 (2006) 1013-1022.

[16] J. H. Lin, Bisphosphonates: A Review of Their Pharmacokinetic Properties, Bone, 18 (1996) 75-85.

[17] N. B. Watts, D. L. Diab, Long-Term Use of Bisphosphonates in Osteoporosis, Journal of Clinical Endocrinology & Metabolism, 95 (2010) 1555-1565.

[18] K. A. Kennel, M. T. Drake, Adverse Effects of Bisphosphonates: Implications for Osteoporosis Management, Mayo Clinic Proceedings, 84 (2009) 632-638.

[19] E. Morey-Holton, R. K. Globus, A. Kaplansky, G. Durnova, The Hindlimb Unloading Rat Model: Literature Overview, Technique Update and Comparison with Space Flight Data, Advances in Space Biology and Medicine, 10 (2005) 7-40.

[20] S. A. Bloomfield, M. R. Allen, H. A. Hogan, M. Delp, Site- and Compartment-Specific Changes in Bone with Hindlimb Unloading in Mature Adult Rats, Bone, 31 (2002) 149-157.

[21] World Health Organization, Assessment of Fracture Risk and Its Application to Screening for Osteoporosis, WHO Technical Report Series, (1994) 843.

[22] Y. Shirazi-Fard, J. S. Kupke, S. A. Bloomfield, H. A. Hogan, Discordant Recovery of Bone Mass and Mechanical Properties During Prolonged Recovery from Disuse, Bone, 52 (2013) 433-443.

[23] R. B. Martin, D. B. Burr, A. N. Sharkey, D. P. Fyhrie, Skeletal Tissue Mechanics, first ed., Springer, New York, 1998.

[24] J. D. Currey, Bones: Structure and Mechanics, second ed., Princeton University Press, Princeton, NJ, 2002.

[25] British Broadcasting Company, GSCE Bitsize: Bone Growth. http://www.bbc.co.uk/schools/gcsebitesize/pe/appliedanatomy/2_anatomy_skeleton_rev4.shtml, 2014 (accessed 10.09.16).

[26] L. Kamibayashi, U. P. Wyss, T. D. V. Cooke, B. Zee, Changes in Mean Trabecular Orientation in the Medial Condyle of the Proximal Tibia in Osteoarthritis, Calcified Tissue International, 57 (1995) 69-73.

[27] T. M. Keaveny, E. F. Morgan, G. L. Niebur, O.C. Yeh, Biomechanics of Trabecular Bone, Annual Review of Biomedical Engineering, 3 (2001) 307-333.

[28] H. M. Frost, Wolff's Law and Bone's Structural Adaptations to Mechanical Usage: an Overview for Clinicians, The Angle Orthodontist, 64 (1994) 175-188.

[29] A. J. Roelofs, C. A. Stewart, S. Sun, K. M. Błażewska, B. A. Kashemirov, C. E. McKenna, R. G. G. Russell, M. J. Rogers, M. W. Lundy, F. H. Ebetino, F. P. Coxon, Influence of Bone Affinity on the Skeletal Distribution of Fluorescently Labeled Bisphosphonates In Vivo, Journal of Bone and Mineral Research, 27 (2012) 835-847.

[30] G. H. Nancollas, R. Tang, R. J. Phipps, Z. Henneman, S. Gulde, W. Wu, A. Mangood, R. G. G. Russell, F. H. Ebetino, Novel Insights into Actions of Bisphosphonates on Bone: Differences in Interactions with Hydroxyapatite, Bone, 38 (2006) 617-627.

[31] M. A. Lawson, Z. Xia, B. L. Barnett, J. T. Triffitt, R. J. Phipps, J. E. Dunford, R. M. Locklin, F. H. Ebetino, R. G. G. Russell, Differences Between Bisphosphonates in Binding Affinities for Hydroxyapatite, Journal of Biomedical Materials Research, 92B (2010) 149-155.

[32] C. T. Leu, E. Luegmayr, L. P. freedman, G. A. Rodan, A. A. Reszkea, Relative Binding Affinities of Bisphosphonates for human Bone and Relationship to Antiresorptive Efficacy, Bone, 38 (2006) 617-627.

[33] P. D. Chilibeck, K. S. Davison, S. J. Whiting, Y. Suzuki, C. L. Janzen, P. Peloso, The Effect of Strength Training Combined with Bisphosphonate (Etidronate) Therapy on

Bone Mineral, Lean Tissue, and Fat Mass in Postmenopausal Women, Canadian Journal of Physiology and Pharmacology, 80 (2002) 941-950.

[34] E. Lespassailles, C. Jaffre, H. Beaupied, P. Nanyan, E. Dolleans, C. L. Benhamou, D. Courteix, Does Exercise Modify the Effects of Zoledronic Acid on Bone Mass, Microarchitecture, Biomechanics, and Turnover in Ovariectomized Rats?, Calcified Tissue International, 85 (2009) 146-157.

[35] P. A. Sengupta, Scientific Review of Age Determination for a Laboratory Rat: How Old Is It in Comparison with Human Age?, Biomedical International, 2 (2012) 81-89.

[36] C. M. Bagi, D. Wilkie, K. Georgelos, D. Williams, D. Bertolini, Morphological and Structural Characteristics of the Proximal Femur in Human and Rat, Bone, 21 (1997) 261-267.

[37] H. M. Frost, W. S. S. Jee, On the Rat Model of Human Osteopenias and Osteoporoses, Bone and Mineral, 18 (1991) 227-236.

[38] R. K. Fuchs, R. J. Phipps, D. B. Burr, Recovery of Trabecular and Cortical Bone Turnover After Discontinuation of Risedronate and Alendronate Therapy in Ovariectomized Rats, Journal of Bone and Mineral Research, 23 (2008) 1689-1697.

[39] Y. Hasegawa, P. Schneider, C. Reiners, Age, Sex, and Grip Strength Determine Architectural Bone Parameters Assessed by Peripheral Quantitative Computed Tomography (pQCT) at the Human Radius, Journal of Biomechanics, 34 (2001) 497-503.

[40] C. H. Turner, D. B. Burr, Basic Biomechanical Measurements of Bone: A Tutorial, Bone, 14 (1993) 595-608.

[41] D. D. Bilke, E. R. Morey-Holton, S. B. Doty, P. A. Currier, S. J. Turner, B. P. Halloran, Alendronate Increases Skeletal Mass of Growing Rats During Unloading by

Inhibiting Resorption of Calcified Cartilage, Journal of Bone and Mineral Research, 9 (1994) 1777-1787.

[42] J. M. Swift, S. N. Swift, M. I. Nilsson, H. A. Hogan, S. D. Bouse, S. A. Bloomfield, Cancellous Bone Formation Response to Simulated Resistance Training During Disuse Is Blunted by Concurrent Alendronate Treatment, Journal of Bone and Mineral Research, 26 (2011) 2140-2150.

[43] L. I. Mosekilde, J. S. Thomsen, M. S. Mackey, R. J. Phipps, Treatment with Risedronate or Alendronate Prevents Hind-Limb Immobilization-Induced Loss of Bone Density and Strength in Adult Female Rats, Bone, 27 (2000) 639-645.

[44] L. Vico, S. Bourrin, J. M. Very, M. Radziszowska, P. Collet, C. Alexandre, Bone Changes in 6-Mo-Old Rats After Head-Down Suspension and a Reambulation Period, Journal of Applied Physiology, 79 (1995) 1426-1433.

[45] E. R. Spector, S. M. Smith, J. D. Sibonga, Skeletal Effects of Long-Duration Head-Down Bed Rest, Aviation, Space, and Environmental Medicine, 80 (2009) A23-A28.

[46] J. D. Sibonga, H. J. Evans, H. G. Sung, E. R. Spector, T. F. Lang, V. S. Oganov, A. V. Bakulin, L. C. Shackleford, A. D. Leblanc, Recovery of Spaceflight-Induced Bone Loss: Bone Mineral Density After Long-Duration Missions as Fitted with an Exponential Function, Bone, 41 (2007) 973-978.

[47] Y. Shirazi-Fard, R. A. Anthony, A. T. Kwaczala, S. Judex, S. A. Bloomfield, H. A. Hogan, Previous Exposure to Simulated Microgravity Does Not Exacerbate Bone Loss During Subsequent Exposure in the Proximal Tibia of Adult Rats, Bone, 56 (2013) 461-473.

[48] M. R. Allen, D. B. Burr, Bisphosphonate Effects on Bone Turnover, Microdamage, and Mechanical Properties: What We Think We Know and What We Know That We Don't Know, Bone, 49 (2011) 56-65.

[49] J. A. Guy, M. Shea, C. P. Peter, R. Morrissey, W. C. Hayed, Continuous Alendronate Treatment Throughout Growth, Maturation, and Aging in the Rat Results in Increases in Bone Mass and Mechanical Properties, Calcified Tissue International, 53 (1993) 283-288.

[50] R. Balena, B. C. Toolan, M. Shea, A. Markatos, E. R. Myers, S. C. Lee, E. E. Opas, J. G. Seedor, H. Klein, D. Frankenfield, H. Quartuccio, C. Fioravanti, J. Clair, E. Brown, W. C. Hayes, G. A. Rodan, The Effects of 2-Year Treatment with the Aminobisphosphonate Alendronate on Bone Metabolism, Bone Histomorphometry, and Bone Strength in Ovariectomized Nonhuman Primates, Journal of Clinical Investigation, 92 (1993) 2577-2586.

[51] S. Y. Tang, M. R. Allen, R. Phipps, D. B. Burr, D. Vashishth, Changes in Non-Enzymatic Glycation and Its Association with Altered Mechanical Properties Following 1-Year Treatment with Risedronate or Alendronate, Osteoporosis International, 20 (2007) 887-894.

[52] Y. Cao, S. Mori, T. Mashiba, M. S. Westmore, L. Ma, M. Sato, T. Akiyama, L. Shi, S. Komatsubara, K. Miyamoto, H. Norimatsu, Raloxifene, Estrogen, and Alendronate Affect the Processes of Fracture Repair Differently in Ovariectomized Rats, Journal of Bone and Mineral Research, 17 (2002) 2237-2246.

APPENDIX A. STATISTICAL ANALYSIS

Table A1. Statistical Analysis of Metaphysis pQCT at the End of Pre-Treatment (Day 28).

Parameter	Statistical Test	Post Hoc	Comparison	P-Value
Total BMC	ANOVA	N/A	Overall	0.865
Total vBMD	ANOVA	N/A	Overall	0.169
Cancellous BMC	ANOVA	N/A	Overall	0.616
Cancellous vBMD	ANOVA	N/A	Overall	0.594
Cortical BMC	ANOVA	N/A	Overall	0.869
Cortical vBMD	Kruskal-Wallis	N/A	Overall	0.13
Total Area	ANOVA	N/A	Overall	0.381
Endocortical Area	Kruskal-Wallis	N/A	Overall	0.39
Cortical Area	ANOVA	N/A	Overall	0.583
PAMOI	Kruskal-Wallis	N/A	Overall	0.33
BSI	ANOVA	N/A	Overall	0.785

Table A2. Statistical Analysis of Metaphysis pQCT at the End of Hindlimb Unloading (Day 56).

Parameter	Statistical Test	Post Hoc	Comparison	P-Value
Total BMC	ANOVA	Tukey	Overall	0.0012
			C-A	0.198
			H-A	0.034
			R-A	0.99
			H-C	0.001
			R-C	0.327
			R-H	0.022
Total vBMD	ANOVA	N/A	Overall	0.063
Cancellous BMC	ANOVA	N/A	Overall	0.0523

Table A2. Continued

Parameter	Statistical Test	Post Hoc	Comparison	P-Value
Cancellous vBMD	ANOVA	Tukey	Overall	0.0000725
			C-A	0.999
			H-A	0.001
			R-A	0.684
			H-C	0.007
			R-C	0.799
			R-H	0.0000604
Cortical BMC	ANOVA	Tukey	Overall	0.002
			C-A	0.023
			H-A	0.381
			R-A	0.999
			H-C	0.001
			R-C	0.033
			R-H	0.374
Cortical vBMD	ANOVA	N/A	Overall	0.999
Total Area	ANOVA	N/A	Overall	0.409
Endocortical Area	ANOVA	N/A	Overall	0.852
Cortical Area	ANOVA	Tukey	Overall	0.004
			C-A	0.033
			H-A	0.393
			R-A	0.999
			H-C	0.002
			R-C	0.05
			R-H	0.363
PAMOI	Kruskal-Wallis	N/A	Overall	0.064
BSI	ANOVA	Tukey	Overall	0.0000198
			C-A	0.0779
			H-A	0.003
			R-A	0.836
			H-C	0.0000212
			R-C	0.313
			R-H	0.000461

Table A3. Statistical Analysis of Metaphysis pQCT at the End of Recovery (Day 112).

Parameter	Statistical Test	Post Hoc	Comparison	P-Value
Total BMC	ANOVA	N/A	Overall	0.708
Total vBMD	ANOVA	N/A	Overall	0.23
Cancellous BMC	ANOVA	N/A	Overall	0.187
Cancellous vBMD	ANOVA	Tukey	Overall	0.012
			C-A	0.159
			H-A	0.061
			R-A	0.999
			H-C	0.994
			R-C	0.118
			R-H	0.04
Cortical BMC	ANOVA	N/A	Overall	0.624
Cortical vBMD	ANOVA	N/A	Overall	0.51
Total Area	ANOVA	N/A	Overall	0.712
Endocortical Area	ANOVA	N/A	Overall	0.587
Cortical Area	ANOVA	N/A	Overall	0.911
BSI	ANOVA	N/A	Overall	0.923
PAMOI	ANOVA	N/A	Overall	0.734

Table A4. Statistical Analysis of Mid-Diaphysis pQCT at the End of Pre-Treatment (Day 28).

Parameter	Statistical Test	Post Hoc	Comparison	P-Value
Cortical BMC	ANOVA	N/A	Overall	0.671
Cortical vBMD	ANOVA	N/A	Overall	0.78
Endocortical Area	ANOVA	N/A	Overall	0.722
Cortical Area	ANOVA	N/A	Overall	0.583
PAMOI	Kurskal-Wallis	N/A	Overall	0.814
SSI	ANOVA	N/A	Overall	0.77
Total Area	ANOVA	N/A	Overall	0.863

Table A5. Statistical Analysis of Mid-Diaphysis pQCT at the End of Hindlimb Unloading (Day 56).

Parameter	Statistical Test	Post Hoc	Comparison	P-Value
Cortical BMC	ANOVA	N/A	Overall	0.49
Cortical vBMD	Kruskal-Wallis	N/A	Overall	0.3
Endocortical Area	ANOVA	N/A	Overall	0.795
Cortical Area	ANOVA	N/A	Overall	0.264
PAMOI	ANOVA	N/A	Overall	0.372
SSI	ANOVA	N/A	Overall	0.678
Total Area	ANOVA	N/A	Overall	0.643

Table A6. Statistical Analysis of Mid-Diaphysis pQCT at the End of Recovery (Day 112).

Parameter	Statistical Test	Post Hoc	Comparison	P-Value
Cortical BMC	ANOVA	N/A	Overall	0.863
Cortical vBMD	Kruskal-Wallis	N/A	Overall	0.68
Endocortical Area	ANOVA	N/A	Overall	0.77
Cortical Area	ANOVA	N/A	Overall	0.264
PAMOI	ANOVA	N/A	Overall	0.945
SSI	ANOVA	N/A	Overall	0.932
Total Area	ANOVA	N/A	Overall	0.89

Table A7. Statistical Analysis of 3-Point Bending at the End of Pre-Treatment (Day 28).

Parameter	Statistical Test	Post Hoc	Comparison	P-Value
Maximum Force	ANOVA	N/A	Overall	0.999
Stiffness	ANOVA	N/A	Overall	0.695
Energy to Fracture	Kruskal-Wallis	N/A	Overall	0.42
Displacement at Fracture	Kruskal-Wallis	N/A	Overall	0.51
Post-Yield Displacement	Kruskal-Wallis	N/A	Overall	0.61

Table A7. Continued

Parameter	Statistical Test	Post Hoc	Comparison	P-Value
Ultimate Stress	Kruskal-Wallis	N/A	Overall	0.167
Modulus	ANOVA	N/A	Overall	0.834
Pre-Yield Toughness	Kruskal-Wallis	N/A	Overall	0.257

Table A8. Statistical Analysis of 3-Point Bending at the End of Hindlimb Unloading (Day 56).

Parameter	Statistical Test	Post Hoc	Comparison	P-Value
Maximum Force	ANOVA	N/A	Overall	0.627
Stiffness	Kruskal-Wallis	N/A	Overall	0.36
Energy to Fracture	ANOVA	N/A	Overall	0.364
Displacement at Fracture	ANOVA	N/A	Overall	0.393
Post-Yield Displacement	ANOVA	N/A	Overall	0.528
Ultimate Stress	ANOVA	N/A	Overall	0.378
Modulus	ANOVA	N/A	Overall	0.12
Pre-Yield Toughness	ANOVA	N/A	Overall	0.445

Table A9. Statistical Analysis of 3-Point Bending at the End of Recovery (Day 112).

Parameter	Statistical Test	Post Hoc	Comparison	P-Value
Maximum Force	ANOVA	N/A	Overall	0.178
Stiffness	ANOVA	N/A	Overall	0.908
Energy to Fracture	Kruskal-Wallis	N/A	Overall	0.18
Displacement at Fracture	Kruskal-Wallis	N/A	Overall	0.23
Post-Yield Displacement	Kruskal-Wallis	N/A	Overall	0.46
Ultimate Stress	ANOVA	N/A	Overall	0.262
Modulus	ANOVA	N/A	Overall	0.93
Pre-Yield Toughness	ANOVA	N/A	Overall	0.337

Table A10. Statistical Analysis of RPC Test at the End of Pre-Treatment (Day 28).

Parameter	Statistical Test	Post Hoc	Comparison	P-Value
Maximum Force	Kruskal-Wallis	N/A	Overall	0.81
Stiffness	Kruskal-Wallis	N/A	Overall	0.88
Ultimate Stress	Kruskal-Wallis	N/A	Overall	0.84
Modulus	Kruskal-Wallis	N/A	Overall	0.93
Strain at Yield	ANOVA	N/A	Overall	0.829

Table A11. Statistical Analysis of RPC Test at the End of Hindlimb Unloading (Day 56).

Parameter	Statistical Test	Post Hoc	Comparison	P-Value
Maximum Force	Kruskal-Wallis	Dunn's Test	Overall	0.01
			C-A	0.066
			H-A	0.0693
			R-A	0.04
			H-C	0.005
			R-C	0.497
			R-H	0.002
Stiffness	Kruskal-Wallis	Dunn's Test	Overall	0.01
			C-A	0.056
			H-A	0.0922
			R-A	0.0251
			H-C	0.006
			R-C	0.469
			R-H	0.001
Ultimate Stress	Kruskal-Wallis	Dunn's Test	Overall	0.02
			C-A	0.1
			H-A	0.0417
			R-A	0.1086
			H-C	0.005
			R-C	0.417
			R-H	0.004

Table A11. Continued

Parameter	Statistical Test	Post Hoc	Comparison	P-Value
Modulus	Kruskal-Wallis	Dunn's Test	Overall	0.03
			C-A	0.111
			H-A	0.051
			R-A	0.106
			H-C	0.008
			R-C	0.444
			R-H	0.004
Strain at Yield	ANOVA	N/A	Overall	0.615

Table A12. Statistical Analysis of RPC Test at the End of Recovery (Day 112).

Parameter	Statistical Test	Post Hoc	Comparison	P-Value
Maximum Force	Kruskal-Wallis	N/A	Overall	0.36
Stiffness	Kruskal-Wallis	N/A	Overall	0.44
Ultimate Stress	Kruskal-Wallis	N/A	Overall	0.4
Modulus	Kruskal-Wallis	N/A	Overall	0.42
Strain at Yield	Kruskal-Wallis	N/A	Overall	0.1

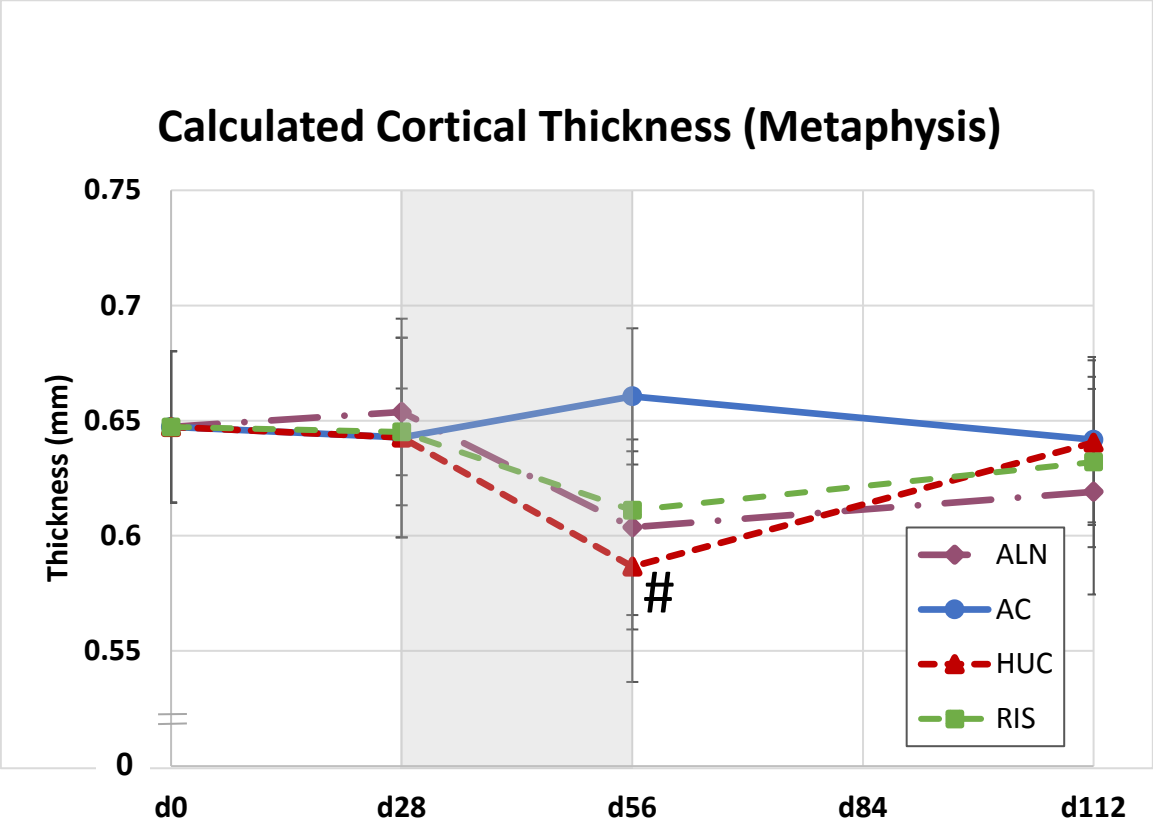

Figure B1. Calculated Cortical Thickness for Tibia Metaphysis from Ex Vivo pQCT.
Gray region represents HU. The HUC group had a significantly lower thickness compared to AC at day 56. ALN and RIS were both lower than AC, but not significantly. Cortical thickness was recovered by day 112. Values are presented as mean ± SD.
 # - Indicates significant difference compared to AC ($p < 0.05$)

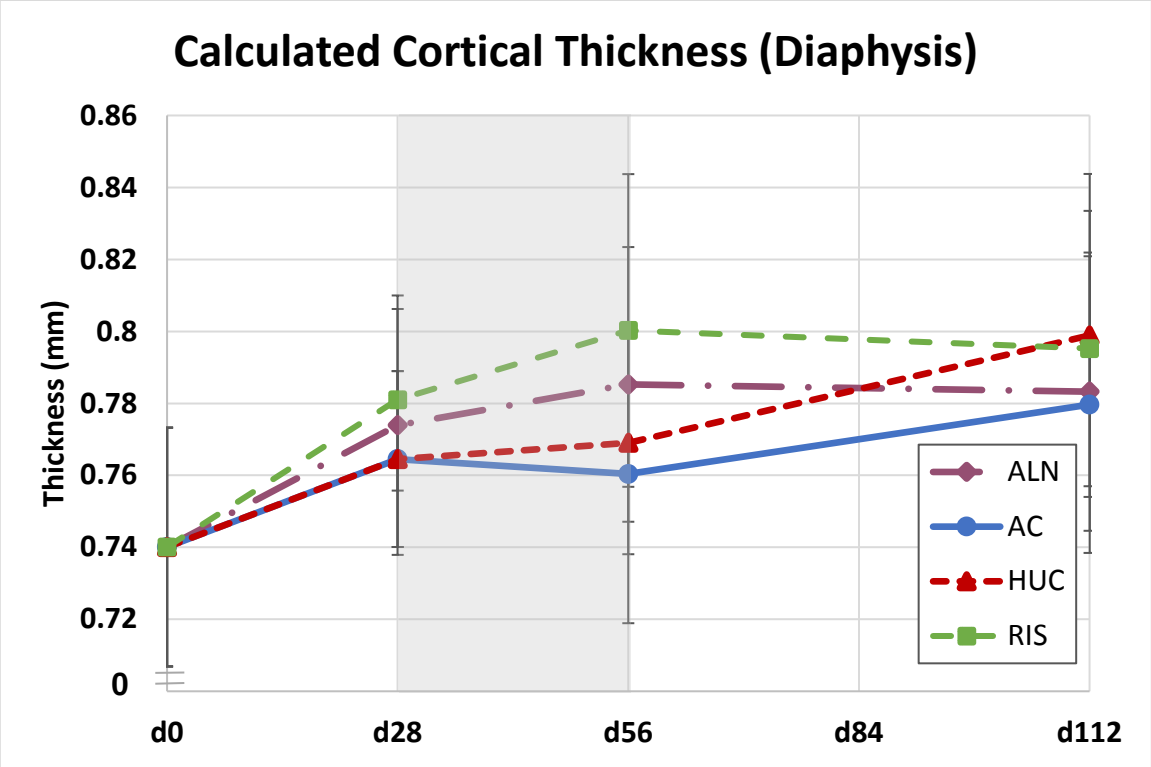

Figure B2. Calculated Cortical Thickness for Tibia Diaphysis from Ex Vivo pQCT. Gray region represents HU. There were no significant differences for this measurement. Values are presented as mean ± SD.

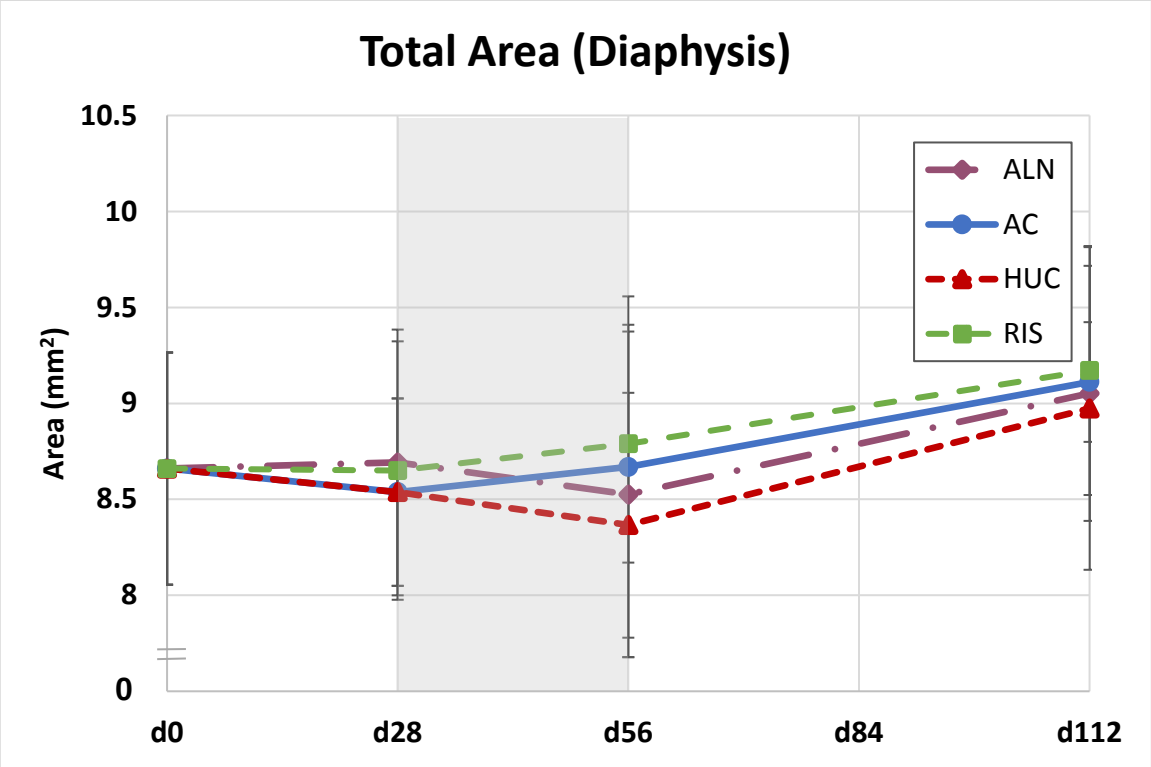

Figure B3. Total Bone Area for Tibia Diaphysis from Ex Vivo pQCT. Gray region represents HU. There were no significant differences for this measurement. Values are presented as mean ± SD.

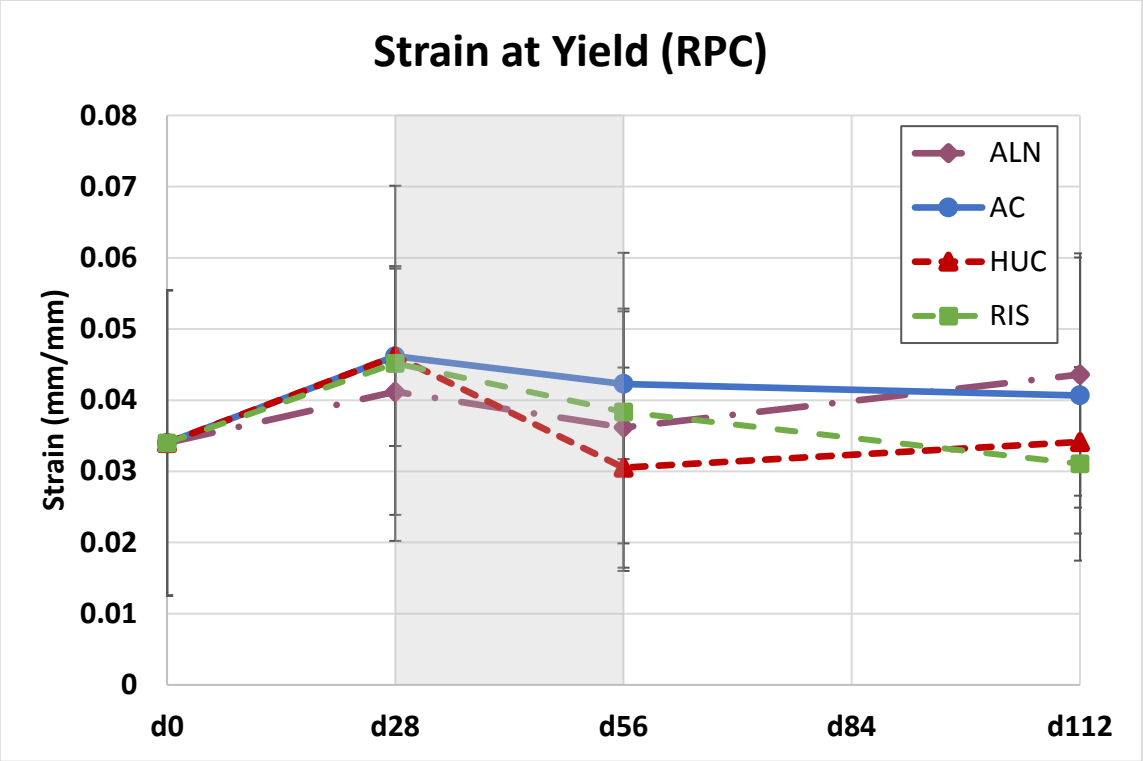

Figure B4. Strain at Yield for Tibia Metaphysis in RPC Test.
Gray region represents HU. Strain was not significantly different at any time point.
Values are presented as mean ± SD.